Prediction of catalytic activity of Pt_3Re_1 alloy for C-C bond cleavage in the ethanol oxidation reaction

Alejandro Esteban Pérez Mendoza

Universidad Nacional de Colombia
Facultad de Minas, Escuela de Procesos y Energía
Ciudad, Colombia
2016

Prediction of catalytic activity of Pt_3Re_1 alloy for C-C bond cleavage in the ethanol oxidation reaction

Alejandro Esteban Pérez Mendoza

Thesis submitted as partial requirement to obtain the Degree of:
Master in Engineering-Chemical Engineering

Advisor:
Rafael Esteban Ribadeneira Paz, Ph.D.

Universidad Nacional de Colombia
Facultad de Minas, Escuela de Procesos y Energía
Medellín, Colombia
2016

A mis padres

Acknowledgments

I thank my advisor, Professor Rafael Ribadeneira for his constant support, guidance and the chance to discuss different topics related with this work. I am grateful for the constructive feedback and patience during the preparation of this written work.

I also would like to thank to my colleagues and friends Luis Ramirez and Laura Gaviria for making the studying journey at National University much more enjoyable. Thank to Sergio Castañeda and Laura Nuñez for the time sharing at multiscale simulation meetings and their support.

Finally I wish to express my gratitude to my loving parents for their love, sacrifice and the efforts to improve my welfare. They make possible that I reach this goal.

Abstract

Design of catalysts able to cleave C-C bond in ethanol oxidation reaction at low temperatures is primordial for improving the direct ethanol proton exchange membrane fuel cells. Pt-Re alloy seems to be an appropriate material for C-C bond cleavage in ethanol decomposition, but yet, it has not been studied in-depth the reactivity of this alloy for this step. Then, in this work, the reactivity of Pt_3Re_1 surface for the C-C bond cleavage is studied and compared with reactivity of pure metal surfaces Pt(111) and Re(0001), using Density Functional Theory (DFT) and the descriptor based approach for catalyst design. Adsorption energy of CH, CO and CHCO are proposed as descriptors since they are the molecules involved in C-C bond cleavage of CHCO, which is considered the most likely reaction step for C-C bond cleavage in ethanol oxidation reaction. Consequently, the energetic and geometrical properties of the adsorption of these molecules on Pt, Re and Pt_3Re_1 are studied and analyzed respect to the electronic structure of the surface in order to understand the reactivity for C-C bond cleavage of the studied surfaces. It was found that the addition of Re to Pt leads to form active sites with Re atoms, which are more reactive for the C-C bond cleavage in CHCO, but the sites without Re are less reactive for this step. These findings suggest that despite higher ability to interact with carbon atoms of Re, the Re addition to Pt does not enhance significantly the C-C cleavage in ethanol oxidation reaction, since the higher reactivity of sites with Re atom in Pt_3Re_1 should not compensate the lower reactivity of the sites without Re.

Keywords: PtRe alloy, C-C bond cleavage, Ethanol Oxidation Reaction, Fuel cell, Density Functional Theory.

Resumen

El diseño de catalizadores capaces de romper el enlace C-C durante la reacción de oxidación de etanol a bajas temperaturas es primordial para la mejora de las celdas de combustible de membrana de intercambio protónico alimentadas directamente con etanol. La aleación Pt-Re parece un material apropiado para la desestabilazación del enlace C-C en la descomposición de etanol, sin embargo no se ha estudiado en profundidad la reactividad de esta aleación para el paso mencionado. Por tanto, este trabajo estudia la reactividad de Pt_3Re_1 para la desestabilización del enlace C-C y la compara con la de los metales puros Pt y Re utilizando la Teoría del Funcional de la Densidad (DFT) y el enfoque basado en descriptores de la actividad. Las adsorciones de CH, CO y CHCO se proponen como descriptores ya que son las moléculas implicadas en la desestabilizaciión del enlace C-C en el CHCO, considerada la etapa más probable para el paso de interés. En consecuencia, en este trabajo se calculan las propiedades energéticas y geométricas de la adsorción de estas moléculas sobre Pt, Re y Pt_3Re_1 y se analizan respecto a la estructura electrónica de las superficies consideradas con el fin de comprender la reactividad de las mismas. Se encontró que la adición de Re a Pt deriva en la formación de un sitio activo con un átomo de Re que es más reactivo para la romper el enlace C-C, pero los sitios sin Re son menos reactivos para este paso. Este hallazgo sugiere que aunque el renio presenta una fuerte interacción con los átomos de carbono en las moléculas estudiadas, la aleación de Pt con Re no tiene un efecto significativo en la promoción del rompimiento del enlace C-C, ya que la mayor reactividad de los sitios con átomos de Re no compensa la menor reactividad de los sitios sin Re.

Palabras clave: Aleación Pt-Re, rompimiento enlace C-C, reacción de oxidación de etanol, celdas de combustible, teroría del funcional de densidad.

Contents

List of Figures

List of Tables

Introduction

Fuel cells are promising devices as clean energy converters, since they have greater efficiency than conventional combustion systems (theoretical energy efficiency can be as high as 97% compared with 43% for combustion engine), which allows to obtain energy from hydrocarbon fuels in an environmentally friendly way with reduced CO_2 emissions. A common type of fuel cell is proton exchange membrane fuel cell (PEMFC), it has drawn a great attention in recent years due to their high energy density and low operating temperature [10, 11, 12]. Generally, hydrogen is the preferred fuel due to high activity in the anode of this device, furthermore it does not release greenhouse gas. Nevertheless, the use of hydrogen as fuel is limited due to the technologies for its production, storage and safe handling are still under development [13, 14].

Alcohol is an interesting choice and could contribute to accelerate the commercialization of this technology. Although methanol is most widely chosen as fuel, it has drawbacks such as low boiling point and toxicity, then ethanol has been established as a potential alternative fuel. It offers advantages such as its non-toxicity, renewability, high energy density (8.0 kWh/kg, compared with 33 kWh/kg for hydrogen and about of 11 kWh/kg for gasoline), and its easy production in large quantities [12, 13, 15].

However the PEMFC that uses ethanol as fuel, named direct ethanol proton exchange membrane fuel cell (DE-PEMFC), is still far from the efficiency obtained with hydrogen. Since the direct ethanol fuel cells technology is still at an early stage of development with many studies on laboratory prototypes. There are only few examples of DE-PEMFCs demonstrated at prototype level [7]. One of them developed by researchers in Offenburg University for an small vehicle [16, 17], and another by NDC power [18]. Both of them are based on anion exchange membrane fuel cells.

The low efficiency of DE-PEMFCs is mainly associated to the low reaction rate of ethanol oxidation reaction (EOR), ethanol crossover and cathode flooding. Another limitation in the development of this technology is the high materials costs which is mainly attributed to the cost of platinum-based catalysts [11,19]. In order to overcome these mentioned challenges, it

is required to develop materials for different parts of DE-PEMFC, among the most important ones, catalytic materials. [11, 14, 20].

Regarding the catalytic materials is found that Pt-based alloys are the most used catalysts for ethanol oxidation, particularly bimetallic and trimetallic alloys, which show a higher performance than pure platinum [20, 21, 22, 23]. But yet it is necessary to improve the DE-PEMFC performance looking for materials with higher specific activity towards CO_2 splitting [12, 20]. Pt-Re mixture is a material used as catalyst in oil reforming industry, this suggests that this alloy could work properly in formation and breakage of C-C, C-H and C-O bonds [24, 25, 26], so it seems to be promising for ethanol oxidation.

Since it is known that the catalytic activity of materials depends on its interaction with molecules and this in turn depends on its electronic structure [27, 28], this work aims to determine the adsorption energy of representative molecules for C-C bond cleavage on Pt_3Re_1 surface and the electronic structure of Pt_3Re_1, in order to predict the reactivity of this surface for C-C bond cleavage in EOR.

This work is developed in various sections, beginning with the research problem statement in the first chapter. In which contextual information about alternative energy technologies, particularly DE-PEMFCs is provided. After the main insights of the catalytic ethanol oxidation mechanism in fuel cells and the limitations of current materials to oxydize the ethanol are discussed. These ideas are summarized, identifying the issues that need to be addressed. Then the particular problem addressed by this study is outlined and it is presented the purpose or desired results envisioned to accomplish with this work.

The second chapter provide a review of works intended to address the research problem that concern to this work. So the research works about development of electrocatalysts for anode of DE-PEMFC and studies of their catalytic activity for the ethanol oxidation reaction are presented. Also, some studies of heterogeneous catalysis using a computational approach, particularly those which uses ab-initio methods to model catalysts are described.

In the third chapter, theoretical concepts used in this work are introduced. In particular, Density Functional Theory, and the pseudopotential method to deal with core electrons, are discussed. Also a description of heterogeneous catalysis, the key concepts to study it, and the approaches proposed for estimating catalytic properties of materials, particularly the descriptor based approach are presented. The fourth chapter explain as the reactivity descriptors for C-C bond cleavage used in this work are chosen, also the specific procedures and equations used for calculating the significant properties from density functional theory calculations are described.

The fifth chapter presents the results on the reactivity of Pt_3Re_1 for C-C bond cleavage in ethanol oxidation reaction, emphasizing in the interaction between CHCO, CH, CO molecules and Pt_3Re_1 surface, which are considered as descriptors of reactivity for C-C bond cleavage in the ethanol oxidation reaction. From the analysis of the data obtained, some conclusions are drawn about usefulness of rhenium as co-catalyst in the ethanol oxidation reaction. The main result is that despite the higher ability to interact with carbon atoms of Re, the Re addition to Pt does not enhance significantly the C-C cleavage in ethanol oxidation reaction, since the higher reactivity of sites with Re atom in Pt_3Re_1 should not compensate the lower reactivity of the sites without Re. This result, other important results and the recommendations are summarized in the final chapter.

Chapter 1

Research Problem

1.1 Research Justification

Currently, electric power generation is a key element to the worldwide development. Due to depletion of fossil fuel resources, global warming and growth in energy demand, the renewable energy sources and the effective use of fossil fuels has become very important to the point of being a strong driving force in economic development, hence as well in the improvement of human living conditions [14, 29, 30].

Several types of renewable energy technologies, such as wind energy, biomass and solar power (technologies with highest global investment) have experienced a global widespread and continuous growth during the last decade. As can be seen in Table **1-1** the investment in renewable energy capacity has grown since 2005, for instance in 2014 a total of 270 billion USD were invested while in 2005 the investment was only of 40 billion USD. Also, the renewable power installed capacity has increased notably in recent years, from 117 GW in 2005 to 657 GW in 2014. This growth has been helped by supportive government policies aiming to boost renewable power generation. It is evidenced by the growing number of countries with renewable energy targets, which reached a total of 164 countries, among them Colombia, where law was enacted in order to enhance the development and using of non conventional energy sources, primarily renewable energies [31]. Also in Colombia is established in the national energy plan, the including of wind, solar photovoltaic and biomass power in the energy mix [32].

One of the renewable energy technologies is photovoltaic modules, they are attractive for their low chemical wastes, their using of energy source (solar radiation) practically infinite

Table **1-1**: Renewable energy indicators. Data from Energy Information Administration (EIA) [5] and that reported annually by Renewable Energy Policy Network for the 21st Century [6]

Indicator	**2005**	**2007**	**2009**	**2011**	**2012**	**2013**	**2014**
New investment in renewable power in billion USD	40	104	169	257	249.5	232	270
Renewable power capacity in GW (% respect total power)	117 (3%)	161 (4%)	238 (5%)	390 (7%)	480 (8%)	560 (10%)	657 (11%)
Countries with policy targets	52	68	89	118	138	144	164

on the scale of human needs, their favourable legal framework in many countries [33]. Their main barriers are the high costs, the low efficiency of these devices due to weakness in light absorption properties and the intermittent of source itself (it is available a few hours per year) [30, 34, 35].

Other technology is wind power, a well established alternative which is playing a major role in power supply in an increasing number of countries. Over past years capital costs of wind power have declined, primarily through competition and technological advances [33]. The challenges of this technology are related with the grid and range from lack of transmission structure to difficulties to integrate variable power with the current management systems, and with the dependence on wind speed, which should be at least 13-15 m/s, because it is not always windy [30, 34, 36].

Among the renewable energy technologies are also the fuel cells, but they are not still developed in Colombia. They are a versatile technology, with systems ranging from single watts to megawatts, which can be well-suited for stationary, transportation and portable applications. They are now recognized as better option than conventional internal combustion engine respect to environmental aspects and efficiency [37, 38].

However the PEMFCs, the most popular fuel cell technology, have critical barriers for their widespread commercialization such as cost and durability [20, 39, 40]. Other barrier for the commercialization of PEMFCs is the use of hydrogen as fuel due to the non-availability of cost effective technologies and infrastructure for production, storage and safe handling of hydrogen, which are still under development [40]. Thus, it is required meaningful advances in order to obtain a device that compete with fossil fuel energy, and renewable energy alternatives as wind power, which is now well established in the market, or solar energy, which is receiving the highest investment among the renewable energy alternatives.

Therefore, it has been made efforts on the direct use of alcohol as fuel. Methanol and ethanol have been proposed as alternatives, in Table **1-2** is shown a comparison of various PEMFC fuels. As can be seen, ethanol is a attractive fuel since it has the advantages of being less toxic and has a higher energy density by mass (8.0 vs. 6.1 kWh/kg) than methanol [7,15,41]. Also, it is easier to transport and to store, and has higher energy density by volume than hydrogen. Other advantage is its availability on industrial scale as renewable bio-fuel generated from biomass sources. In fact, bio-ethanol dominates the global bio-fuel production, in 2013 87.2 billion litres were produced, which accounted for around to 80 % of all biofuels produced [5,33]. Colombia has implemented policies to promote the production of bio-fuels, in 2012 the production of bio-ethanol reached 362 million litres [42,43]. Thus the use of bio-ethanol would offer availability, renewability and the existence of infrastructure for its production, transportation and storage.

Table **1-2**: Properties and conversion efficiencies of Hydrogen, methanol, and ethanol as fuels for PEMFC [7].

Property	**Hydrogen**	**Methanol**	**Ethanol**
Energy density (kWh/kg)	33.0	6.1	8.0
Energy density (kWh/L)	3×10^{-3}	4.8	6.3
E°_{cell} (V)	1.23	1.21	1.14
ϵ^{rev}_{cell} (%)	83	97	97
ϵ_{cell} (%)	54	27	14
Availability and infrastructure	No	No	Yes
Toxic	No	Yes	No

E°_{cell}: equilibrium cell voltage

ϵ^{rev}_{cell}: reversible cell efficiency

ϵ_{cell}: Actual overall efficiency of the cell ($\epsilon^{rev}_{cell} \times \epsilon_f \times \epsilon_V$)

In Table **1-2** can be seen some properties for the fuel cells fed with different fuels. Such as the equilibrium cell voltage E°_{cell}, which is calculated from Gibbs free energy change (ΔG°) for the overall reaction involved in the fuel cells. The reversible cell efficiency ϵ^{rev}_{cell} (defined as analogue of thermal efficiency $\frac{W_{out}}{Q_{in}}$), is defined as the ratio between the maximum value of electrical work that can be obtained, that is ΔG°, and the total heat that would be produced by burning the fuel, that is the enthalpy change (ΔH°) of the overall fuel oxidation reaction. And the overall efficiency (ϵ_{cell}), which considers the losses of efficiency due to incomplete fuel oxidation ϵ_f, and overvoltages associated to electrochemical reactions, mass and charge transport ϵ_V. These overvoltages lead to the operation voltage (E_{cell}) smaller than the equilibrium cell voltage, and the incomplete oxidation leads to a number of electrons (n_{act}) involved in the oxidation reaction smaller than the theoretical number of electrons (n_{theo}) involved in the complete fuel oxidation reaction. Then, the overall efficiency can be expressed

as:

$$\epsilon_{cell} = (\epsilon_{cell}^{rev}) \times (\epsilon_V) \times (\epsilon_f) = \left(\frac{\Delta G^\circ}{\Delta H^\circ} \times 100\right) \times \left(\frac{E_{cell}}{E_{cell}^\circ} \times 100\right) \times \left(\frac{n_{act}}{n_{theo}} \times 100\right) \quad (1\text{-}1)$$

Although the reversible cell efficiency for PEMFC fed with ethanol is high, the current performance of this device is far from the required values for the commercialization, as it is reflected by the actual overall cell efficiency (14%) shown in Table **1-2**. The principal reasons for low efficiency are the slow reaction rate of the ethanol oxidation reaction, the formation of many intermediate products (e.g. aldehyde, acetic acid, etc.) rather than the desired complete conversion to CO_2, the ethanol crossover through the polymer membrane. Also, the performance of this device is decreased by fuel cell degradation, including membrane swelling and softening, catalyst coarsening/agglomeration (reduction in the surface area) and catalyst poisoning. In order to overcome these mentioned challenges, it is required to develop materials for different parts of DE-PEMFC, among the most important ones, catalytic materials.

As it is mentioned above, these devices should be improved in order to reach the performance targets for its commercialization. Consequently, in recent years, they have received much attention of industrial and academic institutions, as shown in Figure **1-1** publications about direct ethanol fuel cells have increased substantially since 2003, and have remained constant since 2011. Despite these efforts, it should be overcome major technical gaps, wherein catalysts are the principal factor [11, 13, 15].

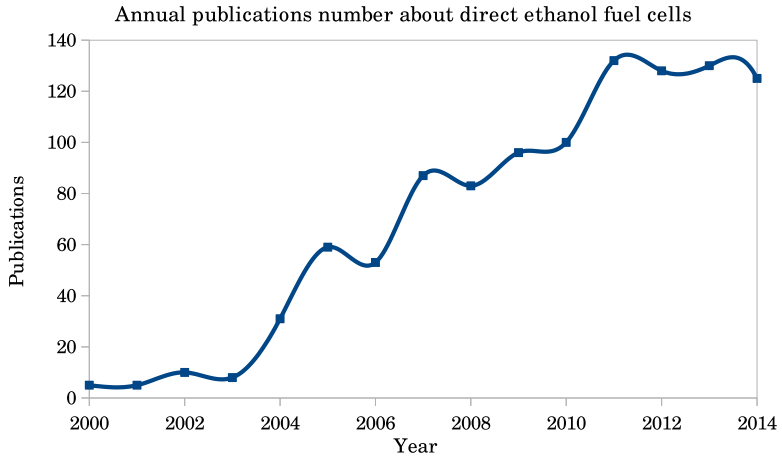

Figure **1-1**: Annual Publications Number About Direct Ethanol Fuel Cell Since 2000

Summarizing the renewable energy sources as alternative to fossil fuel are a driving force in economic development. The PEMFCs are an alternative for energy conversion that shows

attractive features as high theoretical efficiency, low operation temperature, scalability to suit a wide range of power requirement (from 1 W to 1 MW), and wide range of applications including transportation, stationary and portable power applications. The use of ethanol as fuel in the PEMFC is an interesting choice due to availability of ethanol on an industrial scale from renewable sources (bio-ethanol from biomass), high energy density (70 % of gasoline) and low toxicity. However the PEMFCs fed with ethanol require the improvement of their performance, a principal factor for their performance is the ethanol oxidation reaction, which requires the development of materials with high catalytic activity. Precisely the next section summarizes the findings about catalytic ethanol oxidation, focusing in the principal problems of this process.

1.2 Problem Definition

Catalytic ethanol oxidation involves C-H, C-O and C-C bond cleavage on the catalytic surface, ethanol should be oxidized to CO_2 in order to achieve the maximum chemical energy from this fuel [12]. The complete oxidation reaction at the anode is:

$$CH_3CH_2OH + 3H_2O \rightarrow 12H^+ + 12\ e^- + 2CO_2 \tag{1-2}$$

Ethanol oxidation mechanism on Pt-based surfaces have been extensively studied using both experimental and theoretical approach, a scheme of simplified reaction mechanism proposed is shown in Figure **1-2** [1].

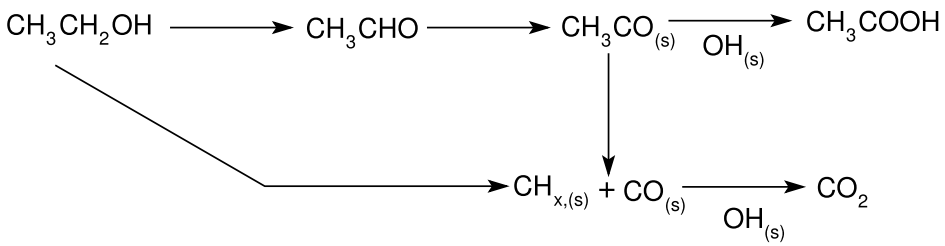

Figure **1-2**: Scheme of the most representative reaction pathways for the ethanol oxidation reaction on Pt metals. Figure based on [1]

A comprehensive description of the mechanism of ethanol oxidation reaction (EOR) is still under research, but some general steps are largely accepted, they are depicted in Figure **1-2**. In general terms, ethanol oxidation on Pt-based catalyst occurs through an adsorption step. After a series of dehydrogenation reactions, adsorbed acetaldehyde $CH_3CHO_{(s)}$ an then acetyl $CH_3CO_{(s)}$ is formed, it can react with $OH_{(s)}$ molecules, formed by H_2O oxidation, to produce acetic acid CH_3COOH, considered a final product in ethanol oxidation because of

the difficulty of further oxidation. Partial oxidation of ethanol is the most favourable route on actual catalysts, but it only releases 4 electrons [1, 10, 13, 44, 45, 46]. Complete oxidation of ethanol releases 12 electrons, but it implies the cleavage of the C-C bond. As is shown in Figure **1-2**, it has been proposed that C-C cleaving could occur mainly in acetyl, however C-C bond breaking may also occur in ethanol, forming $CH_{x,(s)}$ and $CO_{(s)}$ species. Subsequently, $CH_{x,(s)}$ and $CO_{(s)}$ react with $OH_{(s)}$ species forming CO_2.

As can be seen above, C-H and C-C cleavage steps occur at the catalytic surface. But unlike partial oxidation, complete ethanol oxidation implies cleavage of the C-C bond, which is a limiting step due to its high kinetic barriers attributed to high directionality of C-C bond. Despite of the large amount of research conducted in last years about ethanol oxidation on Pt-based surfaces, many aspects still remain unclear, such as the C-C bond splitting mechanism, the ethanol adsorbate and the intermediate species leading to the cleavage of the C-C bond, and the nature of the active site for the C-C bond cleavage [1]. Furthermore, it is pointed out that the development of catalysts with higher specific activity for C-C bond cleavage during the ethanol oxidation process is required [11, 12, 20]. In this sense a deeper understanding in the reaction mechanisms leading to the desired complete oxidation would help to design better catalysts and improve the performance of direct ethanol fuel cells.

Looking for better catalysts is an important challenge, current methods to develop new materials still use trial and error method [14], but a comprehensive approach that involves theory and simulation combined with experiments is needed to understand the reasons for which a particular material is an efficient catalyst for a given reaction, and to elucidate useful principles to design new catalysts [47, 48]. It is found to date that a material has a high performance as catalyst due to its electronic structure [28], in fact, alloys often exhibit improved catalytic performance compared to their constituent because of introduction of a guest element modifies its electronic structure [49].

Likewise, it has been proposed different relationships between catalytic activity and other properties of a material, and some principles for catalyst design using a theoretical approach. The importance of computational catalysis has grown over the past decade, particularly, in the modelling of matter at atomistic level with the introduction of Density Functional Theory (DFT), which has become in an useful tool for investigate a complex processes as is heterogeneous catalysis [3, 48]. Indeed kinetics of catalytic reaction has been evaluated using data calculated with DFT [50, 51, 52], also some atomic-scale properties of materials linked with its catalytic activity can be calculated, allowing the screening for catalytic materials [53, 54].

An interesting alloy is PtRe, it has been found that it is substantially more active in C-C bond cleavage than pure Pt and Re, and that Re addition promotes the rate of glycerol

reforming and increases the rates of alkane formation reactions, by facilitating water activation, producing OH species which are involved in C-O bond cleavage reaction [25, 55]. On the other hand, few studies on Pt-Re alloys for fuel cells are found, it was concluded that this alloy is more active for CO oxidation than other catalysts [56]; more recently, the addition of Re to Pt-Sn anodes have been proposed for DE-PEMFCs, leading to a superior performance [57, 58]. Consequently, Pt-Re is a suitable material to study reactivity trends in the catalytic ethanol decomposition reaction.

Additional to the former, there is few theoretical works in the literature, analyzing this issue. The adsorption and dehydrogenation on Pt_3Re_1 was studied using density functional theory, finding that Re alloying slightly enhances the adsorption of the hydroxyl group on the Pt site, but it does not favour the adsorption through methylene group (CH_2) [59]. However, additional steps in ethanol decomposition including C-C bond cleavage are not investigated in that work. Further, the few found studies demonstrate that the description of this system is still in development and this requires to complement this information. Thus, it is of interest to model Pt-Re catalysts in order to determine qualitative insights for their activity in this primordial step of this reaction as is C-C cleavage.

Summarizing it is remarkable that the design of selective catalysts for the complete oxidation of ethanol is primordial for improving the DE-PEMFCs, then it is important to achieve the C-C bond cleavage in order to fully oxidized ethanol. Pt-Re seems to be an appropriate material for C-C bond cleavage in ethanol decomposition. But yet, the reactivity of this alloy for the C-C cleavage has not been studied for the ethanol oxidation reaction, and there are scarce studies that links the catalytic properties of this alloy with its surface electronic structure in order to understand the nature of the active sites.

For that reason, this work aims to improve the DE-PEMFCs with the design of selective catalysts for the complete oxidation of ethanol, clarifying the usefulness of rhenium as co-catalyst in the ethanol oxidation reaction.

1.3 Objectives

1.3.1 General Objective

- To describe C-C bond cleavage in ethanol reaction on a Pt_3-Re_1 catalytic surface evaluating the electronic structure of the adsorption of representative molecules using DFT.

1.3.2 Specific Objectives

- To propose the representative molecules for the C-C bond cleavage step in order to achieve a successful descriptor based-catalyst study.

- To determine insights about the ability of Pt-Re surface for C-C bond destabilization in ethanol oxidation reaction using the reactivity descriptors (reactivity descriptors are binding energies of representative molecules).

- To theorize about Pt_3-Re_1 surface reactivity for C-C bond cleavage in representative molecules of ethanol oxidation reaction, using electronic structure calculations and chemical bonding theories based on DFT.

Chapter 2

State of the Art

2.1 Direct Ethanol Proton Exchange Membrane Fuel Cells (DE-PEMFC)

DE-PEMFCs are under development, materials of construction for cathode, anode and electrolyte have been investigated in order to improve the performance of this device. The other fuel cell components (bipolar plate or interconnects and seals), the cell and stack designs, and the membrane electrode assembly fabrication processes are somewhat similar to conventional hydrogen based proton exchange membrane (PEM) fuel cells [7, 60]. Although considerable efforts have been made to improve DE-PEMFCs the cell performance remains low, even at high operating temperatures as 110 °C. As can be seen in Table **2-2** the maximum power density reported for a single cell does not exceed 82 mW/cm^2, while the power density of a fuel cell fed with hydrogen is superior to 800 mW/cm^2 [40].

In this section are reviewed some developments in electrolyte, cathode and anode materials. Particularly, developments in anode materials are dealt with greater detail, since the slow rate of EOR is considered the principal factor behind the low performance of DE-PEMFCs [60,61].

Electrolyte. Nafion® is most commonly used membrane in DE-PEMFCs, however it has high permeation rates for ethanol, leading to fuel wastage and competing with oxygen adsorption sites on the cathode [62,63]. Mitigation strategies applied to reduce ethanol crossover include using lower concentration of ethanol [64], a thicker catalyst layer [62], modification of the Nafion® [65] and synthesis of new membranes [66, 67, 68, 69].

For example, it was proposed the modification of Nafion® membrane using neodymium

triflate, obtaining a reduction of alcohol permeation around to 48% and an increasing of proton conductivity around to 24% [65]. Also new membranes were synthesized, an example is the polymer based on sulfonated poly(ether ether ketone) (sPEEK) and polyimide which reduced substantially the ethanol crossover and had better performance in DE-PEMFCs tests than Nafion® 117 despite of its lower proton conductivity [66], also it was proposed inorganic-organic mixed matrix consisting of sPEEK and fumed silica particles modified with dihydrogenimidazole, which exhibited a lower ethanol permeation but also a lower proton conductivity than Nafion ® 117 [67]. Acid polymeric electrolytes for DE-PEMFC are under development aiming to diminish ethanol crossover and to obtain reasonable ionic conductivity and stability.

Cathode. The catalytic material most used at the cathode is platinum supported on high surface area carbon, which is also used in traditional PEMFCs. Although Pt have shown a superior catalytic activity for oxygen reduction reaction, the activity should be improved in order to reduce the large loss in potential of 0.3-0.4 V, which leads to a lower fuel cell efficiency. A part of this polarization is attributed to the irreversible behavior of Pt in the ORR which leads to the formation of hydroxide compounds, causing the inhibition of O_2 reduction [70, 71]. Another problem is the ethanol crossover through the membrane, which causes mixed potential resulting from the oxygen reduction reaction and the alcohol oxidation occurring simultaneously. This problem can be addressed by developing new cathode materials with higher alcohol tolerance than Pt [71].

Table **2-1**: Summary of the performance of DE-PEMFCs with different cathode materials. The catalyst material is reported along with metal weight percentage in parenthesis and catalyst loading used in the membrane electrode assembly after hyphen. The word Pt in catalyst loading indicates that this item is based on Pt content only.

Catalysts		**Electrolyte**	**Operation conditions**				**Power dens.**	**Ref.**
Anode (metal wt%)- loading (mg/cm^2)	Cathode (wt%) - loading (mg/cm^2)	Nafion type	T (°C)	Conc. (M)	Flow (ml/min)	pressure (MPa)	(mW/ cm^2)	
Pt/C (20%)-1	Pt_3Co_1/C (20%)-1Pt	115	90	1	—	0.3	9	[72]
Pt/C (20%)-1	Pt_3Pd_1/C (20%)-1Pt	115	90	1	—	0.3	8	[73]
$Pt_{34}Ru_{66}$/C (60%)-1.5Pt	Pt_9Bi_1/C (40%)-1	117	75	1	—	0.2	25	[74]
PtSn/C (40%)-2	$PtTiO_2$/C (40%)-2	117	70	2	2	0.1	41	[75]

Some authors considered other materials to improve the performance of the cathode, the materials proposed are based on a precious metal as Pt, since the acidic fuel cells present a corrosive environment wherein many metals are unstable. The enhancement of DE-PEMFCs performance achieved with Pt alloys is not noticeable as can be seen in Table **2-1**, that is because of predominance of the slow rate of the EOR. But this alloys can be promising,

since they have tolerance to ethanol and intermediates species derived from ethanol, which can cross through the membrane from the anode [70, 76, 77]. It has been proposed bimetallic alloys such as Pt-Bi [74], Pt-Co [72, 78, 79], Pt-Ni [80] and Pt-Pd [73]. These alloys have approximately the same oxygen reduction reaction (ORR) activity, but a higher ethanol tolerance than Pt. It could be attributed to the blocking of adsorption ethanol due to the existence of a foreign metal atom adjacent to Pt atom [76].

Anode. Ethanol oxidation reaction is considered a principal limiting factor in the performance of DE-PEMFCs. Consequently, most of the research activity in the development of this technology is focused on materials developments for increasing the ethanol oxidation reaction (EOR) rate, several experimental works proposing Pt-based bimetallic and trimetallic alloys have been carried out, as can be seen in Tables **2-2** and **2-3**.

Table **2-2**: Summary of DE-PEMFCs performance using different Pt-based bimetallic catalysts. The catalyst material is reported along with metal weight percentage in parenthesis and catalyst loading used in the membrane electrode assembly after hyphen. The word Pt in catalyst loading indicates that this item is based on Pt content only.

Catalysts		**Electrolyte**	**Operation conditions**				**Power dens.**	**Ref.**
Anode (metal wt%)- loading (mg/cm^2)	Cathode (wt%) - loading (mg/cm^2)	Nafion type	T (°C)	Conc. (M)	Flow (ml/min)	pressure (MPa)	(mW/cm^2)	
Pt/C (20%)-1	Pt/C (20%)-1	115	90	1	—	0.3	7	[81]
Pt_1Ru_1/C (20%)-2	Pt/C (20%)-1	115	75	1	1	0.2	19	[82]
Pt_1W_1/C (20%)-1.3Pt	Pt/C (20%)-1	115	90	1	1	0.2	10	[83]
Pt_1Pd_1/C (20%)-1.3Pt	Pt/C (20%)-1	115	90	1	1	0.2	9	[83]
$Pt_{80}Ir_{20}$/C (40%)-2	Pt/C (40%)-2	117	90	2	—	0.3	10	[84]
Pt_1Sn_1/C (20%)-2	Pt/C (20%)-1	115	90	1	1	0.2	52	[85]
Pt_1Sn_1/C-CeO_2 (20%)-1	Pt/C (20%)-1	117	80	2	2	0.2	50	[86]
$Pt_3Sn_1O_2$/C(20%)-1.5Pt	Pt/C (20%)-1	115	90	1	1	0.2	80	[87]
$Pt_7(SnO_x)_3$/C(20%)-1.5Pt	Pt/C (20%)-1	115	90	1	1	0.2	59	[88]
Pt_3Sn_1/C (48%)-1	Pt/C (40%)-2	115	90	1	5	0.2	82	[89]

Next section provides a brief state-of-the-art of catalysts for the Ethanol Oxidation Reaction in DE-PEMFCs, explanations of the improvement achieved with the catalysts used are included, particularly it is reviewed the efforts to obtain a catalyst able to cleavage the C-C bond in order to oxidise completely the EtOH molecule towards CO_2.

Table **2-3**: Summary of DE-PEMFCs performance using different Pt-based trimetallic catalysts. The catalyst material is reported along with metal weight percentage in parenthesis and catalyst loading used in the membrane electrode assembly after hyphen. The word Pt in catalyst loading indicates that this item is based on Pt content only.

Catalysts		**Electrolyte**	**Operation conditions**				**Power dens.**	**Ref.**
Anode (metal wt%)- loading (mg/cm^2)	Cathode (wt%) - loading (mg/cm^2)	Nafion type	T (°C)	Conc. (M)	Flow (ml/min)	pressure (MPa)	(mW/ cm^2)	
$Pt_3Sn_1P_2$/C (20%)-1.5	Pt/C (20%)-1.5	117	70	2	5	0.2	62	[90]
$Pt_{86}Sn_{10}Ru_4$/C(60%)-3Pt	Pt/C (40%)-2	117	80	2	2	0.3	50	[91]
$Pt_1Sn_1Ru_{0.3}$/C (20%)-1	Pt/C (20%)-1	115	110	1	—	0.3	32	[92]
$Pt_{85}Sn_8W_7$/C (40%)-1	Pt/C (40%)-1	117	90	2	—	0.3	33	[93]
$Pt_1Sn_1Mo_{0.6}$/C (40%)-1	Pt/C (20%)-0.7	115	90	1	2.5	0.11	26	[94]
$Pt_4Sn_5Ir_1$/C (40%)-1	Pt/C (40%)-1	117	90	2	1	0.15	29	[95]
$Pt_4Sn_5Re_1$/C (40%)-2	Pt/C (40%)-2	117	100	5	1	0.1	30	[57]
$Pt_8Sn_1Rh_1$/C (40%)-2	Pt/C (40%)-2	117	80	1	—	0.3	10	[96]
$Pt_8Sn_1Ni_1$/C (40%)-2	Pt/C (40%)-2	117	80	1	—	0.3	35	[96]
$Pt_5Ru_4Bi_1$/C (20%)-1	Pt/C (20%)-1	117	100	2	2	0.2	25	[97]
$Pt_{75}Ru_{15}Ni_{10}$/C (20%)-2	Pt/C (20%)-1	117	80	1	2	0.1	4	[98]

2.2 Experimental development of anodic catalysts

Activity of catalysts for EOR needs to be greatly enhanced in order to become the DE-PEMFC in a viable alternative [10,20]. Currently Pt-based alloys are the most used catalysts because they show the highest performance. It has been found that bimetallic alloys such as PtSn [21,99,100,101], PtRu [21,100,102], PtRe [101], PtRh [103] and PtPd [104] improve the performance of platinum pure as catalyst, particularly PtSn shows the highest performance [14, 105], as can be seen in Table **2-2** and **2-3**.

Higher catalytic activity of PtSn alloys was explained according to the bifunctional mechanism shown in Figure **2-1**, it proposes that ethanol is adsorbed principally on Pt forming acetyl, acetaldehyde, carbon monoxide in very low amounts, and others intermediates (Figure **2-1**a). Besides, tin adsorbs water and provides OH species (Figure **2-1**b) that allows the oxidation of adsorbed intermediates such as acetyl (CH_3CO) and CO, avoiding the poisoning by strong bind between Pt and CO and forming CH_3COOH and CO_2 (Figure **2-1**c) at lower potentials than Pt [10, 44, 45]. This mechanism also was applied to interpret the enhancement of ethanol oxidation the others Pt-based alloys.

It is noteworthy that reported PtSn catalysts show different catalytic activity (Table **2-2**

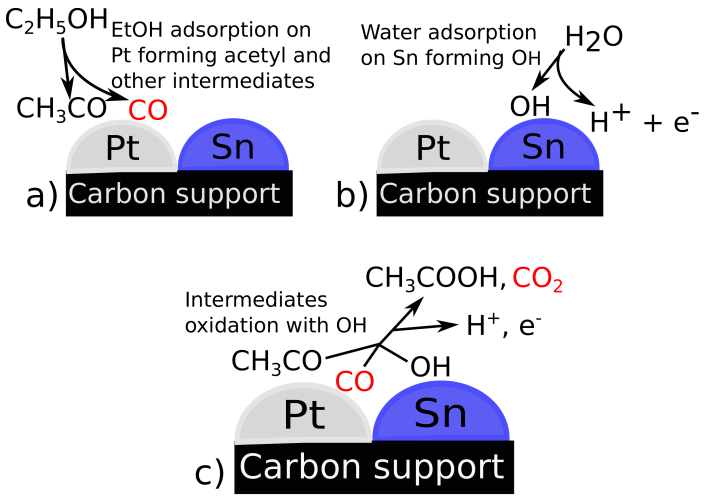

Figure **2-1**: Scheme of bifunctional mechanism.

shows different PtSn alloys with different performance). This can be partly attributed to the different phases formed in PtSn catalyst depending on the synthesis methods. In fact, it is found that PtSn alloyed phase and tin in non-alloyed oxidized state are present in the PtSn catalysts [76, 87, 106, 107]. Some authors have investigated the influence of these phases on catalytic activity finding that catalysts with high alloying degree leads to better performance [89, 108, 109, 110].

The higher catalytic activity of PtSn catalysts with higher alloying degree is explained by the occurrence of both bifunctional mechanism due to the presence of tin and the ligand effect caused by the alloying atom [91, 111]. The ligand effect is the modification of the electronic structure of platinum due to the presence of a foreign atom, which increases the rate of EtOH dehydrogenation [44, 89]. In this regard, it has been showed with a theoretical study that tin exhibits a positive ligand effect and enhance the rate of the dehydrogenation on the Pt site, which explains why PtSn is more active than Pt [23, 59].

Despite the improvement achieved by using PtSn alloys, the activity of these catalysts is still too low to attain an acceptable performing DE-PEMFC for its commercialization. Therefore, it was proposed the development of more active catalysts by adding a third metal, as Ru, Mo, W, Ce or Ni, to binary alloys as PtSn and PtRu. Ternary alloy PtSnRu has been reported in literature [92,112,113,114], finding that the catalytic activity of this alloy depends on the Pt:Sn:Ru atomic ratio [92, 112]. Some authors reported that this catalyst shows a performance inferior to PtSn [113,115], while other authors demonstrated that an appropriate atomic ratio leads to a higher activity for the EOR than PtSn and PtRu [92].

Other alloys widely studied are PtSnNi [98, 116, 117, 118, 119, 120] and PtRuNi [121, 122], authors claim that the addition of Ni increases the activity of Pt-based electrocatalysts,

it was observed a lower charge transfer resistance values for PtSnNi and PtRuNi alloys [118,122]. The Ni increases the oxophilic character of the surface promoting the bifunctional mechanism [117,120], changes the electronic properties of the Pt weakening the adsorption of the intermediate products [117, 119], and improves the stability of the electrocatalyst [119].

Other mixtures studied are PtSnPd catalysts, some authors found that PtSnPd catalysts with atomic ratios (1:1:1), (1:1:0.3) and (1:0.125:0.125) show catalytic activity lower than PtSn catalysts [96, 123]. It was suggested that Pd atoms fully alloyed with Pt atoms in this material leads to lower activity [123]. However, recently was found a better-performing PtSnPd catalyst using combinatorial methods to screen the catalytic activity of PtSnPd with different compositions, the atomic ratio of this particular catalyst was (1:0.3:0.14) [124]. These results indicate the importance of the alloy phases composition on the activity.

The addition of molybdenum for obtaining PtSnMo [94] and PtRuMo [125,126] was proposed, finding that these catalysts show a superior performance than bimetallic alloys based on Pt. The enhanced catalytic activity is attributed to bifunctional mechanism due to use of oxophilic atoms like Mo and Sn, and the migration of H atoms from Pt sites to MoO_x sites which liberates the Pt sites (hydrogen spill-over effect) [94, 126]. The addition of Cerium to PtSn catalysts was also investigated [127, 128, 129], concluding that Ce could increase the EOR activity providing oxygenated species to promote the oxidation of intermediate species [127, 128].

Others considered alloys are PtSnFe [124], PtSnW [93], PtSnIn [130], PtSnOs [131], PtSnPr [132]. It is generally accepted that the presence of oxophilic atoms, as W, Fe, Os and In, allows the formation of metal oxides, which can promote the performance of catalysts via bifunctional mechanism and hydrogen spill-over effect [93, 124], and it is suggested that the addition of a third component modifies the electronic characteristics of the alloys leading to a higher catalytic activity.

Summarizing, the addition of a third metal can enhance the activity of Pt bimetallic alloys. This third metal could form oxides or increase the oxophilic character of the surface, which could promote the bifunctional mechanism and the spill-over effect. Also, it is suggested the ligand effect to explain the higher activity of trimetallic alloys. However, these explanations for the effect of the addition of a third metal are the same that for the Sn addition, then it is not clear yet why the ternary catalysts have better catalytic activity than PtSn. Furthermore, it is remarkable that the higher ethanol oxidation observed in ternary catalysts is due to higher yields of products like acetic acid and acetaldehyde and not from a complete ethanol oxidation to CO_2 [111, 133, 134]. Indicating that despite of efforts to develop materials with higher activity towards ethanol oxidation reaction, the C-C bond cleavage in ethanol oxidation reaction remains as unsolved problem. Consequently, community is

devoting additional efforts toward developing catalysts able to cleavage the C-C bond. Such efforts are presented below.

2.2.1 Catalysts for C-C bond cleavage

Some authors suggest that the addition of some metals to bimetallic electrocatalyst can help in C-C breakage at low temperature ($90°C$), which should lead to complete oxidation of ethanol. In fact, it has been reported that the adittion of metals, as nickel [120], rhodium [135, 136], iridium [137], and rhenium [57], to PtSn bimetallic catalysts would enhance the PtSn performance facilitating the C-C bond cleavage.

The influence in ethanol oxidation reaction mechanism of the addition of a third metal, such as Ni, Pd, Co and Rh to carbon supported PtSn catalysts was investigated using Single Potential Alteration Infrared Reflectance (SPAIRS) [134,136,138]. It was found that addition of Rh and Ni leads to a higher production of CO_2, suggesting that Ni and Rh can promotes the C-C bond cleavage [134, 136]. Also was found that addition of Pd and Ni favours the formation of acetic acid to lower potentials [136], it is attributed to the greater ease for water activation resulting of the more negative charge density in these catalysts [138]. Then the PtSnNi and PtSnRh shows better performance than PtSn, PtSnPd and PtSnCo for oxidizing ethanol towards CO_2.

Ethanol oxidation reaction on $PtRhSnO_2$, $PtSnO_2$ and Pt catalysts was studied using in situ infrared reflection-absorption spectroscopy (IRRAS) and density functional theory calculations. Infrared measurements show weaker bands for acetaldehyde and acetic acid and a stronger band for CO_2 for ternary catalyst, indicating that on this catalyst the C-C bond in ethanol is broken directly. DFT studies show that tin sites are active for water dissociation, and that the presence of Rh decreases the energy barrier for the reaction pathway that involves direct splitting of the C-C bond without acetaldehyde formation [135].

In other study the EOR on $PtRhSnO_2$ was investigated using on-line differential electrochemical mass spectrometry (DEMS) and in situ Fourier transform infrared spectroscopy (FTIR) finding that CO_2 production is higher than acetaldehyde and acetic acid formation on $PtRhSnO_2$, also it was confirmed using CO_2 current efficiency calculation that the complete EOR was favored on $PtRhSnO_2$ [139]. These evidences suggest that the enhancement of the selectivity of this catalyst towards CO_2 respect to Pt and $PtSnO_2$ can be attributed to the synergy between the constituents, that is, SnO_2 provides adsorbed OH species to oxidize the intermediate species, Pt dehydrogenates the ethanol, and the Rh sites facilitate C-C bond breaking [135, 140, 141].

However, some authors found that the CO_2 production in ternary catalysts containing rhodium is similar to that in $PtSnO_2$ [142]. It could be explained by the dependence of catalyst performance on Rh content, this is attributed to the positive effect on C-C bond cleavage and the negative effect on ethanol adsorption of Rh. Then with the increasing of Rh content the negative effect on ethanol adsorption becomes prevalent and hence decreases the CH_3COOH and CO_2 formation [143]. This indicates that there is appropriate arrangement of Pt, Rh and SnO_2 atoms that increases both the activity for ethanol oxidation reaction, it should results in a CH_3COOH production only slightly lower and in a CO_2 formation higher than those obtained using PtSn [143, 144].

Ethanol oxidation on $PtIrSnO_2$ with different iridium content was studied using cyclic voltammetry, and gas cromatography during the potentiostatic electrolysis to detect the formation of CO_2, acetaldehyde, and acetic acid. It was found that the addition of iridium leads to a higher EOR activity, but only the specific composition with atomic ratio Pt:Ir:SnO_2 1:0.07:1 leads to higher selectivity for CO_2 with a CO_2 current efficiency of 18.1%, which is 2.5 and 7 times that of Pt and $PtSnO_2$ respectively [145]. Tayal et al. have studied trimetallic catalysts with Pt, Ir and Sn with different composition. They found that the catalyst with a minor content of Ir, 0.4:0.2:0.5 Pt:Ir:Sn atomic ratio, shows higher catalytic activity towards ethanol oxidation and acetic acid production compared to PtSn and the other trimetallic catalysts prepared, but it was not examined the CO_2 production [95]. Li et al. synthesized and characterized a carbon supported nanoparticulated catalyst comprising SnO_2 core decorated with PtIr nanoislands with high content of iridium, finding that EOR reactivity and selectivity toward CO_2 are improved respect to Pt/SnO_2 catalyst [137].

The different works indicate that the addition of iridium to the binary PtSn catalyst enhances the performance for ethanol oxidation [84, 95]. Also it is reported the enhancement of the selectivity toward CO_2 in catalysts containing iridium with a particular structure and composition [137, 145]. But yet the effects of Ir-Sn heterogeneous structures on the EOR reaction mechanism is not understood, this knowledge is fundamental for the development of catalysts for highly efficient oxidation of ethanol into CO_2 [146].

Likewise, mixtures of platinum, rhenium and tin was proposed as anode for fuel cells. PtRe alloy with atomic composition of Re of 25% was studied for H_2 electro-oxidation, finding that there is no measurable effect of Re on the kinetics of hydrogen oxidation, but this alloy is more active for CO oxidation than other catalysts [56]. Recently the addition of Hf, Os, Re, Ir and Ta to PtSn was studied, finding that PtReSn shows the highest power density among the catalyst tested [58]. Also, it was investigated catalysts with different content of Re for DE-PEMFCs, finding that the addition of small amount of rhenium for obtaining catalysts with 0.4:0.1:0.5 Pt:Re:Sn atomic ratio results in superior activity towards ethanol oxidation compared to PtSn and PtReSn catalysts with different composition [57,58]. It was

suggested that the addition of Re helps in the C-C bond cleavage but a higher percentage of Re in PtReSn blocks the further oxidation of intermediates resulting an adverse effect in cell performance. [57].

Furthermore, PtRe catalysts are mostly used in petroleum-reforming, especially for production of high octane hydrocarbons for automotive fuels [24, 26, 147]. Some experimental research was carried out aiming to get a better understanding of role of rhenium in reforming catalysts. In this way, it has been found that PtRe catalysts are substantially more active in C-C bond cleavage than their monometallic counterparts [25], it has been suggested that Re promotes the rates of glycerol conversion by facilitating water activation, producing OH species which are involved in CO oxidation [25, 55] and promotes CO spillover effect, that is the migration of CO from Pt sites to Re sites on which CO can easily react to form CO_2 [148]. These evidences suggest that Pt-Re could modifying C-C and C-O bonds.

Summarizing, it has been shown that the addition of Ir and Rh as third metal to PtSn alloys leads to improve the selectivity towards CO_2, but only in determined compositions. Also, it is suggested that rhenium helps in the C-C bond cleavage in the ethanol oxidation, but the different works on ethanol oxidation do not provide evidence for this suggestion. However, in different studies about glycerol reforming on PtRe catalysts was found that PtRe is more active in C-C bond cleavage than Pt and Re. But yet the effects of these catalysts on the EOR reaction mechanism is not understood deeply, further work is required to investigate the mechanism of ethanol in the different catalysts that enhances the selectivity towards CO_2, in order to improve the understanding of the EOR electrocatalysis and to help in designing materials with enhanced activity and selectivity in complete ethanol electrooxidation. Theoretical approach allowing the fundamental understanding of determining factors in catalysis is helpful in that task, precisely, next section review some theoretical works in catalysts development focusing in studies about the ethanol oxidation reaction.

2.3 Theoretical development of catalysts

The approaches to develop catalysts with improved activity includes in-depth understanding of determining factors for the catalytic properties of materials [48]. It is possible through computational studies applying atomistic and molecular models, which use quantum mechanical methods and molecular dynamics. Quantum mechanical methods are ideally suited to study adsorbate-catalyst interactions, which allows to determine the potential energy surface and thus the energy barrier of the chemical transformation, also the electronic structure of materials can be calculated, which is useful in understanding bond formation and trends in reactivity [3, 48, 149]. Molecular dynamics (MD) simulations employing reactive empirical

potentials, such as ReaxFF (reactive force field) and charge-optimized many-body (COMB), are suitable for describing reaction process and energetics of intermediates, reactants and products under realistic conditions [150].

Given the reaction events in the system, the behaviour could be averaged over larger length and time scales in order to compute the reaction rates. This can be achieved via statistical mechanics, for instance kinetic Monte Carlo (KMC) method. The reaction rates can be used as kinetic model in a reactor model which takes account gradients in fluid flow, concentration and temperature fields [149]. In this way the information from atomistic/molecular scale can be used in reaction engineering applications, moreover it enables top-down modelling whereby the optimization targets are defined (e.g., maximum activity and/or selectivity) and then searches for materials with appropriate composition and structure [149].

Next section reviews some works conducted about catalysts for the EOR using theoretical approach, including the insights gained with this approach. Particularly, the review focus on the investigations to develop catalysts with improved activity through the understanding of reaction mechanisms and the catalytic properties of materials.

2.3.1 Modelling ethanol oxidation

Some theoretical studies have been performed for ethanol decomposition on different transition metals surfaces as Au [151, 152, 153], Pd [153, 154, 155], Rh [156], Ir [157], Pt [153, 158, 159, 160, 161], PtSn [23, 162], PtRu [23], PtPd, PtRh, PtRe [59, 163] and Iridium alloys [157]. Density Functional Theory (DFT) studies have been carried out to investigate the potential energy surface for the ethanol decomposition process on different surfaces, and in some works this information is used to calculate the energy of the transition state with correlations or methods using DFT calculations, such as nudged elastic band method. Likewise, ab initio molecular dynamics (AIMD) has been used to investigate the ethanol decomposition mechanism on platinum cluster [161]. Otherwise, a micro kinetic model for ethanol partial oxidation and reforming on platinum was developed using experimental and theoretical data to estimate the kinetic parameters of each elemental step of the reaction mechanism proposed, the microkinetic model can assist in chemical reactor design and process optimization. The remarkable results of these works are presented below [160].

The comprehensive mechanism for ethanol decomposition on Pd(111) was investigated using DFT. Finding that the most favourable path is $CH_3CH_2OH \rightarrow CH_3CHOH \rightarrow CH_3CHO \rightarrow CH_3CO \rightarrow CHCO \rightarrow CH + CO$. Also it was found that the Brønsted-Evans-Polanyi (BEP) relation holds true for each of the C-C, C-O, and C-H dissociation reactions [154]. Likewise the reaction mechanism of ethanol oxidation on Au(111) was described employing DFT. It

was found that surface oxygen adatom is necessary in the O-H bond activation of ethanol, which should be the origin of reactivity of gold for ethanol oxidation [152]. Also, the ethanol oxidation reaction was studied on Rh(111) surface using DFT and KMC simulations. The obtained results show that ethanol on Rh(111) is decomposed into C and CO, and the authors point out the CH_2CH_2O as an important intermediate which leads to the formation of CHCO adsorbed the precursor for C-C bond breaking [156].

Alcalá et al. [158, 159] studied the nature of surface intermediates that may be formed on Pt(111) and the transition states for C-C and C-O bond cleavage during the decomposition of ethanol using DFT. It was found that 1-hydroxyethylidene (CH_3COH) and ketenyl (CHCO) adsorbed species have the lowest energy transition states for C-O and C-C bond cleavage respectively. In a subsequent study reaction intermediates and transition states for C-C, C-O, C-H and O-H bond cleavage on Pt_3Sn_1 (111) surface was studied, and the results was compared with those on Pt(111). Finding that the activation energy for C-C and C-O bond cleavage on Pt_3Sn_1 are 25-60 kJ/mol higher than on Pt, it suggests that the addition of tin inhibits the C-C and C-O bond cleavage. Also, it was found that the energy of transition state for CH_3CO-OH bond cleavage in acetic acid on Pt_3Sn_1 is 12 kJ/mol higher compared to Pt. These findings are in agreement with the experimental results that PtSn catalysts are selective for ethanol decomposition toward acetic acid [162].

Ferrin et al. [47] used the Brønsted-Evans-Polanyi (BEP) correlation that relates the transition-state energy of an elementary step to the reaction enthalpy in a linear way, and other linear correlation between the binding energy of molecular adsorbates (for instance CH_3CH_2OH) to the binding energy of the atom through which it adsorbs on the surface (for instance C, H or O). The combination of these correlations allows to develop the potential energy surface for ethanol decomposition on different catalytic surfaces (Pt, Pd, Ir, Rh, Re, Ru and Ni) with few inputs: parameters for the two correlations and the binding energy of atomic adsorbates (i.e. C, H, O). The potential energy surface allowed to construct a simple kinetic model for five of the metals studied (i.e. Pt, Pd, Ru, Rh, Ir) to provide qualitative trends in activity and selectivity for ethanol decomposition. For example, it was found that for all metals studied the predicted rate-determining step (RDS) for C-C cleavage is the cleavage through the CH-CO intermediate. And that all the five metals studied with the kinetic model show higher selectivity toward C-C cleavage than toward C-O cleavage [47].

A similar approach was used by Curtuois et al. [157] for screening iridium based catalysts with overlayer and underlayer structures. They used DFT calculations of CO, CH and CHCO adsorption energy on different Ir-based alloys and the BEP linear scaling correlation to calculate the activation energies for C-C bond cleavage in CHCO species, which is considered as the rate determining step for C-C cleavage in ethanol decomposition reaction. It was concluded that some iridium-based underlayer structure catalysts as Ru-Ir, Rh-Ir, Zr-Ir and

V-Ir are promising for the ethanol oxidation reaction, because they shows good CO tolerance and low activation energy for C-C cleavage on CHCO molecule.

In a recent study was investigated the adsorption and dehydrogenation reaction of ethanol on platinum based bimetallic clusters (Pt_3M) with different metals M (Sn, Ru, Re, Rh, Pd) [59]. It was considered adsorption through hydroxyl group (OH) and methylene group (CH_2) on Pt and M site. The effects of alloyed metal on the catalytic activity of Pt for ethanol partial oxidation, including adsorption energy, energy barrier, electronic structure, and rate constant was discussed. Finding a positive ligand effect of Sn that enhance the rate constant of the dehydrogenation by the methylene path on the Pt site of Pt_3Sn comparing with Pt alone. Re alloying slightly enhances the adsorption of the hydroxyl group on the Pt site, but it does not favour the adsorption through CH_2. Ru and Rh decrease both adsorptions on the Pt site [59]. Furthermore the water adsorption and dissociation on the same bimetallic clusters were studied, finding that the activation energy for water dissociation is lower on tin and rhenium atoms, hence the kinetic activity for water dissociation increases in the sequence of Pd < Rh < Pt < Ru < Sn < Re [163]. These findings allow to explain why PtSn is the most active catalyst for partial ethanol oxidation [59, 163].

In a most recent approach, ethanol decomposition on a Pt cluster was studied with ab initio molecular dynamics [161]. It was found that dehydrogenation of the methylene carbon occurs more frequently than that of the methyl carbon (CH_3). Also, it was observed that the charge of methylene carbon becomes positive with the dehydrogenation and the methyl carbon remains negative, that could explain the C-C bond cleavage observed in the CH_xCO molecules. It is remarkable that the discussion based on the charge transfer during the reaction is attributed to the ab initio simulation, since such discussion is hard to attain by a classical MD simulation [161].

In other work, classical MD simulations were used to study the difussion and structure of ethanol-water system in presence of Pt(111) surface [164]. It was found that an adsorption layer is mostly formed with ethanol molecules and the ethanol molecules push the water molecules away from the surface. It indicates that Pt (111) surface has a interaction with ethanol stronger than with water.

Molecular dynamics simulations employing reactive empirical potentials to study ethanol oxidation reaction have not found so far. But, it has been developed ReaxFF potentials to study kinetics of hydrocarbon reaction on metal surfaces, obtaining results consistent with experimental reactivity data and quantum mechanics energy surfaces [165]. For instance, the adsorption and decomposition of different molecules as ethyne, ethene, propene and benzene on nickel, finding that the species decompose by breaking C-H bonds prior to the eventual breaking of C-C bonds, which usually involves the formation of nickel carbide [166].

Also ReaxFF potentials were used to study the reaction behavior of CH_x plasma species on nickel [167], the initial stages of phenolic polymer pyrolysis [168] and the reaction barriers for hydrogen adsorption and dissociation on iron [169].

2.3.2 Theoretical approach for this work

From previous ideas, it is remarkable that the different theoretical studies on bimetallic alloys allow to explain the superior performance of PtSn for the partial oxidation of EtOH, it is pointed out that tin inhibits the C-C bond cleavage, exhibits a positive ligand effect enhancing the rate of the dehydrogenation on the Pt site, and has a lower activation energy for water dissociation than Pt, which supports the explanation given by the bifunctional mechanism [59]. Also, it was found that PtRe alloy has higher activity for water dissociation than PtSn, but this alloy does not enhance the dehydrogenation rate on Pt [163]. However, it has not been found works about other ethanol oxidation reaction steps including the C-C bond cleavage on this alloy.

This step is primordial to achieve the total oxidation of ethanol, and as was mentioned in the state of art the bimetallic and most of trimetallic Pt based catalysts are not able to cleavage C-C bond. But it is suggested that the addition of metals as Re, Rh and Ir to Pt could promote C-C cleavage in the EOR. Some theoretical works have been done aiming to clarify the effects of iridium [157] and rhodium [135], but it is not found theoretical works studying the effect of rhenium in C-C bond cleavage. Then, this work intends to describe C-C bond cleavage in a particular PtRe alloy in order to gain understanding into this step and clarify the usefulness of rhenium as co-catalyst in the ethanol oxidation reaction. A theoretical approach using atomistic-molecular modeling would enable this description.

Classical MD models the nucleus together with electrons as a single object, approximating the effects of electrons by means of inter-atomic potentials with adjustable parameters [170, 171, 172]. Then, a critical step of the modeling process using MD is tune the parameters to match well-studied experimental properties or ab initio data [171, 172, 173]. Hence, these interatomic potentials are not generic, since different parameter combinations for the same system can be obtained fitting data to different properties [171, 172]. For instance, in a work on proton transfer reaction using reactive force-field ReaxFF were obtained forty five different parameter combinations by fitting to DFT data modifying the weights of the properties used as *training set* [174]. Also, since electrons are not treated explicitly MD are unable to describe the electronic structure of the system studied, which is a property that can describe and explain chemical reactivity of the systems and the catalytic activity of the surfaces.

Ab-initio methods describe explicitly the electrons in the system with very few approxima-

tions. Then Ab-Initio methods can produce more accurate and reliable results than classical MD without using tunable parameters, also the electronic structure can be calculated to gain additional insight into catalytic activity. However, ab-initio methods have higher computational cost than classical MD, restricting their applicability to systems on the order of thousands of atoms, which could be not sufficient to observe the phenomena of interest [171, 172, 173].

In order to achieve the objectives of this work an ab-initio method is appropriate, since the catalytic activity of a material is fundamentally attributed to the electronic interaction between molecules and surface. Then, catalytic activity can be better understood describing the electronic structure of the system. Classical MD does not allows to explain the surface reactivity for C-C bond cleavage in terms of electronic structure, then the discussion of the C-C bond cleavage and the usefulness of rhenium as co-catalyst would be limited. In addition, a practical aspect is the development of satisfactory interatomic potentials for the systems considered, which requires experimental or ab-initio data, which is limited for the Pt_3Re_1 alloy.

The C-C bond cleavage in EOR can be described taking into consideration different intermediate molecules and reaction steps, likewise different surfaces with well-defined facets in addition to edges, corners, steps and kinks. However, the complete kinetic description of a given system is a quite demanding task. Rather, knowledge about catalytic activity could be gained studying properties at the atomic scale, which determine the macroscopic kinetics and can be calculated in a simpler way [3, 48, 175, 176]. This approach have been pioneered by Jens Nørskov group applying it to different reactions, it is named descriptor-based design approach and is implemented in this work. Next chapter reviews the principal concepts in catalysis used for this approach.

Chapter 3

Theoretical Background

This section presents theoretical concepts used to study catalytic processes. In particular principles which are used to understand the main characteristics of the heterogeneous catalysed reactions and the basics concepts of Ab-initio methods used in this work to study chemical reactions and the concepts. Therefore, on this section is described briefly the basic ideas of Density Functional Theory, implemented to calculate all quantities required for the description of the surfaces reactivity for a determined reaction. And some concepts such as Sabatier principle, Brønsted-Evans-Polanyi (BEP) relationship and the d-band model which are used to describe the main trends observed in heterogeneous catalysis.

3.1 Heterogeneous Catalysis Concepts

Catalysis is a phenomenon by which the rate of desired reactions, thermodynamically feasible, are accelerated by foreign substances, called catalysts. In heterogeneous catalysis, the catalyst is in a different phase with respect to reactants [177]. Overall heterogeneous catalytic reactions involve different steps, first the reactants are chemically adsorbed at the surface of the catalyst, followed by reaction steps involving bond breaking and bond making to form products and the final step is the desorption of products.

The current theories are not entirely capable to describe the catalytic phenomenon, covering the entire range of reaction conditions and observed reaction rates. But there are several general principles and concepts useful to study catalysis. Any chemical reaction can be described as a transition between two local minima on the *potential energy surface* of the system as a function of the spatial coordinates of all the involved atoms. The reaction path is

defined as the minimum energy path which connects the configuration of the reactants with minimum energy (R) to the configuration of the products with minimum energy (P), along the reaction path there is a configuration with the highest energy that is called *transition state* (TS) [176, 178]. The energy difference between the TS and R is the activation energy (E_a), with this the rate of an elementary step can be calculated using an Arrhenius expression such as:

$$r = \upsilon e^{-\frac{E_a}{k_B T}} \tag{3-1}$$

Where υ is a pre-factor interpreted as an attempt frequency, k_B is the Boltzmann's constant and T is the temperature, an schematic representation of the chemical reaction through the transition state theory is shown in Figure **3-1**.

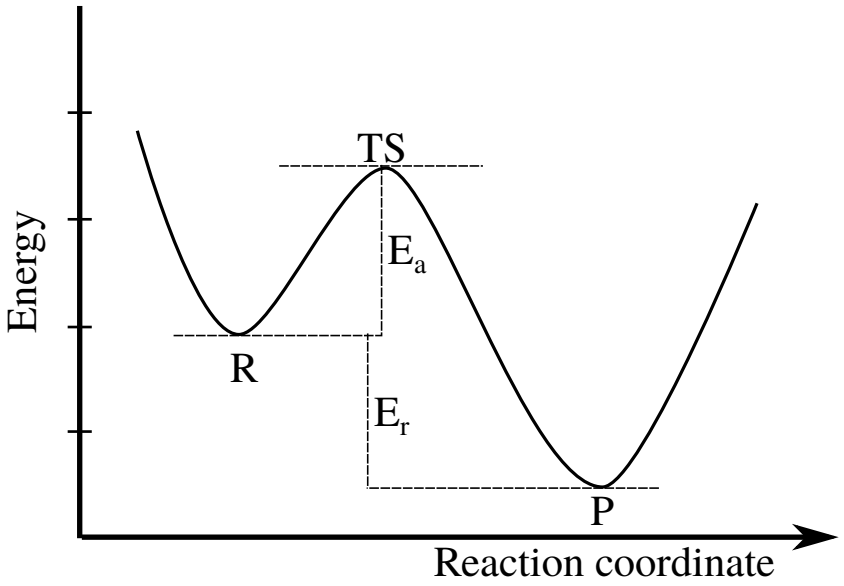

Figure **3-1**: Potential energy surface of a processes between locally stable states

It has been found that the transition energies show a linear correlation with adsorption energies. This type of relationship is a well-established approach in the understanding of trends in chemical reactions that dates back to Brønsted in 1928, also Evans and Polanyi in 1938 [179], they established a linear relationship between activation energies (E_a) and reaction energies (E_r) of a reaction. Which is called *Brønsted-Evans-Polanyi*(BEP) relationship.

$$E_a = b + aE_r \tag{3-2}$$

This relation has been held true until now, it has been demonstrated for different classes of catalytic reactions, such as hydrogenation [180, 181], dehydrogenation [180, 181, 182] and dissociation reactions on different surfaces [180, 182, 183]. Using electronic structure calculations for obtaining the transition state and the adsorption energies and hence the activation

and the reaction energies it has been possible to establish transition state scaling relations with sufficient statistical significance. This scaling relationship provides a straightforward way of defining the effect of the surface on the activity for a given reaction, as it enables the estimation of reaction barriers from the adsorption energies, which could be calculated with computational calculations or experimentally.

A valuable principle for catalyst "design" is the *Sabatier principle*, which is related to linear free energy relationships. It states that the bond between the catalyst and the key adsorbate should be not too weak, such that the reactants do not bind, and not too strong, since this leads to catalyst poisoning [177, 184].

It allows an interpretation of volcano curves, which show the catalytic activity for a given elementary reaction step as a function of the adsorption energy of an intermediate compound. As shown in volcano curve in Figure **3-2** at low values of adsorption energy, the reaction is slow because the rate of adsorption is slow and rate-limiting, whereas at high values of adsorption energy, desorption becomes the rate-limiting step. Then it is required intermediate values of adsorption energies in order to obtain the highest activity (top of the volcano) [2, 176, 177, 185].

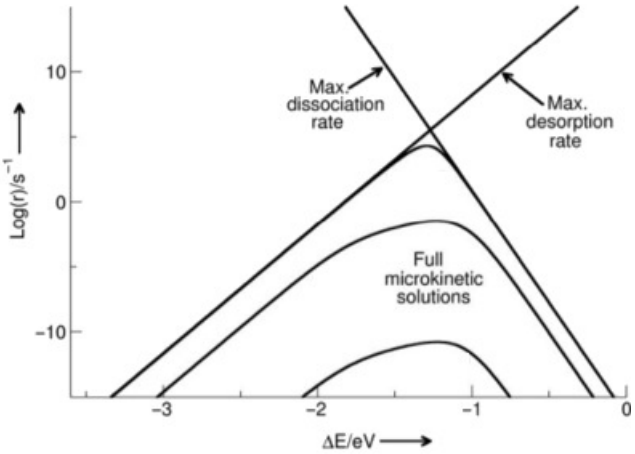

Figure **3-2**: Interpretation of volcano curves obtained from full microkinetic models using Sabatier principle. Reprinted from [2]

Heterogeneous catalysis requires chemical bonding (*chemisorption*) of reactants to the surface, this bond can be described in terms of electronic structure of the surface and adsorbate molecule. In particular, for transition metals, it is described in terms of d-bands of metals, as is proposed in the "d-band model", which is presented in the next subsection.

3.1.1 d-band Model

A simplified picture of the electronic structure in transition metals (Figure **3-3** shows a broad s-band and a much narrower d band. The interaction of the adsorbate valence state with the broad s-band can be assumed to be similar for different transition metals, hence the chemisorption energy should be mainly determined by the interaction with the d electrons. The interaction of an adsorbate state with the d-electrons of a surface causes a split into bonding and antibonding states, as in the case of molecular orbitals [3, 176, 186].

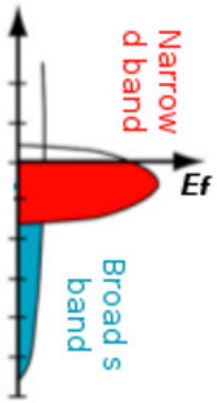

Figure **3-3**: Schematic projected density of states (PDOS) of transition metals. Reprinted form [3]

The strength of the bond is determined by the filling of antibonding states, if more of them are empty, the molecule is strongly bound to the surface. Since electrons will fill up all states located below the Fermi level, the energy of these states respect to Fermi energy (E_f) is useful to characterize strength of the bond between adsorbate and surface. It has been found that if d-bands of metals shift up in energy, anti-bonding states would become empty (shift up above E_f) and hence the bond with the molecule is stronger.

Furthermore, the energy-weighted average of the density of d-states (center of d-band) can be used to characterize the d states and therefore the adsorption strength. If d-band center is more below in energy respect to Fermi energy (blue d-bands in Figure **3-4**), more of antibonding states would be below E_f and hence more occupied, resulting in a weaker bond. This is the so-called *d-band model* proposed by Hammer and Nørskov [27, 186]. Figure **3-4** illustrates this chemisorption model.

As is mentioned above, the interaction between reactants and surface, specifically between molecule atoms and local surface atoms, is a central point in heterogeneous catalysis. The local surface atoms constitutes the *active site*, the active sites can be defined as atoms or groups of atoms accessible for chemisorption and active for reaction. A solid catalyst can have different active sites with different reactivities, they exposes different well-defined sur-

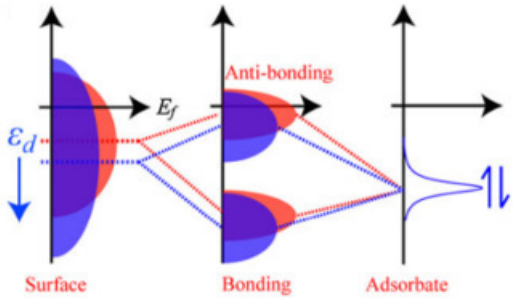

Figure **3-4**: Illustration of the d-band model. The interaction of an adsorbate valence orbital with metal d-states forms bonding and anti-bonding states. As the d-band center of the metal shift down in energy, more of antibonding states are below E_f and hence more occupied, resulting in a weaker bonding. [4]

faces together with surface defects such as steps, kinks, edges, and corners with different coordination number. The variation of coordination numbers will lead to different reactivities, in general low coordination will lead to improved reactivities as in the case of surface defects [185, 187, 188].

Additionally the reactivity of a given metal can be changed substantially by variations of the lattice parameter (*strain*), overlayers of one metal on another and alloying. The different ways to modify the reactivity of the active sites affect the electronic properties of the surface. In alloying, the addition of one or more chemical elements to a metallic surface changes the electronic structure from that of the pure metallic surface alone. It is due to new interactions between the metals, which cause a shift in metal d-bands, it is called the *ligand effect*. Furthermore, alloying increases the possible bonding geometries of adsorbate and reaction complexes [186].

3.1.2 Descriptors approach

The concepts presented represent the basic theoretical instruments usually used to investigate catalytic chemical reactions and to provide satisfactory descriptions. Summarizing, it is observed that different properties of a material can be related with its catalytic activity. For instance, BEP expression 3-2 relates the reaction energy of given reaction and the activation energy, which allows estimate the reaction rate with 3-1. Sabatier principle shows that a relation between the catalytic activity and the adsorption energy can be established. Finally it is mentioned that variations in lattice parameter and modification of the electronic structure changes the catalytic activity.

Furthermore, it seems that adsorption energy is a key property to understand the catalytic activity. It can be expected that the rate of a reaction depends on the adsorbate-surface interaction strength. This fact is confirmed with the volcano curves observed when activity is graphed as function of adsorption energy. Also, BEP relation would imply a relationship between activation energy and adsorption energies, since in heterogeneous catalysis the reaction energy depends on adsorption energy of reactants and products.

In order to understand trends in catalytic activity, it could be proposed a full kinetic description considering each possible intermediate and its binding energy, and different reaction steps and their barrier energies. But, the needed information to be calculated could be reduced considering the fact that the catalyst activity for a given reaction can be described using a limited set of properties, named descriptors [175,176], as is suggested by the relations above remarked.

The first step in a descriptor based study is find the most suitable reactivity descriptor. Scaling relations and Sabatier principle suggest that adsorption energies are descriptors for a given reaction. The identification of particular adsorption energies that are descriptors is usually achieved studying the underlying reaction mechanism and identifying the rate-limiting step, also an adsorption energy descriptor can be found through an educated guess, resulting of the knowledge on the particular or similar reactions. The second step is quantify that descriptors [175, 176].

Additionally, it can be noted that the interaction adsorbate-molecule is a phenomenon attributable to the electrons, then this interaction can be described in terms of electronic structure. Moreover, the electronic structure is considered as the origin of the surface specificity of adsorption energies and activation energies for surface reactions [48,175]. Hence the analysis of the electronic structure also can be a descriptor of the catalytic activity.

The description of the chemical bond between surface and molecule is the fundamental basis for understanding surface chemical reactivity. An appropriate approach to study it is the Density Functional Theory (DFT) based on quantum physics. In recent years, a great deal of progress has been made on DFT calculations, becoming in a powerful tool to evaluate materials and complex process such as catalysis. It can describe the electronic structure and provide the interaction energy of molecules and surfaces with sufficient accuracy, giving a bonding picture between surfaces and molecules that allows one to explain trends in reactivity [3, 48]. Next section review the basic concepts beyond DFT.

3.2 Density Functional Theory

First-principles or ab initio calculations are based on the quantum physics that describes with accuracy the behavior of small particles, such as electrons. It requires the solution of the fundamental equation, namely the Schrödinger equation:

$$\hat{H}\Psi = \epsilon\Psi \tag{3-3}$$

In equation 3-3 Ψ is a function that describes a quantum state of one or more particles, containing all the information about the entire system. ϵ is a real number associated with the energy corresponding to each state Ψ. $\hat{H}$ is a operator associated with the total energy of the system, then it contains the operations associated with the kinetic and potential energies. The operation on the wavefunction with the Hamiltonian produces the energies value ϵ. The Hamiltonian is defined according to the physical system of interest, since potential energy operation depends on the physical situation. In this case we are interested in multiple electrons interacting with multiple nuclei, then $\hat{H}$ is defined as:

$$\hat{H} = \underbrace{\frac{\hbar}{2m}\sum_{i=1}^{N}\nabla^2}_{kinetic\ energy\ of\ electrons} - \overbrace{\frac{1}{2}\sum_{i=1}^{N}\sum_{j=1}^{M}\frac{Z_j e^2}{|r_i - R_j|}}^{electron-nucleus\ interaction} + \underbrace{\frac{1}{2}\sum_{i\neq j}\frac{e^2}{r_i - r_j}}_{electron-electron\ interaction} \tag{3-4}$$

The Hamiltonian in 3-4 do not includes the nuclear kinetic energy and nucleus-nucleus interaction. This is because nuclei and electrons are considered separately, then in the study of electrons the nuclear kinetic energy can be neglected and the nuclei are considered as fixed ions acting as an external potential. The validity of this separation is founded in that nuclei move with much smaller velocities than electrons and the time-scales of nuclear and electronic motion will be well separated [171, 189, 190]. This separation is known as Born-Oppenheimer approximation [190].

Unfortunately the equation 3-3 is useful in practice only for the simplest system due to the many-body nature of interactions, it is still too complicated to be solved for systems with several atoms. Density functional theory (DFT) developed by Kohn and Sham is a successful ab initio approach for systems with larger number of atoms. It made possible the application of quantum physics to materials science, so much that DFT calculations is now a "standard theory" for materials modelling problems in physics, chemistry and engineering [191, 192, 193, 194]. Next subsection review the basic ideas and concepts underlying the theory.

3.2.1 Electron density and Hohenberg-Kohn theorems

The main variable in the Kohn and Sham approach is the electron density $\rho(r)$. It is an observable quantity and denotes the probability to find any electron in a certain volume dr [191, 192]. The electron density, similar to the wave function, describes everything in an n-electron quantum system and is defined by the sum over a set of squares of non-interacting orbitals $\phi(r)$.

$$\rho(r) = \sum_i |\phi_i(r)|^2 \tag{3-5}$$

It is remarkable that the usual wavefunctions ψ_i are replaced by orbitals ϕ_i, implying that the electronic orbitals at a point determine an electron density at that particular point. With this new approach the problem changes to an electron density dependent problem, which describes any property of a system of interacting particles in external potential. It is demonstrated by Hohenberg and Kohn in their two theorem [195].

Theorem 1: For a system of interacting particles in an external potential V_{ext}, the potential V_{ext} is determined uniquely by the ground-state electron density $\rho_0(r)$, and V_{ext} determines completely the Hamiltonian. This implies that any properties can be deduced from the ground state electron density, then an universal functional for the system energy $E[\rho(r)]$ can be defined in terms of the density $\rho(r)$ corresponding to any external potential V_ext

Theorem 2: The electron density that minimizes the energy functional $E[\rho(r)]$ is the exact ground state density $\rho_0(r)$. Then varying electron density the energy system can be reach the minimum E_0, but never below it.

$$E[\rho(r)] \geq E[\rho_0(r)] \qquad E[\rho_0(r)] = E_0 \tag{3-6}$$

The theorem expressed in equation 3-6, so called variational principle, offers a powerful means of finding the ground state. It requires only the minimization of a functional of the electron density.

3.2.2 Kohn-Sham equations

The Hohenberg-Kohn theorems show that the electron density is the fundamental quantity and allows calculate any property if the functional is known. Kohn and Sham formulated the equations which allows to calculate the properties based on electron density [196]. They first assumed that the electrons in the system are non-interacting, that means that every electron is regarded as moving in an effective single particle potential V_{ext} and the terms considered in

the energy functional $E[\rho(r)]$ are the density functionals associated with kinetic energy E_{kin} of electrons and the energy due to external potential E_{ext}. After they returned to the problem of interacting electrons and added new terms: one term that take account the interaction between electrons E_H and another that regroup all other electron interacting contributions called the exchange-correlation E_{xc}. Then the energy functional can be expressed as:

$$E[\rho(r)] = \overbrace{T[\rho(r)]}^{E_{kin}} + \overbrace{\int V_{ext}(r)\rho(r)dr}^{E_{ext}} + \overbrace{\frac{1}{2}\int \frac{\rho(r)\rho(r')}{|r-r'|}drdr'}^{E_H} + \overbrace{\underset{xc}{E_{xc}[\rho(r)]}}^{E} \tag{3-7}$$

From expression 3-7 is derived the Kohn Sham (KS) equations by applying the variational principle (minimizing energy respect electron density), the result is:

$$\left(-\frac{1}{2}\nabla^2 + V_{ext}(r) + \int \frac{\rho(r')}{|r-r'|}dr' + v_{xc}(r)\right)\phi_i(r) = \left(-\frac{1}{2}\nabla^2 + V_{eff}(r)\right)\phi_i(r) = \epsilon_i\phi_i(r) \tag{3-8}$$

This is the (KS) one electron equation analogous to the Schrödinger equation, ϕ_i are the KS orbitals constructed from electron density, and ϵ_i are its corresponding energies. In this equation $v_{xc}(r)$ is the exchange correlation potential which depends on electron density and is given by the following equation:

$$v_{xc} = \frac{\delta E_{xc}[\rho(r)]}{\delta\rho(r)} \tag{3-9}$$

and the electron density defined in terms of KS orbitals as:

$$\rho(r) = \sum_i |\phi_i(r)|^2 \tag{3-10}$$

The equation 3-8, with exchange correlation potential given by 3-9 and the electron density given by 3-10 are now called the Kohn-Sham (KS) equations. If v_{xc} is known any property can be calculated solving 3-8. Then the attention should be directed to $E_{xc}[\rho(r)]$, since practical usefulness of DFT depends on whether sufficiently simple and accurate approximations for the functional could be found $E_{xc}[\rho(r)]$. The next section briefly review the approximations for exchange correlation functional.

Exchange correlation functional

For the construction of XC functional is useful the concept of XC hole, which is a consequence of the fact that the presence of an electron in a region inhibits the proximity of other electrons around it, thus there is a reduction of electron density [192,194]. Then the exchange correlation energy can be attributed to the interaction between electron density and XC hole, and the correlation energy E_{xc} is calculated from a purely local integral over the density [191, 192]

$$E_{xc}[\rho(r)] = \int \rho(r)\epsilon_{xc}[\rho(r)]dr \tag{3-11}$$

The term $\epsilon_{xc}[\rho(r)]$ denotes the local (at point r) exchange-correlation energy density, there are many approximations to calculate this term, as the local density approximation (LDA) and the generalized gradient approximation (GGA). In the LDA method the system is assumed as many regions with different uniform local electron density, for each region the XC energy is assumed to be identical to the exchange-correlation energy density for an homogeneous electron gas of the same density. Analytical formula for the exchange energy density and some approximations and analytical forms for the correlation energy are available [191].

This assumption was expected to be useful for densities varying slowly on the scales of the local Fermi wavelength which depends on Fermi energy of the system, it is below 1 nm for metals. This condition is rarely satisfied in atomic systems, nevertheless the LDA give accurate results for many systems. This is partly due to cancellation of errors estimating exchange and correlation energies. Some implementations of LDA functionals are those of Perdew and Zunger (PZ) [197], and Perdew and Wang (PW) [198]. LDA give accurate results for nearly free electron metals and covalent systems, it is found that LDA overestimates dissociation and cohesive energies and gives bond lengths and geometries of the systems with an accuracy of 1%.

In GGA method information about both local electron density and its gradient is accounted. Then an special dimensionless functional $F_{xc}[\rho(r), |\nabla\rho(r)|]$ is included to modify the LDA energy. This term is like an enhancement factor related with variations in different order of the electronic density of the system, for which numerous formulas have been proposed. Some of them are those of Perdew and Wang (PW91) [199], Perdew, Burke and Enzerhof (PBE) [200], and the combination of the exchange functional of Becke (B88) [201] and correlation functional of Lee, Yang and Parr (LYP) [202] which is named BLYP. GGA describes in high degree almost all systems, giving structural properties with in 1 to 3% error and correct the overbinding problems of LDA.

The choice of the XC potential always depends on the studied system and its particular properties to be calculated. But there is no general rule that allows to unambiguously

choose the XC functional for given system, a reasonable way is comparison of the results of test calculations between each other and with available experimental data.

With the specification of energy exchange correlation are completed the KS equations above presented and all that remains is solve them. The next subsection presents the algorithm for solving this set of equations, which requires an iterative procedure.

3.2.3 Solving Kohn-Sham equations

Solve the KS equations imply minimizing the energy by finding a self consistent solution, whose orbitals are subject to constraints. A self consistent solution is a set of KS orbitals that leads to a KS Hamiltonian whose solution is the same orbitals. The iterative method used for DFT calculations is outlined below:

1. Set the initial $\rho(r)$ using equation 3-10, it is needed to define initial KS orbitals ϕ_i. A good initial supposition is superimposing the orbitals of electrons in the isolated atom, or orbitals obtained from calculations performed for a slightly different geometry. Usually, KS orbitals are constructed from a *basis set*.

2. Construct V_{eff} using the actual $\rho(r)$ to evaluate selected E_{xc} functional, E_H term and the V_{ext}. The Coulomb potentials are usually replaced by effective ionic *pseudopotentials* that account for the screening effects of the core electrons.

3. Solve the set of coupled KS equations by diagonalization and obtain the KS orbitals $\phi_i(r)$. The procedure involves expansion of the orbitals in terms of a *basis of functions*. The choice of a basis leads to distinct but equivalent descriptions of the underlying electronic structure.

4. Use the new $\phi_i(r)$ to calculate new electron density $\rho_{new}(r)$, compare with the previous $\rho(r)$ to verify self consistency. The iteration can be stopped when the density change becomes less than a pre-set stopping criterion.

5. If self consistency is not reached, a new guess for $\rho(r)$ is constructed mixing the new and the previous electron density, and the steps 2 and 3 are repeated. The way the mixing is made can affect the convergence and the possibility to achieve self consistency quickly

Two important issues in solving KS equations is the chosen basis set, and the pseudopotential (PP) approach which leads to a significant reduction in the numbers of electrons in a system.

Basis set

The basis set is a set of functions f_k of known properties that is used to represent the KS orbitals ϕ_i. The orbital is a linear combination of these functions:

$$\phi_i(r) = \sum_k c_{ik} f_k(r) \tag{3-12}$$

Most important criteria for the choice of basis include: the asymptotic completeness, computational complexity, efficiency and accuracy of the calculations, conceptual simplicity and ease of implementation, meaningfulness of the physical interpretation. Plane wave methods are very widely used for periodic systems due to their conceptual simplicity (Fourier transforms) and generality achieved by not making assumptions regarding the specific features of the orbitals. This also means that hundreds of plane waves per atom are necessary to achieve good accuracy.

Pseudopotential (PP) approach

The pseudopotential approach divides electrons into two groups, core electrons that are close to nucleus and the valence electrons that are in the outer shells of the atoms [192, 203]. The core electrons are tightly attached to the nucleus, their orbitals do not extend far from it, therefore have less contributing significance to interatomic interaction. Valence electrons are almost delocalized and are responsible for the formation of atomic bonds, having most impact on the material properties. Then the PP approach consider core electrons freeze together the nucleus, an exclude them from the calculations, but take account for their effect by constructing effective pseudopotentials. This leads to a much easier description and computation of valence electron orbitals without significant errors.

The differentiation between core and valence atoms is usually based on electronic configuration, for instance the Pt and Re atoms which are studied in this work are divided as follows.

Pt: $\underbrace{1s^2 2s^2 2p^6 3s^2 3p^6 3d^{10} 4s^2 4p^6 5s^2 4d^{10} 5p^6 4f^{14}}_{core\ electrons} \overbrace{5d^9 6s^1}^{valence\ electrons}$ Re: $\underbrace{1s^2 2s^2 2p^6 3s^2 3p^6 3d^{10} 4s^2 4p^6 5s^2 4d^{10} 5p^6 4f^{14}}_{core\ electrons} \overbrace{5d^5 6s^2}^{valence\ electrons}$

Several procedures of pseudopotential generation have been developed, leading to different type of pseudopotentials. Some approximations are those proposed by Vanderbilt [204], and Troullier and Martins [205].

Chapter 4

Methods and simulation parameters

This work aims to describe C-C bond cleavage in ethanol oxidation reaction on a Pt_3-Re_1 surface using a descriptor based approach. This chapter describe the procedure followed to apply this approach to study the C-C bond cleavage. The first part present the descriptor proposed, that is CH, CO and CHCO adsorption. Also, this part explains why they are the most suitable reactivity descriptor. The second part describe the surface model, the equations and the computational parameters used to quantify the reactivity descriptors chosen.

4.1 The reactivity descriptor for C-C bond cleavage

As is mentioned in chapter 2 the different works carried out in order to understand the reaction mechanism for ethanol decomposition show that the C-C cleavage in molecules with more hydrogen atoms attached to the carbon atoms, as ethanol molecule (CH_3CH_2OH) or acetaldehyde (CH_3CHO), has the highest activation energies [154, 156, 158]. It can be attributed to the high directionality of the σ-orbital of C-C bond in these molecules, which is constrained straightway along the bond axis, also there are several substituents (hydrogen and oxygen atoms) on both carbon atoms constraining sterically this bond. Then, the interaction of the metal with this bond is more difficult than with C-C double bond or a C-H single bond. These bonds are less sterically constrained than the σ-orbital of C-C bond, also the π-orbital of a C-C double bond is oriented sideways, making its interaction with the metal simple [206].

According to the mentioned above, it seems that the C-C bond cleavage in ethanol oxida-

tion requires breaking of C-H bonds prior to the eventual breaking of C-C bonds, which is more feasible in dehydrogenated molecules with π orbitals in C-C bond. It is similar to the found in hydrocarbons reaction on metal surfaces, where molecules decompose forming dehydrogenated species, which are further decomposed by cleaving C-C bond into lower hydrocarbons [166]. Likewise, the works on ethanol oxidation points out that the first steps in ethanol oxidation involves dehydrogenation reactions, forming acetyl CH_3CO, this molecule could be further dehydrogenated forming CH_2CO and CHCO [1]. In all these molecules is more feasible the C-C bond. Then they would be good descriptors of C-C bond cleavage.

Also, it is found that the step with the lowest transition energy for the C-C bond cleavage on transition metals as Pd, Rh and Pt is the following surface reaction: [154, 158]

$$CHCO_{(s)} + s \rightarrow CH_{(s)} + CO_{(s)} \tag{4-1}$$

The subscript (s) indicates that the species are adsorbed on surface. Also, it is pointed out that for most transitions metals, the rate determining step for C-C cleavage in ethanol oxidation reaction involves the transformation of CHCO intermediate into CH and CO [47]. Then, it is considered that significant insights on C-C cleavage on Pt_3Re_1 surface can be gained by studying this step.

Additionally, it is found that the transition state for C-C bond breaking in CH_xCO (x=1, 2 or 3) on metal surfaces is linearly related with the energy of products (like Brønsted-Evans-Polanyi relation, BEP), this one single relation is hold true for different transition metals such as Ni, Ru, Rh, Pd, Ir and Pt [181]. Similarly, other works has established transition state scaling relations for the reactions involving different intermediates of EOR, including the C-C dissociation reactions, on surfaces as Pd [154] and Pt [158]. The linear relationship originates from the close similarity between the transition state geometries and the final state geometries. This is case for the breaking of strong bonds, which have to be stretched very far from equilibrium to sufficiently mix with the surface states [181]. The relationships can be expressed as:

$$E_{TS} = \alpha E_P + \beta \tag{4-2}$$

E_P is the energy of the adsorbed products of the particular reaction respect to the energy of reactants in gas phase and the clean surface, E_{TS} is the energy of transition state respect to the same reference. Then the activation energy E_a can be calculated as:

$$E_a = E_{TS} - E_R = \alpha E_P + \beta - E_R \tag{4-3}$$

E_R is the energy of the reactants. In the reaction step proposed in this case, the products (P) are the CH and CO species adsorbed, and the reactant is the adsorbed CHCO. Hence the activity of the metallic surface is related with the adsorption energies of CH, CO and CHCO, which are the descriptor proposed in this work.

4.2 Atomistic surface model

The surface is modeled with the slab approach, that is a portion of solid with periodicity in two dimensions(X,Y), but finite in the third dimension (Z) to form a surface, then empty space has been left above the atoms in the top portion of the supercell [193]. So when the supercell is repeated in all three dimensions, it defines a series of stacked solid material separated by empty spaces.

The surface is constructed using the lattice parameters obtained with DFT calculations of the Pt_3Re_1 bulk system, which is modeled as face centered cubic (FCC) structure with crystal symmetry defined by $pm\hat{3}m$ space group, since the experimetal works report that this alloy crystallizes in FCC structure [207]. As depicted in **4-1**, the Pt atoms (gray) occupy the face-centered positions and the Re atoms (red) are located at the corners in the unit cell (represented with the blue cubic boxes). Also can be seen the (2x2x2) supercell used for the calculations, which has 8 unit cells and 32 atoms. Also, Pt is modeled as face centered cubic structure with crystal symmetry defined by $fm\hat{3}m$, using a supercell of 32 atoms, and rhenium as hexagonal close packed crystal symmetry defined by $P63/mmc$, using a supercell with 16 atoms.

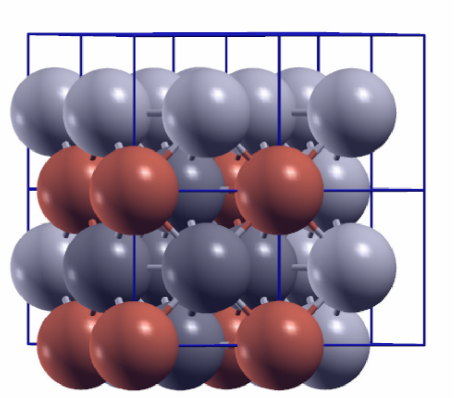

Figure **4-1**: Supercell of fcc Pt_3Re_1 crystal. Gray and red spheres represent Pt and Re atoms, respectively.

As it is observed in Figure **4-2**, for the slab empty space of 9.00 Åis left above atoms in the portion of material in order to obtain the slab, and five layers of atoms are used for representing the portion of solid. These values have been found after several test calculations using different atomic layer and vacuum space under the basis of convergence for all calculations. Convergence tests can be seen in Anexo A, particularly in Figures **A-3** and **A-4**.

The total energies of 4-layer slab Pt_3Re_1 (111) with different vacuum space values have been

calculated, finding that the total energy changes slightly from 9.00 Å, the energy difference between slabs with 14.95 and 9.00 Å of vacuum space is only 0.001 eV, indicating that the top of one slab has essentially no effect on the bottom of the next. Slabs with 3, 4, 5 and 6 atomic layer was tested, finding that the energy difference between 5 and 6 layers is 0.047 eV, the 5 layer slab was chosen considering that offers a considerable physical accuracy in relation to computational cost.

It is important to note that the slab in the Figure **4-2** is a model that represents the surface (111), it has in each layer one atom of Re, and the slab has a configuration A-B-C-A in Z direction, due to the alternative positions of the atoms in each layer. This packing sequence is characteristic of FCC structures and is one of the packing scheme with the highest packing efficiency, allowing to the atoms at intermediate layers have 12 nearest neighbours.

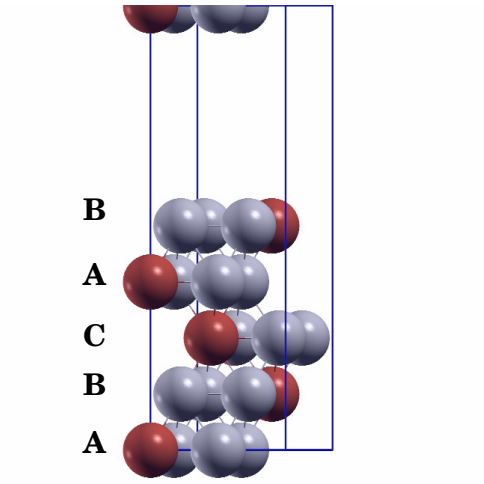

Figure **4-2**: Slab model for Pt_3Re_1 (111) surface. Gray and red spheres represent Pt and Re atoms, respectively.

The arrangement of atoms exposed in the surface depends on the planes along which the crystal can be cleaved, these cutting planes are usually identified by three index which denote the direction of a vector normal to the plane. A representative group of planes for fcc materials are the low-index surfaces (001), (110) and (111), the schemes of the cutting planes in the conventional cell for fcc material are shown in Figure **4-3**.

The three surfaces obtained with these three cutting planes in the Pt_3Re_1 system are shown in Figure **4-4**. These surfaces are all atomically flat, in the sense that every atom on the surface has the same coordination, but have different symmetry and composition. The surface (111) has a composition of 3:1 Pt:Re, while the others two have a composition of 1:1. Additionally, the surface (111) has the highest surface atom densities for fcc crystal structures and is typically the most stable, it is found that this plane represents a significant fraction of the fcc material surface area. For these reasons the surface Pt_3Re_1 (111) was the

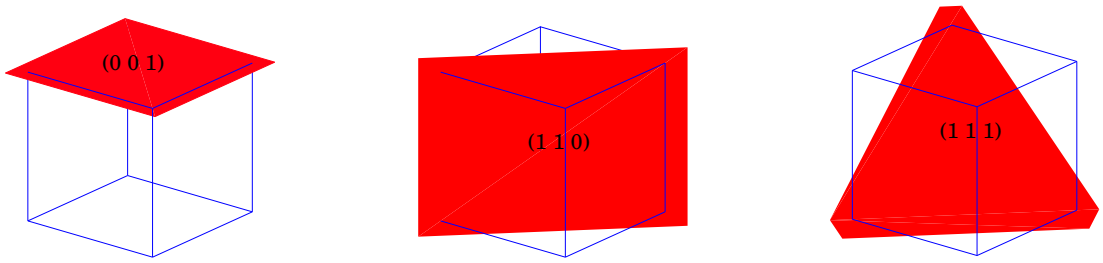

Figure **4-3**: Slab model for Pt_3Re_1 (111) surface. Gray and red spheres represent Pt and Re atoms, respectively.

chosen surface for analysis in this work.

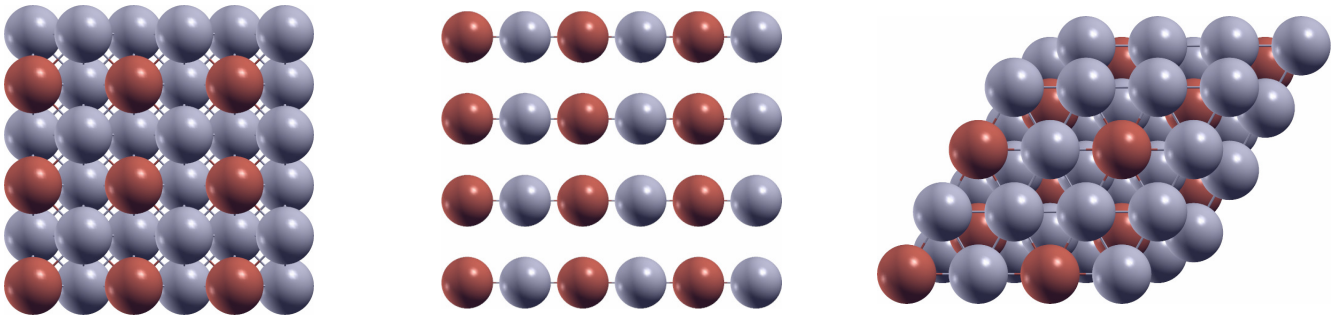

Figure **4-4**: Top views of (a) Pt_3Re_1 (001),(b) Pt_3Re_1 (110),(c) Pt_3Re_1 (111) surface. Gray and red spheres represent Pt and Re atoms, respectively.

4.3 Properties calculation

In order to determine the crystal structure of the systems studied. Lattice constant and bulk modulus are evaluated with total energy DFT calculations of the bulk system at different unit cell volumes, and fitting the DFT data to an analytical expression as the Murnaghan equation of state [208], which is given by:

$$\frac{E(V)}{N} - \frac{E(V_0)}{N} = \frac{B_0 V}{B_0'(B_0'-1)}\left[B_0'\left(1-\frac{V_0}{V}\right)+\left(\frac{V_0}{V}\right)^{B_0'}-1\right] \tag{4-4}$$

V_0 is the unit cell volume at the equilibrium crystal structure, E is the total energy of the solid, N the number of atoms in the crystal and B_0 is the bulk modulus. Also, the cohesive energy, which is a central property of solids, defined as the energy required to pull out the atoms of the solid into isolated atomic species, is determined as follows [209]:

$$E^{coh} = -\sum_i E(V_0) - Eatom_i \tag{4-5}$$

where $Eatom_i$ is the energy of each isolated atom that belongs to the crystal unit cell. The calculations of an isolated atom involve definition of large, empty supercell with just single atom inside. These properties are compared with available data from the literature in order to verify the adequate representation of the system, and proceed with the construction of the slabs, representing the surfaces studied.

As mentioned above, the activity of the metallic surface can be estimated using the adsorption energies of CH, CO and CHCO. The adsorption energy is calculated as the total energy of the slab with the i-specie adsorbed $E_{i/s}$ minus the total energy of clean slab E_s and the energy of the i-specie in gas phase E_i.

$$E_{ads-i} = E_{i/s} - E_s - Ei \tag{4-6}$$

The adsorption energies allow to estimate the activation energy using linear scaling relations. In this work is used the transition state scaling relationship developed by Mavrikakis et al. to calculate the activation energies for CHCO dissociation to CH and CO on Pt(111), Re(0001) and $Pt_3Re_1(111)$.

$$E_{TS} = \alpha E_P + \beta \quad with \;\; \alpha = 0.88eV \; and \; \beta = 1.07eV \tag{4-7}$$

E_{TS} is the energy of the transition state relative to the initial state gas-phase species (that is CHCO species in gas phase) and the clean slab E_s. And E_P is the energy of the final state (products) with the same reference, then for the C-C bond cleavage reaction 4-1 E_P can be write as follows

$$E_P = E_{CO/s} + E_{CH/s} - 2E_s - E_{CHCO} \tag{4-8}$$

This equation can be written in terms of the adsorption energy of CH and CO. Adding and subtracting the energy of the products molecules in gas phase (E_{CH} and E_{CO}), the equation above can be rewritten as

$$\begin{aligned} E_P &= \overbrace{(E_{CO/s} - E_s - E_{CO})}^{E_{ads-CO}} + \overbrace{(E_{CH/s} - E_s - E_{CH})}^{E_{ads-CH}} + \overbrace{(E_{CH} + E_{CO} - E_{CHCO})}^{E_{diss(g)}} \\ &= E_{ads-CO} + E_{ads-CH} + E_{diss(g)} \end{aligned} \tag{4-9}$$

This expression can be seen as the necessary energy to transform the CHCO in gas phase in adsorbed CH and CO. First, the molecule is dissociated, then the CH and CO are adsorbed on the surface. Finally the activation energy E_a is calculated as the difference between the transition state E_{TS} and the initial state (reactants) E_R (in this case CHCO adsorbed), both are expressed relative to the initial state gas-phase species (that is CHCO specie in gas phase).

$$E_a = E_{TS} - E_{ads-CHCO} = \big(\alpha(E_{ads-CO} + E_{ads-CH} + E_{diss(g)}) + \beta\big) - E_{ads-CHCO} \tag{4-10}$$

The above equation states that the activation energy for the reaction studied depends on the adsorption energies of the products, if those are higher (more negative) the activation energy is lower. Also, depends on the bond energy of the molecule, if the bond is stronger (more positive) the activation energy is higher.

Additionally, the adsorption was analyzed in terms of the electronic structure using the d-band model for transition metals which states that the adsorption energy is mainly determined by the interaction of the molecular electronic states with the metal d-electrons. And the center of the d-band of clean surface (the energy-weighted average of the density of d-electrons) can be used to characterize the strength of the adsorption. In general, sites on metals with a higher d-band center respect to the Fermi level bind the molecules more strongly than similar sites on metals with a lower d-band center. The d-band center was calculated as follows:

$$\epsilon_d = \frac{\int_{-\infty}^{\infty} n_d(E) E \mathrm{d}E}{\int_{-\infty}^{\infty} n_d(E) \mathrm{d}E} \tag{4-11}$$

$n_d(E)$ is the projected density of states of the surface atoms d-electrons, the used integration limits were the energy of minimum energy state and the energy of maximum energy state. This model allows to predict qualitative trends in the adsorption energy for metallic surfaces by verifying the clean surface d-band center.

4.4 Computational details

The energetic properties of the systems studied are calculated solving the Khon-Sham equations presented in the previous chapter, these calculations are performed with Quantum Espresso package, which is based on plane waves and pseudopotentials [210]. The exchange correlation functional used for the DFT calculations is the Generalized Gradient Approximation (GGA) by Perdew and Wang (PW91) [199], which is chosen among three different functionals available in the electronic libraries for the atoms considered. The other functionals tested were the local density approximation (LDA) Perdew-Wang (PW) [198], and the GGA Perdew, Burke and Ernzerhof (PBE) [200].

It is found that the PW LDA functional overestimates the binding of the systems, hence overestimates the cohesion energy and the bulk moduli of the metals studied, although the lattice constant and lengths in the system are estimated with high accuracy [94, 211, 212]. The GGA approximations (PBE and PW91) give a better description of binding properties, hence the bulk moduli and cohesive energy are lowered respect to LDA functional.

But the lattice parameter and lengths in the system are overestimated [94, 211, 212]. The energetic description is quite similar for both GGA functionals, PW91 and PBE, but with PBE functional is estimated a lattice constant slightly higher than with PW91 functional. Then the PW91 is chosen for the slightly better description of the geometry of the bulk system. Also, it has been reported that these two GGA functionals give similar values for molecular bond energies in different small molecules [213] and similar chemisorption energies [211] although they are not equivalent [213].

The basis set implemented by Quantum espresso are plane waves, and the core-electrons are represented using ultrasoft pseudopotentials developed by Vanderbilt. Also, in numerical calculations there is always a trade-off between accuracy and computational resources spent on solving given problem. In order to make optimal choice is performed several tests, in this way was determined the minimal (associated computational effort) value for given parameter that will not affect the accuracy in the calculation of relevant system property such as total energy. Some of the most important parameters are the k-mesh and the energy cut-off for the plane waves expansion. The first one set up the fineness of the k-grid used for Brillouin zone sampling using the scheme Monkhorst-Pack. The second one is related with the basis set used to describe the ground state wavefunction for the system, in this case is a plane-wave function, this value define that the plane waves with kinetic energy smaller than this cutoff energy are taken into account. Convergence tests respect to this two parameters can be seen in Anexo A, particularly in Figures **A-1** and **A-2**.

In this work are used a value of 550 eV for the energy cut-off for the plane waves and an scheme 3x3x3 k-mesh for the bulk system and 3x3x1 for the surface system. That is because the first Brillouin zone of a surface in the slab approach is flat, then it is sufficient to choose a two-dimensional mesh. A denser grids of 6x6x6 and 6x6x1 are used for electronic properties calculation (e.g DOS). In order to find the minimum energy geometry, the structure was relaxed without symmetry constraints until the force was less than 0.03 eV/a.u., the total energy of the optimized structures is used to calculate the different properties of the system.

Chapter 5

Results and Discussion

5.1 Crystal structure and physical properties of bulk system

Different properties for this system are calculated and compared with available data from the literature. The Table **5-1** shows the experimental values and the data obtained with DFT calculations. Comparison between experimental and calculated values shows an overall reasonable agreement in terms of lattice constants, structure, bulk moduli and cohesive energy. The lattice constants calculated are very close to the experimental value, considering the obtained relative errors of 1.93 %, 0.18 % and 1.85 % for Pt, Re and Pt_3Re_1 respectively. Similarly the bulk modulus are relatively close to the experimental value, considering the relative errors of 12.6 % and 0.54 % for Pt and Re respectively. The most notable discrepancy is the larger cohesive energy of Re hcp structure (by over 40 %), it can be attributed to the poor description of this property in transition metals with half filled d-orbitals (5, 6 and 7 valence electrons) by the spin-restricted calculations. The contribution to the energy of spin polarized electrons in these metals is more important since they can have 5 or 6 spin polarized electrons, the energy difference between spin polarized and spin restricted energy for these metals ranges from 3.0 to 5.4 eV [214].

Experimental data of cohesive energy and bulk modulus of Pt_3Re_1 is not found, but the results are reasonable in relation to the pure Pt and Re metals, since bulk modulus and cohesive energy is between the values reported for the pure systems. Comparing results of pure Pt, pure Re and Pt_3Re_1 alloy, it is observed that addition of rhenium to platinum leads to a shorter lattice parameter, higher cohesive energy and higher bulk modulus in the alloy compared with pure Pt. Suggesting that Pt-Re binding is stronger than Pt-Pt in agreement

with previous experimental work [26].

Table **5-1**: Comparison of the properties of Pt, Re and Pt_3Re_1 obtained in the present work and the experimental values [8] [9]

Property	**Pt (fcc)**			**Re (hcp)**			**Pt_3Re_1 (fcc)**		
	DFT	Exp.	% Err.	DFT	Exp.	% Err.	DFT	Exp.	% Err.
lattice constant a_0 [Å]	4.000	3.924	1.93	2.766	2.761	0.18	3.967	3.895	1.85
c/a_0	—	—	—	1.605	1.605	—	—	—	—
$E^{coh}[eV/atom]$	-5.91	-5.84	1.20	-11.40	-8.03	42	-7.11	—	—
$B_0[GPa]$	243	278	12.6	370	372	0.54	296	—	—

Also, it should be pointed out that physical properties of Pt_3Re_1 are not found. Then, this work is among the first in estimate the physical properties and the crystalline structure from first-principles, and it is expected that experimental or other theoretical studies be done in order to contrast the results obtained in this work. The bulk system study is the first step to the construction of the Pt_3Re_1 surface-molecule system, which allows to describe the C-C bond cleavage in this alloy.

5.2 Adsorption of molecules

Pt_3Re_1 exhibits several sites with special symmetry that are of interest as probable binding sites, which are illustrated in the Figure **5-1**. The sites on Pt and Re atoms, namely atop sites (A-Pt and A-Re). Sites between Pt and Re atoms or two Pt atoms, namely bridge sites (B-Re and B-Pt). Sites among Re and two Pt atoms or among three Pt atoms with an atom directly below in the subsequent layer, which are called HCP hollow sites (HCP-Re and HCP-Pt). And the site among Re and two Pt atoms or among three Pt atoms without atom in the subsequent layer but with an atom directly below the site two layers further down, namely FCC hollow sites (FCC-Re and FCC-Pt). Adsorption on all these sites is tested.

Pt(111) exhibits sites similar to those found in Pt_3Re_1, but as only a metal type is present, then only exhibit one atop site, one bridge site and two hollow sites (FCC and HCP site). Re(0001) exhibits the same sites but the denominated FCC hollow site is different, since there is no atoms directly below this site in Re(0001), that is because Re has an hexagonal close packed structure (HCP).

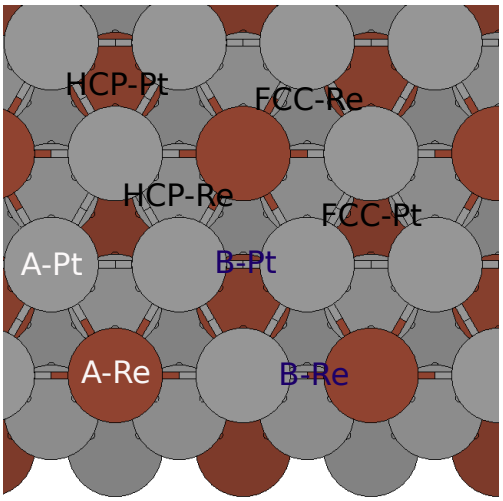

Figure **5-1**: Top view of slab model for Pt_3Re_1 (1 1 1) surface and the different surface sites: atop, bridge, HCP hollow and FCC hollow. Gray and red spheres represent Pt and Re atoms, respectively.

5.2.1 CO adsorption

CO is a product of C-C cleavage in CHCO molecule, so binding energies for CO can be used to calculate activation energies for the C-C bond cleavage step. Also CO is a poison for Pt based catalysts for EtOH oxidation, so it is important the study of CO adsorption for understanding of Pt_3Re_1 activity for the complete decomposition of EtOH.

CO adsorption on Pt_3Re_1(111). Different initial geometries for CO are tested, these involve the different sites: atop, bridge and hollow sites shown in Figure **5-1**, and different orientations of the molecule respect to the surface. The most stable adsorption configurations on Pt_3Re_1 is the linear atop bonded CO with C atom forming a bond with the Re (A-Re) atom, this configuration is shown in Figure **5-2**, and it is in agreement with the experimental findings for Pt based surfaces, which point out that CO molecule is chemisorbed with its molecular axis normal to the surface and its carbon end closer to metal atom [215].

When the CO is adsorbed the C-O bond is slightly stretched from 1.14 to 1.17 Å, carbon atom forms a bond with rhenium atoms, whose bond length (d_{M-A}) is 1.89 Å, also the obtained adsorption energy (E_{ads}) is -2.43 eV. These geometrical parameters are illustrated in Figure **5-2** and are reported in table **5-2** along with adsorption energies. The CO adsorption on Pt atoms also is tested, it is obtained similar geometrical configuration. CO is adsorbed with its axis normal to the surface and with the carbon atom forming a bond with Pt, whose length (d_{M-A}) is also 1.89 Å, the C-O bond is similarly stretched from 1.14 to 1.16 Å, but the obtained adsorption energy is -1.14 eV.

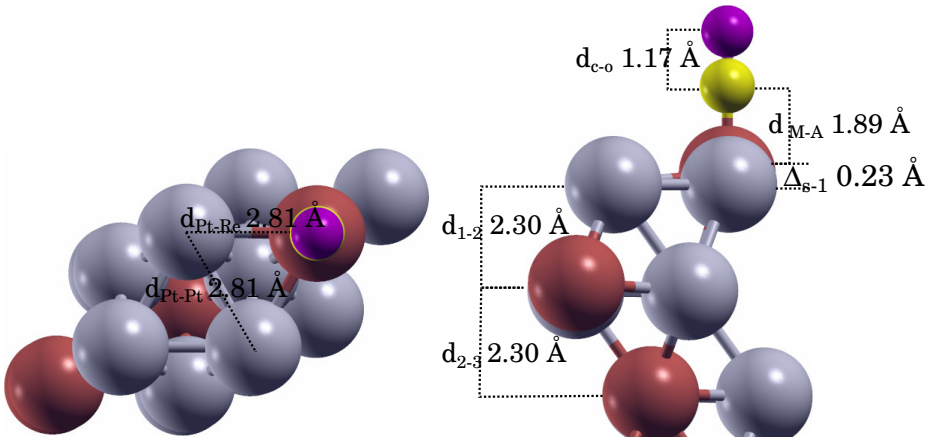

Figure **5-2**: Top and side view of CO adsorption on Pt_3Re_1 surface in the atop-Re site. Gray and red spheres represent Pt and Re atoms. Yellow and purple spheres represent C and O atoms.

These results indicates that CO adsorption on A-Re site is stronger than on A-Pt, consequently the C-O bond length is longer on A-Re, indicating that CO molecule is more destabilized when adsorbs on A-Re site. It is in agreement with theoretical and experimental findings, DFT calculations by Ishikawa et al. [216] and Greeley and Mavrikakis [217] results in a CO binding energy reduced in the cases of Pt-Re clusters or near surface alloys when CO binds to Pt. Experimental works using X-ray photoelectron spectroscopy point out that Pt-CO binding is weakened in the PtRe alloy surface, while the Re-CO bond is strengthened with the presence of Pt [218, 219].

CO adsorption on Pt(111). It is found that the most stable configuration for CO on Pt(111) is at bridge site with CO molecular axis normal to the surface and its carbon end closer to the surface. Geometrical parameters of the adsorption configuration, such as the bond length between surface metal and the adsorbate d_{M-A} and the C-O bond length (d_{C-O}), are shown in Table **5-2**. Carbon atoms form a bond with two Pt atoms, whose bond length is 2.03 Å, which implies that the vertical distance from carbon atom to the surface is 1.47 Å, these values are lower than the reported experimental values, 2.08 Å and 1.55 Å [220]. Also, d_{C-O} is stretched from 1.14 Å to 1.18 Å, which is higher than the experimental one of 1.15 Å [220]. The calculated geometrical parameters d_{M-A} and d_{C-O} are very close to the experimental values as it is reflected by the relative errors of 2.15 % and 2.47 %, which indicates that the geometrical configuration is well described with the approach used.

The adsorption energy calculated (E_{ads}), also reported in Table **5-2**, is -1.86 eV. This value is higher than the experimental values, which range form -1.24 to -1.66 eV [221, 222, 223, 224, 225, 226]. As can be seen in Table **5-2** the calculated values are similar to other DFT calculations, for instance Pedersen et al. [227] obtained a value of -1.80 eV which is very close to the obtained in this work. These results indicates that the CO adsorption energy

on bridge site calculated using DFT is overestimated, leading to predict a preferred site for CO adsorption different to the atop site reported in experimental studies [228, 229, 230, 231]. This difficulty of DFT to achieve the correct prediction of the preferred adsorption site has been discussed by other authors. It is pointed out that DFT calculations using LDA or GGA (PBE, RPBE, PW91) functionals lead to overestimate the adsorption energy for CO on high-coordination sites (bridge and hollow sites) [232].

Different approaches have been proposed to obtain accurate adsorption energies for CO on transition metals, such as: Using GGA+U functional for restoring the correct prediction of the preferred site on Pt (111), however the value of U is not known a priori [233]. Using all electron relativistic calculations, which are able to predict the correct accurate CO adsorption energy [234, 235]. Using random phase approximation to the correlation energy, which leads to obtain accurate adsorption energies for CO on transition metals [236]. And correcting the adsorption energy with an expression which involves the frequency of the CO adsorbed stretch mode [237,238]. With the later proposal Pedersen and Andersson [227] calculated the CO adsorption energy on a variety of metals, showing that the adsorption energy on atop site require the smallest correction (less than 0.2 eV). These findings indicate that the calculated energy adsorption for the atop site could be considerably close to the experimental results. So, in this work would be considered the adsorption at atop site to posterior calculations and analysis.

The adsorption energy of CO on the atop site obtained is -1.68 eV, which is close to the experimental value of -1.66 eV reported by Yeo et al. [225] for a CO coverage (θ) that ranges from 0.17 to 0.33, as reflected by the relative error of 1.19 %. Other experimental results range from -1.24 to -1.66 eV [221, 222, 223, 224, 226]. The distance d_{M-A} and d_{C-O} obtained are 1.86 and 1.15 Å respectively, which are in agreement with the experimental ones of 1.85 and 1.15 Å [220], as is reflected by the relative error of 0.48 % and 0.78 % for d_{M-A} and d_{C-O} respectively.

CO adsorption on Re(0001). The most stable configuration for CO adsorption on Re(0001) is at the atop site with with C atom forming a bond with Re, this configuration is the same as the reported in experimental studies [247, 248, 249]. The distance d_{M-A} is 1.96 Å, and d_{C-O} is stretched from 1.14 to 1.17 Å, which are the same values reported by Hahn and Mavrikakis in their DFT study [246]. The E_{ads} is -1.91 eV, which is similar to the values calculated in other theoretical works [227, 246], for instance Pedersen et al. [227] reports a value of -1.97 eV.

Comparing the CO adsorption for pure metal surfaces, it can be noted that CO adsorption on Re(0001) surface is stronger than Pt(111), since the adsorption energy and the stretching of C-O bond is higher for Re(0001) surface. Suggesting a stronger chemical bond between

Table **5-2**: Adsorption energies E_ads and geometrical parameters, d_{C-O} and d_{M-A} for CO adsorption on the different surfaces studied. CO bond length d_{C-O} in gas phase is 1.14 Å

Surface	Site	E_{ads} [eV]		d_{C-O} [Å]		d_{M-A} [Å]	
		This work	Other works	This work	Other works	This work	Other works
Pt(111)	atop	-1.68	-1.66[e1], -1.43[e2]	1.15	1.15[e3]	1.86	1.85[e3]
			-1.67[t1], -1.59[t2]		1.15[t3], 1.16[t4]		1.84[t4], 1.85[t5]
	bridge	-1.86	-1.61[t6], -1.80[t7]	1.18	1.15[e3], 1.18[t6]	2.03	2.08[e3], 2.04[t6]
Re(0001)	atop	-1.91	-1.17[e4], -1.24[e5]	1.17	1.17[t8]	1.96	1.96[t8]
			-1.97[t7], -2.02[t8]				
$Pt_3Re_1(111)$	atop-Re	-2.43	—	1.17	—	1.89	—
	atop-Pt	-1.14	—	1.16	—	1.89	—

*e*1: Experimental study [225] *e*2: Experimental study [226] *e*3: Experimental study [220] *e*4: Experimental study [239]

*e*5: Experimental study [240] *t*1: Theoretical study [241] *t*2: Theoretical study [242] *t*3: Theoretical study [243]

*t*4: Theoretical study [244] *t*5: Theoretical study [245] *t*6: Theoretical study [235] *t*7: Theoretical study [227]

*t*8: Theoretical study [246]

the adsorbate and rhenium, hence a higher reactivity of rhenium material. It is in agreement with the experimental studies, which report that Re can form a strong CO-metal complex, which eventually leads to dissociate the C-O bond, it is more likely in atoms with low coordination (with less neighbor atoms) [240]. But CO does not dissociates on Pt [223, 228], in general transition metals that are able to dissociate CO lie to the left of the periodic table (from group 8 to the left) [240]. However it can affect negatively the activity, since the surface would be blocked by strongly adsorbed CO. This negative aspect could be overcome if these molecules react with oxidant species that help to remove the strongly adsorbed species, precisely other theoretical [163] and experimental works [25, 55] show that Re promotes the water activation producing OH species which can react with CO to form CO_2.

Comparing the CO adsorption for the alloy and pure metal surfaces, it is noted that addition of Re to the Pt surface leads to higher adsorption energy on Re sites and lower adsorption energy on Pt sites than on the pure metals. Suggesting that the bonding of Pt with Re decreases the ability of Pt for interacting with CO, and increases the reactivity of Re, it could be attributed to a rehybridization of Pt d-states to s-p states, as is proposed in other works [219].

Surface deformation on CO adsorption. It is quantified by the vertical and horizontal displacements respect to the clean slab. In the horizontal direction, the Pt-Pt Re-Re and Pt-Re bond lengths (d_{Pt-Pt}, d_{Re-Re} and d_{Pt-Re}) in the respective surfaces after adsorption are similar to those in clean slab (2.81 Å), as can be seen in Figure **5-2** for adsorption on Pt_3Re_1. Then the difference between these lengths after adsorption and in the clean slab (Δ_{M-M}

and Δ_{Pt-Re}) are close to zero, as is reported in Table **5-2**. In the vertical direction, the distance between top layers (1) and the layer immediately below (2) (d_{1-2}) is quantified, the difference in this distance respect to clean slab (Δ_{1-2}) is reported in Table 2. Also, after adsorption, the site on which the molecule is adsorbed is repositioned respect to other atoms in the top layer, the difference in the height of the site respect to the height of the top layer (Δ_{s-1}) after adsorption also is reported in Table 2.

It is found that the interlayer distances d_{1-2} is slightly modified, for instance, for CO adsorption on Pt Δ_{1-2} is 0.05 Å, which is in agreement with the reported expansion of the topmost Pt atomic layer of 0.05 Å [250, 251], indicating that the surface is relaxed after CO adsorption. The position of the adsorption site respect the top layer is significantly modified, the atoms in the site move out of the surface towards the adsorbate. It can be expected in any adsorption process with a preferred adsorption site, and can be attributed to the weakening of bond between surfaces atoms when the molecule approaches to surface. The adsorbate induces an electron density redistribution in the surface which is partly relocated between the surface and the molecule [175]. Δ_{s-1} ranges from 0.19 to 0.24 Å, the value for Re (0.19 Å) is close to the values of 0.15 Å reported in other theoretical work [246]. For the alloy are obtained values slightly higher, suggesting that the electron redistribution in this surface is more pronounced.

These results, which are summarized in Table **5-3**, indicate that the alloy structure is not reconstructed, since formation of new bonds between metal surface atoms does not take place. But the CO adsorption induces a relaxation in the surface, modifying slightly the interlayer distances, and moving out the atoms at adsorption site towards the adsorbate, as can be expected in any adsorption process [251].

Table **5-3**: Geometric parameters of different surfaces after the CO adsorption. Δ_{M-M}, Δ_{Pt-Re} and Δ_{1-2} are the differences respect to clean slab. Δ positive represents an increment in the respective distance. Δ_{s-1} is the difference between the vertical positions of site and top layer. At the end of the table is reported the distances in the clean slab.

Surface	Site	Δ_{M-M} [Å]	Δ_{Pt-Re} [Å]	Δ_{1-2} [Å]	Δ_{s-1} [Å]
Pt(111)	atop	0	—	0.05	0.19
Re(0001)	atop	0	—	0.01	0.19
Pt_3Re_1	atop-Re	0	0	0.05	0.23
	atop-Pt	0.01	0.01	0.03	0.24
		Clean Slab			
		d_{M-M} [Å]	d_{Pt-Re} [Å]	d_{1-2} [Å]	
Pt(111)		2.83	—	2.34	
Re(0001)		2.77	—	2.11	
Pt_3Re_1		2.81	2.81	2.25	

5.2.2 CH adsorption

CH adsorption on Pt_3Re_1. CH adsorption is tested on the different sites at surface, obtaining that the minimum energy configuration is at hollow sites with a rhenium atom (HCP-Re, FCC-Re) and with the molecular axis of CH normal to the surface and the carbon atom closer to the surface, as can be seen in Figure **5-3**. This configuration is the same as for other theoretical studies of CH adsorption on metallic alloys [157, 252] and transition metal surfaces, such as Re(0001) [246], Pt(111) [253, 254], Ru(0001) [255], Ni(111) [256], Pd(111) [257].

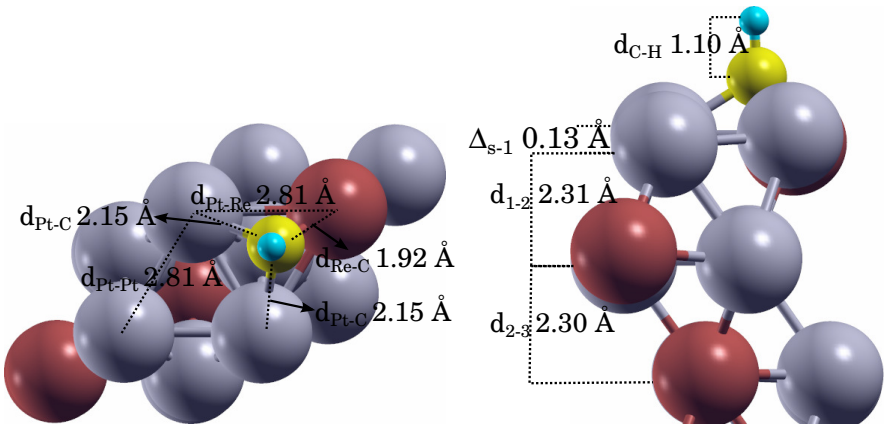

Figure **5-3**: Top and side view of CH adsorption on Pt_3Re_1 surface in the HCP-Re site. Gray and red spheres represent Pt and Re atoms. Yellow and cyan spheres represent C and H atoms

The adsorption in the hollow-Re sites, FCC-Re and HCP-Re, present similar geometrical parameters and adsorption energy (energy is different only by 0.02 eV). Table **5-4** presents the geometrical parameters and adsorption energy, it is obtained that Re-C distance d_{Re-C} (1.92 Å) is shorter than the Pt-C distance d_{Pt-C} (2.15 Å), which suggests that Re interacts more strongly with the CH molecule. The C-H bond length (d_{C-H}) is slightly shortened from 1.13 Å to 1.10 Å, and the E_{ads} is -7.40 eV. This value is similar to the values obtained in other theoretical works for CH adsorption on pure transition metal and alloys, which range from -6.00 eV to - 8.00 eV. For instance, Curtuois et al. [157] calculated for Re-Ir and Pt-Ir ovelayer alloys a value of -7.25 and -6.09 eV.

Also for CH adsorption on HCP-Pt is found a geometrical parameters similar to hollow-Re sites, d_{C-H} is 1.10 and Pt-C distance 2.03 Å. But the adsorption energy is -5.91 eV, which is significantly lower than the obtained for hollow-Re sites. this result confirms that the interaction of CH with Re atoms is stronger than with Pt atoms in the Pt_3Re_1 surface.

CH adsorption on Pt(111) and Re(0001) the most stable configuration for the adsorption on pure surfaces also is at the hollow sites, for the HCP site in Pt(111) surface is found

Table **5-4**: Adsorption energies E_ads and geometrical parameters, d_{C-H} and d_{M-A} for CH adsorption on the different surfaces studied. The calculated CH bond length d_{C-H} in gas phase is 1.13 Å. For HCP-Re site in $Pt_3Re_1(111)$ is reported two d_{M-A} values, the first corresponds to Pt-C length and the second to Re-C length.

Surface	Site	E_{ads} [eV]		d_{C-H} [Å]		d_{M-A} [Å]	
			Other works		Other works		Other works
Pt(111)	HCP	-7.18	-7.15^{t1}, -7.22^{t2}	1.10	1.10^{t1}	2.01	2.02^{t1}, 1.95$t2$
Re(0001)	HCP	-7.66	-6.89^{t3}	1.10	1.10^{t3}	2.06	2.03^{t3}
$Pt_3Re_1(111)$	HCP-Re	-7.40	—	1.10	—	2.15, 1.92^{Re}	—
	HCP-Pt	-5.91	—	1.10	—	2.03	—

$t1$: Theoretical study [254] $t2$: Theoretical study [258] $t3$: Theoretical study [246] Re: Re-C bond length

a d_{Pt-C} distance of 2.01 Å, a d_{C-H} of 1.10 Å and an energy adsorption of -7.18 eV. And for FCC Re(0001) site is found similar geometrical parameters, d_{Re-C} distance of 2.06 Å, a d_{C-H} also is 1.10 Å, but the adsorption energy is -7.66 eV. which is 0.48 eV higher than Pt(111), suggesting that the electronic interaction of CH with Re is stronger than with Pt. These results are similar to other theoretical works for instance in [254] reports an adsorption energy of -7.15 eV, a d_{C-H} of 1.10 Å and d_{Pt-C} of 2.02 Å.

The results for CH adsorption indicate that the interaction of CH with Re atoms is stronger than Pt atoms. The adsorption energy is higher on Re(0001) than Pt(111) and adsorption energy on Pt_3Re_1 is higher if Re atom is present in the adsorption site. So the adsorption on HCP-Re site (with one Re atom) is higher than the adsorption on HCP-Pt (without Re atoms). Also, when CH adsorbs on hollow-Re sites in Pt_3Re_1, the carbon atom is closer to the rhenium atom than to the Pt atom. Furthermore it is remarkable that the addition of Re to Pt surface leads to a lower adsorption energy on hollow-Pt sites compared with the hollow site in Pt(111) surface. Reinforcing the idea that the bonding of Pt with Re decreases the ability of Pt for interacting with the molecules (CH and CO).

Surface deformation after CH adsorption. As can be seen in Table **5-4** the surface is deformed after CH adsorption, it is evidenced in the increment of interlayer distance, Δ_{1-2} is around 0.06 Å for all surfaces when CH adsorbs on HCP site. Deformation is more noticeable in the change of position of the adsorption site respect the top layer, it is moved out toward the molecule. If CH is adsorbed on HCP site in Pt(111) surface (Δ_{s-1}), the metal atoms at the site are 0.19 Å higher up, while for Re(0001) is only 0.07 Å. This suggests that the charge redistribution induced by the formation of new bonds has a considerable effect for Pt atoms, weakening the bond of these atoms with the subsequent layer atoms. For Pt_3Re_1 Δ_{s-1} for HCP-Pt site is 0.27, whereas for HCP-Re site is 0.13 Å, which follows a trend similar to the found in pure metals, for Pt the effect is more considerable. Also, these values are slightly

higher than in pure metals, suggesting that the electron redistribution in the alloy surface is more pronounced.

Table **5-5**: Geometric parameters of different surfaces after the CH adsorption. Δ_{M-M}, Δ_{Pt-Re} and Δ_{1-2} are the differences respect to clean slab. Δ positive represents an increment in the respective distance. Δ_{s-1} is the difference between the vertical positions of site and top layer.

Surface	Site	Δ_{M-M} [Å]	Δ_{Pt-Re} [Å]	Δ_{1-2} [Å]	Δ_{s-1} [Å]
Pt(111)	HCP	-0.02	—	0.07	0.19
Re(0001)	HCP	0	—	0.05	0.07
Pt_3Re_1	HCP-Re	0	0	0.06	0.13
	HCP-Pt	0	0.01	0.10	0.27

5.2.3 CHCO adsorption

CHCO adsorption on Pt_3Re_1. CHCO is the intermediate molecule of ethanol decomposition, in which C-C cleavage is likely to occur [47, 154, 156, 158]. The most stable adsorption configuration on Pt_3Re_1 is shown in Figure **5-4**. In this geometry the CH is located in a bridge-like position between Re and Pt atom (B-Re), whereas the CO is located close to a Pt atom in a Pt-atop-like position. For both groups, the C atom is closer to the surface. This configuration is similar to the found in other theoretical studies for transition metals [47,158] and metallic alloys [157].

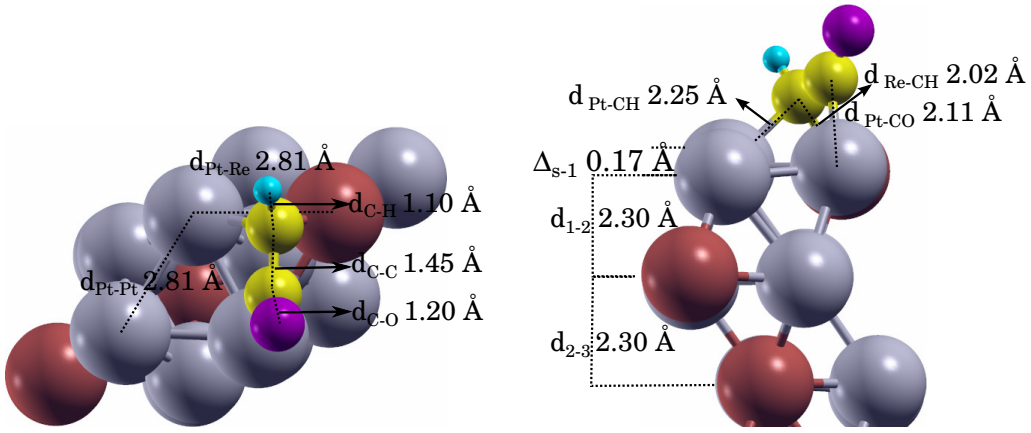

Figure **5-4**: Top and side view of CHCO adsorption on Pt_3Re_1 surface. Gray and red spheres represent Pt and Re atoms. Yellow, purple and cyan spheres represent C, O and H atoms

As can be observed in Table **5-6**, it is found that the bond length between Pt and CO group of the molecule is 2.11 Å (d_{Pt-CO}), and the CH group at B-Re site is located at a distance of 2.25 Å from Pt (d_{Pt-CH}) and 2.02 Å from Re (d_{Re-CH}). The C-H bond is slightly stretched

from 1.07 Å to 1.10 Å, the CO bond length is 1.20 Å, which is the same as in gas phase, and C-C bond length is significantly stretched from 1.26 Å to 1.45 Å. Also, the E_{ads} is -3.97 eV, this value is similar to the obtained in other theoretical works for CHCO adsorption on pure transition metal and alloys, whose range is between -3.00 eV and -6.00 eV. For instance, Curtuois et al. [157] calculated for Re-Ir and Pt-Ir ovelayer alloys a value of -4.26 and -3.15 eV.

Initial configurations close to Pt atoms and FCC-Pt site (and far of the sites with Re atoms) converge to a configuration, where only the carbon atom linked to the hydrogen atom is bound to the surface, whereas the carbon atom linked to oxygen is far from the surface. Then the molecule forms an angle of approximately 45 degrees with the surface. The adsorption energy for that configuration is -2.69 eV, which indicates that the interaction between this sites and CHCO is lower than those sites where Re atom is present. A similar configuration is found in other theoretical work for Ir-Au alloys whit Au exposed in the surface, to which is reported an E_{ads} of -2.24 eV [157]. It is interesting that the sites that involves only Pt atoms show a behavior similar to a noble metal alloy.

Table **5-6**: Adsorption energies E_{ads} and geometrical parameters, d_{C-H}, d_{C-C}, d_{C-O}, d_{M-CH} and d_{M-CO} for the CHCO adsorption on the different surfaces studied. The calculated d_{C-H}, d_{C-C} and d_{C-O} in gas phase are 1.07, 1.26 and 1.20 Å

Surface	Site	E_{ads} [eV]		d_{C-H}, d_{C-H}, d_{C-O} [Å]		d_{M-CH}, d_{M-CO} [Å]	
			Other works		Other works		Other works
Pt(111)	bridge-CH atop-CO	-3.97	-4.15[t1]	1.10, 1.45, 1.20	1.10, 1.45, 1.21[t2]	2.08, 2.05	2.08, 2.06[t2]
Re(0001)	HCP-CH FCC-CO	-4.51	—	1.10, 1.43, 1.28	—	2.22, 2.21	—
$Pt_3Re_1(111)$	(B-Re)-CH (A-Pt)-CO	-3.97	—	1.10, 1.45, 1.20	—	2.25, 2.02[Re], 2.11	—

*t*1: Theoretical study [157] *t*2: Theoretical study [158] Re: Re-CH bond length

CHCO adsorption on Pt(111) and Re(0001) The most stable configuration for CHCO adsorption on Pt(111) surface is similar to that found on Pt_3Re_1, with CH located in a bridge position and CO located close to an atop position. d_{Pt-CO} and the d_{Pt-CH} are 2.08 and 2.05 Å respectively. The bond lengths in the molecule after adsorption d_{C-H}, d_{C-C}, and d_{C-O} are 1.10, 1.45 and 1.20 Å respectively, indicating that the C-C bond is significantly destabilized after adsorption as well as in Pt_3Re_1. The E_{ads} is -3.97 eV, which is similar to the found for Pt_3Re_1. The values of geometrical parameters are similar to the theoretical values obtained by Alcala et al. [158] for the same system.

The most stable configuration for CHCO adsorption on Re(0001) surface is shown in Figure

5-5, in this configuration CH and CO are located at the hollows site. It is found that the d_{Re-CO} and the d_{Re-CH} are 2.21 Å and 2.22 Å. d_{C-H}, d_{C-C}, and d_{C-O} are 1.10, 1.43 and 1.28 Å respectively, and the E_{ads} is -4.51 eV.

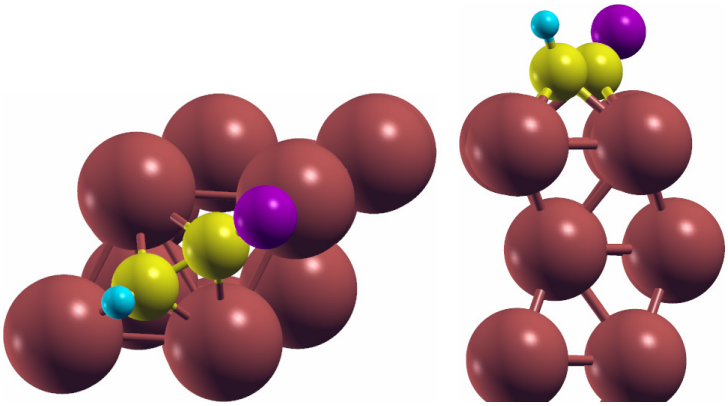

Figure **5-5**: a.) Top and side view of CHCO adsorption on Re surface. red spheres represent Re atoms. Yellow, purple and cyan spheres represent C, O and H atoms

The results of CHCO adsorption on the different surfaces studied indicate that the CHCO molecule requires two adjacent sites, which bind each carbon atom in CHCO molecule and destabilize the C-C bond stretching it by around of 0.18 Å. The bond lengths between carbon atoms and metal atoms in the adsorption of CHCO are similar for Pt(111) and Pt_3Re_1(111) surface, whereas these lengths in Re(0001) are slightly higher due to the different adsorption configuration. Since for Re(0001) CH and CO groups in the CHCO molecule bind hollow sites, while for Pt(111) and Pt_3Re_1(111) CH and CO groups in the CHCO molecule bind a bridge and atop site respectively.

Comparing the adsorption energy of the pure metal surfaces can be noted that the Re(0001) surface shows stronger interaction with CHCO than Pt(111), suggesting that Re atom has higher ability to interact with carbon atom than Pt atoms. Also it is noticed that ensembles with only Pt atoms Pt_3Re_1 surface show a weaker interaction with CHCO than pure metal surfaces, which suggest that the addition of Re decrease the ability of Pt for interacting with CHCO. The ensembles with a Re atom in Pt_3Re_1 surface have an adsorption energy similar to pure Pt surface and lower than Re surface, it can be attributed to a higher ability of Re atom in the Pt_3Re_1 alloy to interact with carbon atoms on the molecule, which should compensate the lower ability of Pt in the alloy for interacting with the carbon atoms in CHCO molecule.

Surface deformation after CHCO adsorption The surfaces are relaxed upon the CHCO adsorption, the displacements respect to clean slab can be seen in Table **5-7**. The surface deformation after CHCO adsorption in the horizontal direction (Δ_{M-M}, Δ_{Pt-Re}) is close to zero for all studied surfaces. The deformation is evidenced in the increment of interlayer

distance between top layer and subsequent layer, Δ_{1-2} is approximately 0.04, 0.05 and 0.06 Å for Re(0001), $Pt_3Re_1(111)$ and Pt(111) respectively. It is more noticeable in the distance between the site on which CHCO is adsorbed and the top layer, for the adsorption on Pt(111) and $Pt_3Re_1(111)$ the metal atoms at the site are 0.18 and 0.17 Å higher up than the topmost layer. For Re(0001) all atoms in surface are attracted towards the molecule, since two hollow sites are involved. But the atoms at site where CO is adsorbed are positioned 0.04 higher up than the atoms at site where CH is adsorbed.

Table **5-7**: Geometric parameters of different surfaces after CHCO adsorption. Δ_{M-M}, Δ_{Pt-Re} and Δ_{1-2} are the differences respect to clean slab. Δ positive represents an increment in the respective distance. Δ_{s-1} is the difference between the vertical positions of site and top layer.

Surface	Site	Δ_{M-M} [Å]	Δ_{Pt-Re} [Å]	Δ_{1-2} [Å]	Δ_{s-1} [Å]
Pt(111)	bridge-CH atop-CO	0	—	0.06	0.18
Re(0001)	HCP-CH FCC-CO	0	—	0.04	0.04
Pt_3Re_1	(B-Re)-CH (A-Pt)-CO	0	0	0.05	0.17

5.2.4 Adsorption trends

Figure **5-6** shows the calculated adsorption energy as a function of the distance between the surface and the molecule (r), the points were obtained from static calculation (without relaxation) and with the molecule located on the preferred adsorption site and oriented in its adsorbed state. This potential energy curve allows scanning the adsorption distance with minimum energy and checking differences for the adsorption on the different surfaces.

It is observed for CO adsorption (Figure **5-6**a) that the shape of the curves is similar for Re(0001) and $Pt_3Re_1(111)$, but these curves differ with Pt(111) curve, since they begin to decrease from higher values of r than Pt(111) curve. It is attributed to the adsorption on different atoms, Re atom (Re and Pt3Re1) and Pt atom. Also it is evidenced that the adsorption on Pt_3Re_1 has the highest adsorption energy, and Pt(111) the lowest. These facts indicate that if Re atom is introduced in Pt, it interacts similarly as in Re(0001) but its ability to interact with CO is increased.

For CH adsorption (Figure **5-6**b) is noted that the shape of the curves is similar for all the surfaces, naturally the adsorption energy and adsorption height are different, Re(0001) presents the highest adsorption energy and Pt(111) the lowest. These facts reflect that the adsorption site is similar for all surfaces (hollow site), and that Re-CH interaction is higher

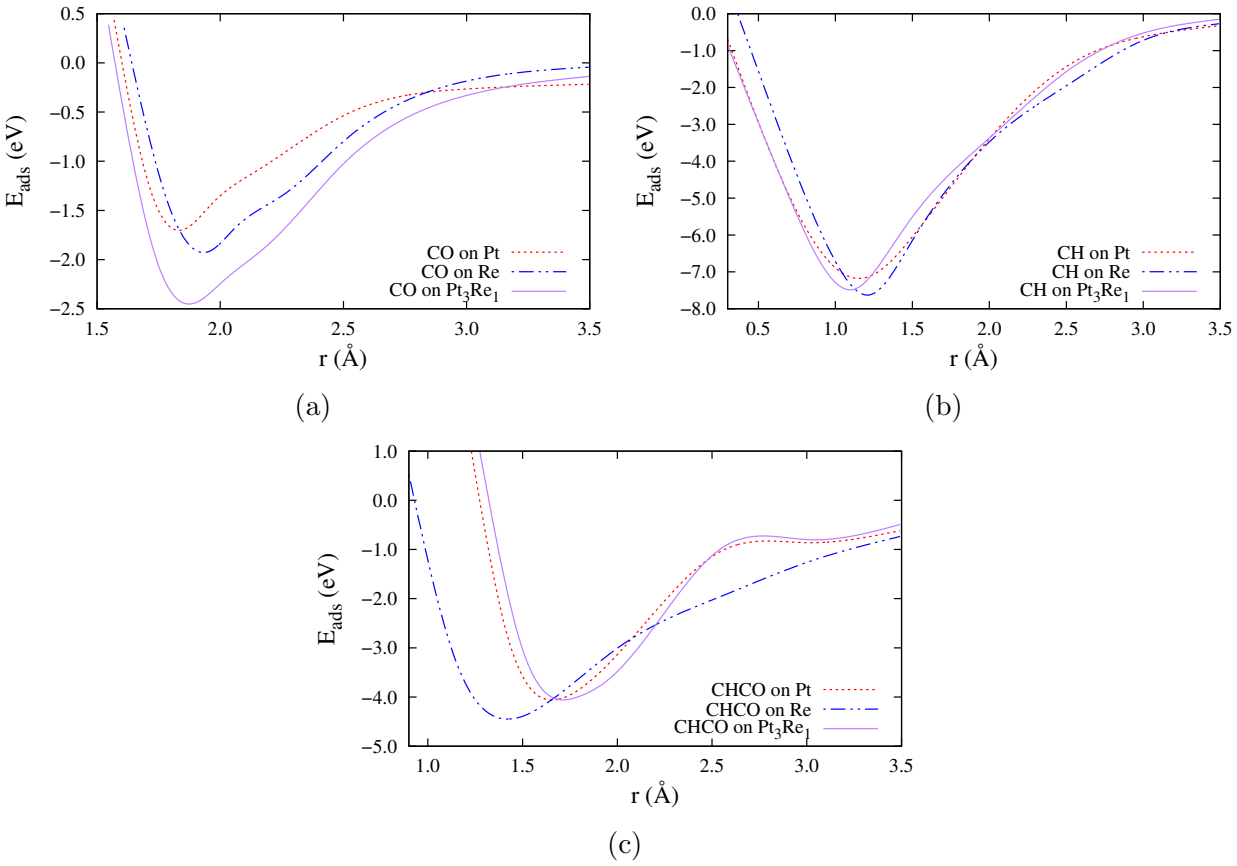

Figure **5-6**: Calculated adsorption energies for the (a) CO, (b) CH and (c) CHCO molecules on Pt (dotted), Re (dot-line) and Pt_3Re_1 (solid line) as function of distance of the distance above the surface (r).

than Pt-CH. Since Pt_3Re_1 (111) has a hollow site with one Re atom and two Pt atoms, its interaction with CH is intermediate respect to Pt and Re surfaces.

For CHCO adsorption (Figure **5-6**c) is noted that the shape of the curves is similar for Pt(111) and Pt_3Re_1(111), but these curves are notoriously different to Re(0001) curve. The adsorption energy is higher for Re(0001) than Pt(111) and Pt_3Re_1(111), which have a similar value. These facts reflect that the adsorption site (and configuration) is similar for Pt and the alloy, and that the mentioned ability to interacts with C atoms of Re is not enough to increase the adsorption energy of CHCO on Pt_3Re_1. This is because of the sites involved in the CHCO adsorption on this alloy, which involves two Pt atoms bonding CO and CH parts, but only a Re atom bonding the CH part. Also, it is remarkable that for Pt and Pt_3Re_1 the energy decrease slightly from 3.5 to 2.5 Å, and decrease more sharply from 2.5 to 1.6 Å. That is due to the orientation of the molecule, which is oblique respect to the surface with the CH closer to the surface than CO, then the interaction with CO is no so significant to higher distances consequently the energy decrease slightly at these distances.

Summarizing, the general trends in the adsorption of molecules show that the Re(0001) surface interacts more strongly with carbon atom in the molecules than Pt(111). Furthermore, it is observed that the addition of Re to Pt surface leads to obtain two active sites with different reactivity. The Re atoms in this alloy has a stronger interaction with the considered molecules than pure metals (Pt and Re), whereas the Pt atoms in this alloy form a weaker bond with CH, CO and CHCO molecules than pure metals. This difference explains the higher CO adsorption energy on Pt_3Re_1 than on pure metals, since CO interacts only with Re atom in the alloy. And the lower CH and CHCO adsorption energy on Pt_3Re_1 than on Re(0001), since these molecules interacts with Pt and Re atoms in Pt_3Re_1. Then the stronger interaction of Re with CH and CHCO compensates the weaker interaction of Pt.

These trends are further studied in terms of the electronic structure of the surface atoms in Pt_3Re_1 alloy and the sites involved in the adsorption of the different molecules, it is found forward in the electronic structure section.

5.3 C-C bond cleavage in CHCO molecule

The activation energies calculated using linear scaling relation (equation 4-10) for each surface are 1.00, 0.91, 0.16 and 1.33 eV for Pt, Re, Rs-sites and Pt sites in Pt_3Re_1 respectively, they are reported in Table **5-8**. These values seem reasonable if are compared with the results obtained using other methods to search the transition state. In a previous work for ethanol decomposition on Pt(111) surface, which uses constrained optimization, was estimated an activation energy of 0.95 eV [158]. For other transition metal surfaces such as Pd(111) [154] and Rh(111) [156] were obtained values of 0.98 and 0.69 eV using linear synchronous transitions (LST) and quadratic synchronous transitions (QST) methods. Pd which is a metal of the same group than Pt has similar activation energy, and Rh reported to be more effective cleaving the C-C bond, has lower activation energy.

Table **5-8**: Calculated activation energies for each surface.

Surface		E_a(eV)
Pt(111)		1.00
Re(0001)		0.91
Pt_3Re_1	Pt	1.33
	Re	0.16

It can be seen that the activation energy for Re-sites in Pt_3Re_1 alloy is minor by 0.84 eV and 0.75 eV than Pt(111) and Re(0001) respectively. Then, according to the transition state theory, the C-C cleavage reaction should be faster in this site, which presents lower

activation energy. But the activation energy for Pt-sites in Pt_3Re_1 alloy is higher than the obtained for pure metals, indicating that part of the Pt_3Re_1 surface exhibits lower activity for the C-C bond cleavage in CHCO than the pure metal surfaces. It can be attributed to the high adsorption energies of the products CH and CO on Re-sites in Pt_3Re_1 surface, as it was established in equation 4-10 the transition state depends on the sum of CH and CO adsorption energies, which is -8.86, -9.57, -9.83 and -7.04 eV for Pt, Re, Re-sites and Pt-sites in Pt_3Re_1. These results can be attributed to the modification of the electronic structure of rhenium and Pt atom if Re is introduced in the Pt structure.

It is remarkable that the high adsorption energy of the products (CH and CO) can affect negatively the activity of this catalyst, since the surface would be blocked by strongly adsorbed species. Then it would not have available sites to adsorb new reactants molecules, leading to a decreasing of the activity of the Pt_3Re_1 catalyst. This negative aspect could be overcome if these molecules react with oxidant species that help to remove the strongly adsorbed species, in other words it is needed to promote the bifunctional mechanism. As it is mentioned in Chapter 2, the tin and other metallic oxides promotes the bifunctional mechanism, likewise it is suggested in experimental studies that Re promotes the rates of glycerol conversion by facilitating water activation [25, 55] and it is reported in a theoretical study [163] that rhenium atom in a Pt cluster is active for water activation producing OH species. So, it seems that the blocking of the surface would not be a problem, but it is an issue to study in further works.

Summarizing, the calculations show that the sites with Re atom in Pt_3Re_1 are more reactive for the C-C bond cleavage in CHCO, but the sites without Re are less reactive in this catalyst. These findings indicate that the alloying of Pt with Re can contribute to a better performance in C-C bond cleavage reactions and hydrocarbons cracking reactions since this metal has higher ability for interacts with carbon atoms than Pt. However, this improvement of C-C cleavage activity is not so significant, since the active site on Pt_3Re_1 is very specific with a low surface density (few sites on determined exposed area) and the CHCO cleavage requires two adjacent sites with similar reactivity which bind each group (CH and CO) in CHCO molecule, then the low surface density is critical for C-C bond cleavage activity. Also Re is oxophilic and may activate water to produce OH species, then Re may be partly occupied with OH species under reaction conditions [55, 101]. Furthermore the pure Re surface has only a slightly lower activation energy for C-C bond cleavage than Pt, then the presence of pure rhenium phase in Pt-Re mixtures contribute to increase only slightly the activity for the C-C bond cleavage of these mixtures.

The mentioned aspects explain the experimental results, which suggests that the Re addition improves performance for C-C cleavage, but this improvement is not much higher. As is shown by Ciftci et al. [25] the Re addition to Pt improves the acetaldehyde decomposition,

increasing the CO yield (product of C-C bond cleavage) from 10% to 18%. Also, it is shown that PtRe electrocatalysts with low content of Re has a positive effect on ethanol oxidation, beyond 0.35 V the current density is higher than pure Pt and beyond 500 V is higher than PtSn, but CO_2 produced is not increased significantly and remains small [101]. Then, the increment of C-C bond cleavage is not so significant since not all of the sites at the surface are more active towards C-C bond cleavage and the advantage of the higher reactivity of Re atom in the alloy is not enough, also C-C bond cleavage involves two available active sites and many intermediates, which can interact strongly with the active sites blocking the surface.

5.4 Electronic structure

The density of states projected on d orbitals (d-DOS) of the surface atoms in the clean slab is calculated in order to gain insight about the adsorption process. The Figure **5-7** shows the density of states of the clean slabs, in that figure, energies are reported relative to respective Fermi energies E_F and the solid lines are the DOS of atoms at the topmost layer and the dotted lines are the DOS of atoms at inner layers.

The difference between the DOS for surface (solid line) and inner layer (dotted lines) atoms reflect that the existence of a surface modifies the electronic properties of the material, and more states are closer to Fermi energy (closer to 0), consequently the center of d-band of surface atoms is shifted towards higher energies than inner layer atoms by around 0.47 eV, as can be verified in Table **5-9**, in which d-band centers (ϵ_d) are reported. This shift is due to the reducing of bonds number at the surface, which leads to decrease the states with minimum energy associated to the bonding states, increasing free states which are available to form bonds and are located closer to Fermi energy. For that reason a large local density of electron states at the Fermi level is related with high reactivity [259].

In Figure **5-7**a and **5-7**b the states dominated by d-band are shown, then it can be expected that d-sates are the predominant contribution to the total DOS and to the energetics. Then, the analysis of density of states is focused on the d-states. Comparing the d-DOS of the Pt(111) and Re(0001) surfaces (Figure **5-7**a and **5-7**b) can be noted that the Pt has higher peaks than Re, that is because Pt has more valence electrons ($Z_val = 10$) than rhenium ($Z_val = 7$). Also, it is noted that Pt has high peaks in -3 and 0 eV, while Re has a high peak in -1 eV and has more states above Fermi energy than Pt. These issues contribute to the higher d-band center of Re, while Re(0001) surface atoms has a d-band center of -1.88 eV, Pt(111) surface atoms has a d-band center of -2.10 eV, as can be seen in Table **5-9**

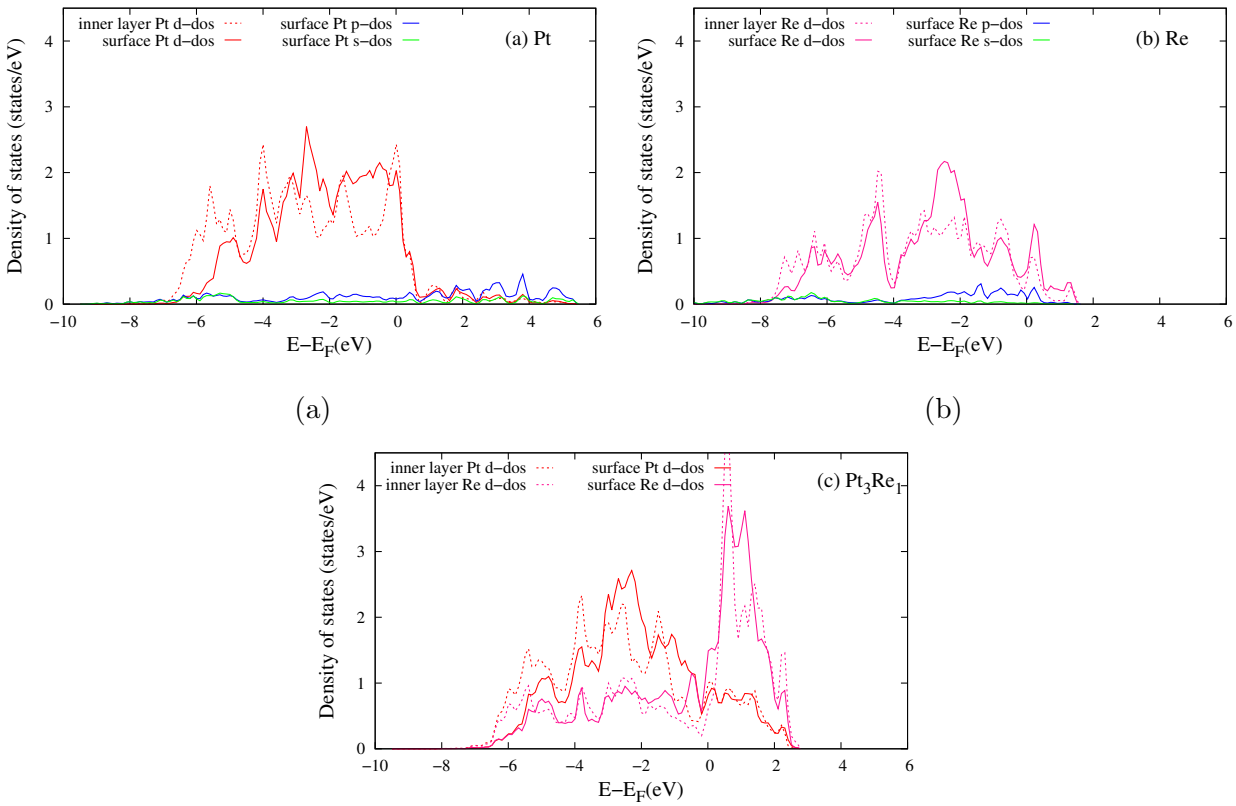

Figure **5-7**: Local density of states of clean slabs (a) Pt, (b) Re and (c) Pt_3Re_1. Dotted lines are the DOS of atoms at the inner layers, while solid lines are for atoms at the topmost layer. Blue and green lines are the s and p states respectively. Red and pink lines are d states of Pt and Re atoms respectively. Energies are shifted by respective Fermi energies E_F.

Figure **5-7**c shows the projected DOS for Pt_3Re_1 alloy, in red and pink are the d-DOS for Pt and Re atoms in this alloy respectively. It is noted that the DOS for Re atom has a high peak at Fermi energy, which is higher than the found in Re(0001) surface, evidencing the modification of electronic structure of Re atom when alloy is formed. It is quantified by the d-band center (reported in Table **5-9**) shift from -1.88 eV in Re(0001) surface to -1.37 eV in Pt_3Re_1 (111) surface. Pt atoms show a decreased peak in Fermi energy and more states below Fermi energy respect to the found in Pt(111) surface. Hence, Pt atoms in the studied alloy has a lower d-band center than Pt(111) surface, the d-band center for Pt atoms in the top layer of the alloy is -2.85 eV while for Pt(111) surface is -2.10 eV.

The mentioned trend in the d-DOS quantified by the d-band center allows to explain the trend in the adsorption energy. When the d-band center is higher, surface forms a stronger bond with the adsorbate [48, 175]. Then the sites with Re in Pt_3Re_1(111) should bind more

Table **5-9**: d-band center $\epsilon - d$ for the top-most layer and inner layer atoms.

Surface		ϵ_d(eV)	
		inner layer	top layer
Pt(111)		-2.64	-2.10
Re(0001)		-2.32	-1.88
	Pt	-3.31	-2.85
Pt_3Re_1	Re	-1.82	-1.37
	total	-2.99	-2.50

strongly the adsorbates than the Pt(111) and Re(0001) surfaces and the sites without Re. The order from higher to lower energy adsorption according to d-band center should be as follows: Re-sites in Pt_3Re_1, Re(0001), Pt(111) and Pt sites in Pt_3Re_1 alloys. This order is in agreement with the trends found for the adsorption energy CO molecule, which was shown in the previous section.

The mentioned order is not followed by CH and CHCO adsorption, since these molecules involve different surface atoms. CH interacts with 2 Pt metal and 1 Re metal atom, it would be expected an adsorption energy that would be some average of the adsorption energy on metal Pt and metal Re, in fact energy adsorption of CH on Pt_3Re_1(111) in the hollow-Re has an intermediate value between those of Pt(111) and Re(0001). CHCO presents different adsorption configurations, and then the adsorption energy for Pt_3Re_1 is not as simple as an average of the adsorption energy on metal Pt and metal Re.

Besides, the trends in the adsorption energy of CH and CHCO molecules for Re(0001), Pt(111) and sites with just Pt atoms in the alloy are in agreement with the d-band center order. This is because the adsorption on the mentioned surfaces and the Pt-site only involves one type of atom, hence the d-band center of the sites involved in the adsorption of these molecules would be the same as calculated above.

These results confirm the usefulness of d-band model for explaining trends in adsorption energy, as is observed a higher d-band center is related with higher adsorption energy [48,175]. This relation is remained true for simple molecules as CH and CO studied in this work, which has similar adsorption configuration on each surface. Also, if the adsorbate binds to different surface metal atoms, the natural approach is to assume that the adsorption strength is a linear combination of contributions from each metal, and the d-band center of interest should be a kind of average of the d-band centers for each atom to which the adsorbate couples, as is mentioned above the CH adsorption on the alloy, which involves two atoms has an intermediate adsorption energy.

The center of the d-band relative to Fermi energy, taking account all atoms in the top layer of Pt_3Re_1, is -2.50 eV. This values is lower than the d-band center of Pt(111) surface. It is due to Pt d-states moving down in energy relative to the Fermi level, suggesting that the overall effect of the Re introduction into Pt lattice is to decrease the ability of this surface to interact with the molecules due to inactivation of Pt atoms. Then the introduction of rhenium in platinum lattice leads to the inactivation of Pt atoms (lower d-band center of Pt) and to the increment of reactivity of rhenium atom. Also the Re(0001) surface has higher reactivity than Pt, then the presence of pure rhenium in catalysts with mixtures of platinum and rhenium can contributes to a better performance in C-C bond cleavage reactions. But considering both effects, the overall result of Re addition in the promotion of C-C bond cleavage is no so significant since the higher reactivity of sites with Re atom in Pt_3Re_1 and pure rhenium phase should not compensate the lower reactivity of the sites without Re.

The changes of the d-band center for Pt_3Re_1 alloy can be attributed to transfer of electronic charge from one atom to another and the change in the width of the d-band, due to the hybridization between the d-orbitals of the atom in question with the valence orbital of the neighboring atoms [4, 260]. In this case can be noted in the d-DOS that the d-band of surface Pt atoms in Pt_3Re_1 changes its shape respect to pure Pt, the main feature is that the states at Fermi energy are decreased and are "relocated" in lower energies. And the d-band of surface Re atoms in Pt_3Re_1 is increased close to Fermi energy and decreased at lowers energies. Löwdin population analysis [261] (similar to Mulliken analysis) was performed to calculate the electronic charge transfer from one atom to another, founding that the charge of Pt and Re atoms in Pt_3Re_1 alloy is similar to the nominal electronic charge of pure Pt and Re atoms (10 and 7). Pt and Re atoms in the alloy have a total charge in d orbitals of 10.02 and 6.93 respectively. Thus, the shift in the d-band center can be attributed to the hybridization between the d-orbitals of the Pt and Re atoms.

Chapter 6

Conclusions

6.1 Conclusions

The PEMFCs fed with ethanol are an alternative for energy conversion and they show attractive features as high theoretical efficiency, low operation temperature, and the availability of ethanol on an industrial scale from renewable sources. However the DE-PEMFCs require the improvement of their performance, a principal factor for that is the C-C bond cleavage in ethanol oxidation reaction. Hence, it requires development of materials with high catalytic activity toward C-C bond cleavage. Pt-Re is proposed as an appropriate material for C-C bond cleavage in ethanol decomposition, since this catalyst is mostly used in petroleum-reforming. This work clarifies the usefulness of rhenium for C-C bond cleavage reaction in the ethanol oxidation reaction on a Pt_3Re_1 catalyst.

In this work is investigated the C-C bond cleavage on a $Pt_3Re_1(111)$ surface and compared with the C-C bond cleavage in pure metal surfaces Pt(111) and Re(0001), using Density Functional Theory (DFT) and the descriptor based approach. This work propose as descriptors the adsorption of CH, CO and CHCO because the most likely reaction step for breaking of C-C bond is through CHCO molecule, and the activation energy for this step can be calculated from CH, CO and CHCO adsorption energies using linear relations (like Brønsted-Evans-Polanyi relation, BEP). A significant contribution of this work relies in the methodology utilized, demonstrating that the catalytic activity for C-C bond cleavage in ethanol oxidation reaction on Pt_3Re_1 is successfully described using a limited set of adsorption energies.

In order to quantify the descriptors selected, the slab approach is used to model the surfaces,

which were constructed from the minimum energy configuration for the bulk system. The bulk system of Pt and Re is investigated mainly as verification of the method used, finding that the final structure of the Pt_3Re_1 crystal is a cubic face centered structure with a lattice parameter of 3.967 Å that is close enough to available experimental value, so the obtained relative error was 1.85 %. DFT data fit well to Murnaghan equation of state allowing to calculate properties as cohesive energy and bulk modulus, which are higher for the alloy than pure Pt, meaning that bonding in Pt_3Re_1 system is stronger than Pt pure system as is suggested in experimental works. Also, the adsorption energy of the different molecules is in agreement with previous work in similar systems, demonstrating that this first description of the system is good enough for studying trends in reactivity. It is remarkable that some physical properties of bulk Pt_3Re_1 are not found. Then, this work is among the first in estimate the physical properties and the crystalline structure from first-principles, and it is expected that experimental or other theoretical studies be done in order to contrast the results obtained in this work.

The analysis of geometrical and energetic properties of the adsorption of different molecules on each surface allows to extend the understanding of C-C bond cleavage and the usefulness of rhenium as co-catalyst in this reaction step. It was found that the cleavage of CHCO involves two adjacent sites, which binds each carbon in that molecule and destabilizes the C-C bond stretching it. Also, it is found that Re atom has higher ability to interact with carbon atoms of the molecules studied as is indicated by the higher energy adsorption of Re(0001) surface and the sites with Re atom in Pt_3Re_1. Also, this work demonstrates that the alloying of rhenium and platinum in Pt_3Re_1 leads to decrease the ability of platinum and increase the ability of rhenium in this alloy for interacting with CH, CO and CHCO.

Brønsted Evans Polanyi relation allows to obtain the activation energy for this cleavage step with the adsorption energy of the product and reactant molecules, this relation is fundamental to describe the activity in terms of adsorption energies. It is found that the activation energy is lower for Re-sites in Pt_3Re_1 and higher for Pt sites in Pt_3Re_1 alloys. The difference in the activation energies is mainly attributed to the difference between the sum of adsorption energies of product molecules (CH and CO), whose order from higher to lower energy adsorption is: Re-sites in Pt_3Re_1, Re(0001), Pt(111) and Pt sites in Pt_3Re_1 alloys. This order matches with that found for activation energies.

These trend is partly explained analyzing the d-DOS of the clean slabs and using the simple d-band model, which establishes that when the d-band center is higher, surface form a stronger bond with the adsorbate. The order from higher to lower d-band center matches with the order of adsorption energies and activation energies: Re-sites in Pt_3Re_1, Re(0001), Pt(111) and Pt sites in Pt_3Re_1 alloys. It confirms the usefulness of d-band model for explaining trends in adsorption energy. Also, it is shown that if the adsorbate binds to different surface metal

atoms, the adsorption strength is a linear combination of contributions from each metal and d-band center of interest should be a kind of average of the d-band centers. Furthermore, the change of DOS after alloying is attributed to the hybridization of d orbitals with s and p orbitals of neighbor atoms.

The mentioned findings leads to the main result of this work. It is proposed that the presence of rhenium atoms (in pure rhenium phase or Pt_3Re_1 alloy phase) in Pt-Re catalysts has not a significant effect on promotion of C-C bond cleavage since Pt_3Re_1 have an active site with low surface density and the C-C bond cleavage requires two adjacent active sites. Also this site interacts strongly with other molecules, which can block the site. Then, it explains the low increment of CO_2 production by C-C bond cleavage in ethanol and other similar molecules when rhenium is added to Pt in Pt_3Re_1 catalyst.

Summarizing the main conclusions of this work are:

- Adsorption energy of the different molecules is in agreement with previous work in similar systems, demonstrating that this first description of the system is good enough for studying trends in reactivity. Also, this work is the first in estimate some physical properties of Pt_3Re_1 alloy from first-principles, and it is expected that experimental or other theoretical studies be done in order to contrast the results obtained.

- This work demonstrates that is possible to describe the catalytic activity for C-C bond cleavage in ethanol oxidation reaction on Pt_3Re_1 using a limited set of adsorption energies through the descriptors methodology.

- It is demonstrated that the alloying of rhenium and platinum leads to decrease the ability of platinum and increase the ability of rhenium in this alloy for interacting with CH, CO and CHCO. Hence sites with rhenium in the alloy has higher reactivity for C-C bond cleavage than pure Pt and Re, whereas sites with Pt in the alloy has lower reactivity.

- This work evidences that the relation between the d-band center and adsorption energies remains true for simple molecules as CH and CO, confirming the usefulness of d-band model for explaining trends in adsorption energy.

- This work demonstrates that the addition of rhenium to Pt forming Pt_3Re_1 alloys, does not have a significant improvement of the C-C bond cleavage activity, since not all of the sites at the surface are more active towards C-C bond cleavage. It explain the experimental results, which suggests that the Re addition improves performance for C-C cleavage, but this improvement is not much higher.

6.2 Future Work

The calculated properties of the systems studied are good enough for the analysis of C-C bond cleavage performed in this work. However, the description of the system with DFT can be further improved including other special issues as Van der Waals interactions and spin orbit coupling in order to take account the possible effects resulting of these considerations.

The adsorption of CH, CO and CHCO are proposed as descriptors of C-C bond cleavage activity, they can be used to studying the activity of other surfaces and for the search of more active catalysts. Also, this work focus on a determined composition of the alloy, it should be extended to other composition in order to get a more complete picture of the role of rhenium in Pt-Re catalysts and reveal the significance of the different phase that can be formed in that catalysts.

In order to get a whole picture of ethanol oxidation reaction, a similar approach can be used for the other important steps. For instance dehydrogenation reactions and water activation reaction (which produces OH specie that oxidizes intermediate species). The presence of water is key in ethanol oxidation reaction in fuel cells, a future work should study the ethanol oxidation in a system which includes water along ethanol.

The density of states is related with the reactivity of the surfaces, also the analysis of that property reveal the effects of alloying on the surface atoms. Then the density of states of other alloys could be studied in a systematic manner to elucidate the effects of alloying on the electronic structure and hence the reactivity. That study will provide significant issues for tuning the reactivity of particular material by means of its modification with alloying elements.

Appendix A

Anexo: Convergence Tests

In numerical calculations there is always a trade-off between accuracy and computational resources spent on solving given problem. In order to make optimal choice is performed several convergence tests, in this way was determined the minimal (associated computational effort) value for given parameter that will not affect the accuracy in the calculation of relevant system property such as total energy of the system. Some convergence tests results are presented here: convergence respect to the most important parameters in DFT calculations, the energy cut-off and k-mesh. And convergence respect to the most important parameters in the slab model, atomic layers and vacuum space.

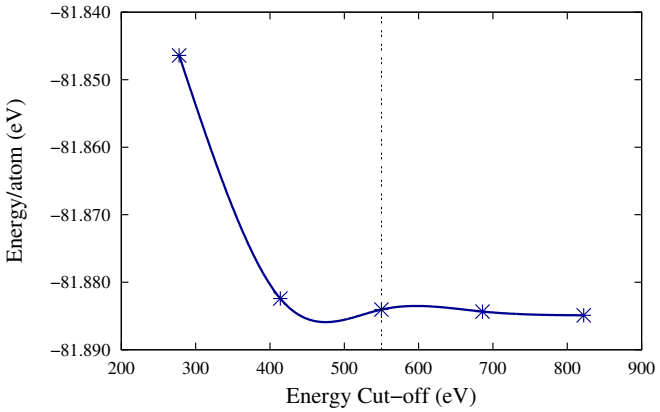

Figure **A-1**: Convergence of total energy by atom in bulk system respect to energy cut-off for the plane waves expansion. The value which is considered that offers a considerable physical accuracy in relation with computational cost is marked with a dotted line.

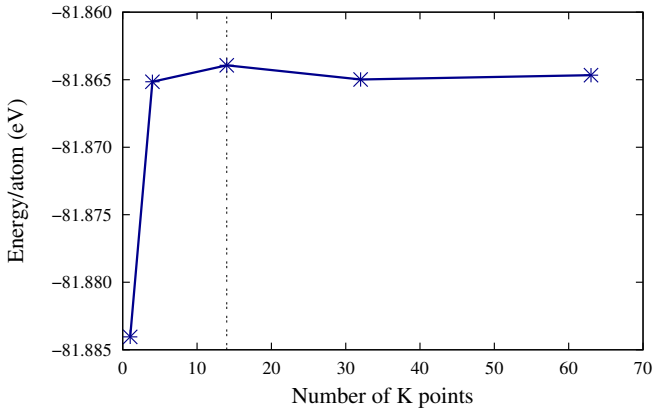

Figure **A-2**: Convergence of total energy by atom in bulk system respect to number of k-points used in the scheme Monkhorst-Pack for Brillouin zone sampling. The value which is considered that offers a considerable physical accuracy is marked with a dotted line.

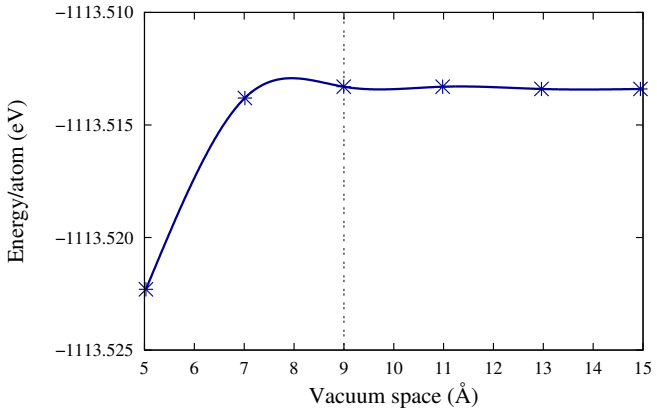

Figure **A-3**: Convergence of total energy by atom in the slab respect to vacuum space (in Å). The value which is considered that offers a considerable physical accuracy is marked with a dotted line.

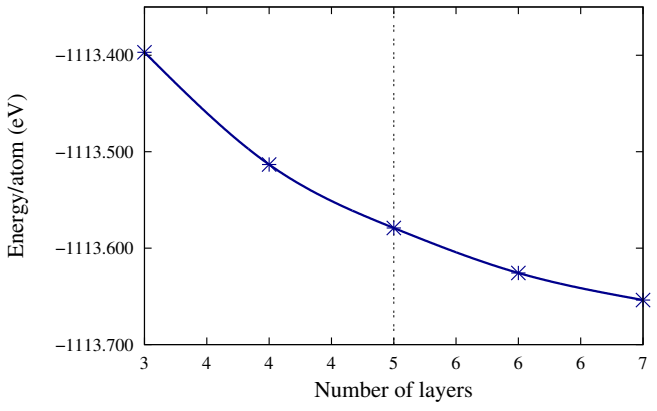

Figure **A-4**: Convergence of total energy by atom in the slab respect to number of layers. The value which is considered that offers a considerable physical accuracy is marked with a dotted line.

Bibliography

[1] S. García-rodríguez, T. Herranz, and S. Rojas, "New and Future Developments in Catalysis," in *Electroctalysts for the Electrooxidation of Ethanol*, pp. 33–67, Elsevier, 2013.

[2] T. Bligaard, J. Nørskov, S. Dahl, J. Matthiesen, C. Christensen, and J. Sehested, "The Brønsted-Evans-Polanyi relation and the volcano curve in heterogeneous catalysis," *Journal of Catalysis*, vol. 224, pp. 206–217, may 2004.

[3] J. K. Nørskov, F. Abild-Pedersen, F. Studt, and T. Bligaard, "Density functional theory in surface chemistry and catalysis.," *Proceedings of the National Academy of Sciences of the United States of America*, vol. 108, pp. 937–43, jan 2011.

[4] S. Linic, H. Xin, A. Holewinski, N. Schweitzer, and E. Nikolla, "Electronic Structure Engineering in Heterogeneous Catalysis: Identifying Novel Alloy Catalysts Based on Rapid Screening for Materials with Desired Electronic Properties," *Topics in Catalysis*, vol. 55, pp. 376–390, apr 2012.

[5] Energy Information Administration (EIA), "International energy data and analysis."

[6] Renewable Energy Policy Network for the 21st Century, "REN21 Annual Reports."

[7] S. Badwal, S. Giddey, a. Kulkarni, J. Goel, and S. Basu, "Direct ethanol fuel cells for transport and stationary applications – A comprehensive review," *Applied Energy*, vol. 145, pp. 80–103, 2015.

[8] W. B. Pearson, *A handbook of lattice spacings and structures of metals and alloys*. Belfast: Pergamon press, 1958.

[9] C. Kittel, *Introduction to solid state physics*. John Wiley & Sons, Inc., eight edit ed., 2004.

[10] A. Brouzgou, A. Podias, and P. Tsiakaras, "PEMFCs and AEMFCs directly fed with ethanol: a current status comparative review," *Journal of Applied Electrochemistry*, vol. 43, pp. 119–136, dec 2012.

[11] S. Abdullah, S. Kamarudin, U. Hasran, M. Masdar, and W. Daud, "Modeling and simulation of a direct ethanol fuel cell: An overview," *Journal of Power Sources*, vol. 262, pp. 401–406, sep 2014.

[12] S. Song and P. Tsiakaras, "Recent progress in direct ethanol proton exchange membrane fuel cells (DE-PEMFCs)," *Applied Catalysis B: Environmental*, vol. 63, pp. 187–193, mar 2006.

[13] C. Lamy, "The direct ethanol fuel cell: a challenge to convert bioethanol cleanly into electric energy," in *Catalysis for Sustainable Energy Production* (P. Barbaro and C. Bianchini, eds.), ch. 1, pp. 1–46, Weinheim, Germany.: WILEY-VCH Verlag GmbH & Co. KGaA, 2009.

[14] J. Zhang, ed., *PEM Fuel Cell Electrocatalysts and Catalyst Layers*. London: Springer London, 2008.

[15] M. Kamarudin, S. Kamarudin, M. Masdar, and W. Daud, "Review: Direct ethanol fuel cells," *International Journal of Hydrogen Energy*, pp. 1–16, sep 2012.

[16] "Acta launches catalyst, supplies electrodes to ethanol FCV," *Fuel Cells Bulletin*, vol. 2007, no. 7, p. 10, 2007.

[17] Biopact, "Interview: University of Offenburg demonstrates world's first 'Direct Ethanol Fuel Cell'," 2007.

[18] D. Montgomery, "Large Scale Direct Ethanol Alkaline Fuel Cells," tech. rep., NDC Power.

[19] G. Andreadis, A. Podias, and P. Tsiakaras, "The effect of the parasitic current on the Direct Ethanol PEM Fuel Cell Operation," *Journal of Power Sources*, vol. 181, pp. 214–227, jul 2008.

[20] A. Rabis, P. Rodriguez, and T. J. Schmidt, "Electrocatalysis for Polymer Electrolyte Fuel Cells: Recent Achievements and Future Challenges," *ACS Catalysis*, vol. 2, pp. 864–890, may 2012.

[21] S. Song, W. Zhou, Z. Zhou, L. Jiang, G. Sun, Q. Xin, V. Leontidis, S. Kontou, and P. Tsiakaras, "Direct ethanol PEM fuel cells: The case of platinum based anodes," *International Journal of Hydrogen Energy*, vol. 30, pp. 995–1001, aug 2005.

[22] F. Colmati, G. Tremiliosi-Filho, E. R. Gonzalez, A. Berná, E. Herrero, and J. M. Feliu, "The role of the steps in the cleavage of the C-C bond during ethanol oxidation on platinum electrodes.," *Physical chemistry chemical physics : PCCP*, vol. 11, pp. 9114–23, oct 2009.

[23] Z. Xu and Y. Wang, "Understanding Electrocatalytic Activity Enhancement of Bimetallic Particles to Ethanol Electro-Oxidation: Ethanol Adsorption and Decomposition on Pt n M (n=6 and 9; M=Pt, Ru, and Sn)," in *Applications of Molecular Modeling to Challenges in Clean Energy*, ch. 8, pp. 135–151, Washington DC.: American Chemical Society, jan 2013.

[24] L. Y. Chen, "Structure Characterization of Platinum/Alumina, Rhenium/Alumina, and Platinum-Rhenium/Alumina Catalysts," *Journal of Catalysis*, vol. 145, pp. 132–140, jan 1994.

[25] A. Ciftci, D. M. Ligthart, a. O. Sen, A. J. van Hoof, H. Friedrich, and E. J. Hensen, "Pt-Re synergy in aqueous-phase reforming of glycerol and the water-gas shift reaction," *Journal of Catalysis*, vol. 311, pp. 88–101, 2014.

[26] G. Meitzner, G. H. Via, F. W. Lytle, and J. H. Sinfelt, "Structure of bimetallic clusters. Extended x-ray absorption fine structure (EXAFS) of Pt–Re and Pd–Re clusters," *The Journal of Chemical Physics*, vol. 87, no. 11, p. 6354, 1987.

[27] B. Hammer and J. K. Nørskov, "Electronic factors determining the reactivity of metal surfaces," *Surface Science*, vol. 343, pp. 211–220, dec 1995.

[28] A. Nilsson, L. G. M. Pettersson, B. Hammer, T. Bligaard, C. H. Christensen, and J. K. Norskov, "The electronic structure effect in heterogeneous catalysis," *Catalysis Letters*, vol. 100, pp. 111–114, apr 2005.

[29] T. Kousksou, P. Bruel, A. Jamil, T. El Rhafiki, and Y. Zeraouli, "Energy storage: Applications and challenges," *Solar Energy Materials and Solar Cells*, vol. 120, pp. 59–80, jan 2014.

[30] V. Nelson, *Introduction to Renewable Energy*. CRC Press, 2011.

[31] C. D. Colombia, "Ley No 1715 Del 13 De Mayo De 2014," 2014.

[32] Upme, "Plan Energético Nacional Colombia: Ideario Energético 2015," tech. rep., Unidad de Planeacion Minero Energética, Colombia, 2015.

[33] REN21, "Renewables Global Status Report 2014," tech. rep., Renewable Energy Policy Network for the 21st Century, Paris, France, 2014.

[34] A. K. Hussein, "Applications of nanotechnology in renewable energies—A comprehensive overview and understanding," *Renewable and Sustainable Energy Reviews*, vol. 42, pp. 460–476, 2015.

[35] C. Karakosta, C. Pappas, V. Marinakis, and J. Psarras, "Renewable energy and nuclear power towards sustainable development: Characteristics and prospects," *Renewable and Sustainable Energy Reviews*, vol. 22, pp. 187–197, 2013.

[36] L. Eltrop, "Renewable Energy: Resources and Technologies," in *Glances at Renewable and Sustainable Energy* (T. Jenssen, ed.), pp. 15–32, Springer-Verlag, 2013.

[37] Y. Wang, K. S. Chen, J. Mishler, S. C. Cho, and X. C. Adroher, "A review of polymer electrolyte membrane fuel cells: Technology, applications, and needs on fundamental research," *Applied Energy*, vol. 88, pp. 981–1007, apr 2011.

[38] L. B. Braga, J. L. Silveira, M. Evaristo Da Silva, E. B. Machin, D. T. Pedroso, and C. E. Tuna, "Comparative analysis between a PEM fuel cell and an internal combustion engine driving an electricity generator: Technical, economical and ecological aspects," *Applied Thermal Engineering*, vol. 63, no. 1, pp. 354–361, 2014.

[39] U. S. C. f. A. R. (USCAR), "Fuel Cell Technical Team Roadmap," Tech. Rep. June, US Department of Energy, 2013.

[40] Energy Office of Energy Efficiency and Renewable (EERE), "FUEL CELL TECHNOLOGIES OFFICE MULTI-YEAR RESEARCH, DEVELOPMENT AND DEMONSTRATION PLAN," 2013.

[41] H. Berg, J. Nyman, P. Erlandsson, P. Johansson, and A. Matic, "Direct ethanol fuel cells: ethanol for our future fuel cells?," tech. rep., Energiforsk, Stockholm, 2015.

[42] Federación Nacional de Biocombustibles de Colombia, "Cifras Informativas del Sector Biocombustibles," tech. rep., Fedebiocombustibles, 2014.

[43] Unidad de Planeación Minero Energética (UPME), "Biocombustibles en Colombia," 2009.

[44] F. Vigier, C. Coutanceau, F. Hahn, E. Belgsir, and C. Lamy, "On the mechanism of ethanol electrooxidation on Pt and PtSn catalysts: electrochemical and in situ IR reflectance spectroscopy studies," *Journal of Electroanalytical Chemistry*, vol. 563, pp. 81–89, feb 2004.

[45] M. H. Shao and R. R. Adzic, "Electrooxidation of ethanol on a Pt electrode in acid solutions: in situ ATR-SEIRAS study," *Electrochimica Acta*, vol. 50, pp. 2415–2422, apr 2005.

[46] R. B. Kutz, B. Braunschweig, P. Mukherjee, R. L. Behrens, D. D. Dlott, and A. Wieckowski, "Reaction pathways of ethanol electrooxidation on polycrystalline platinum catalysts in acidic electrolytes," *Journal of Catalysis*, vol. 278, pp. 181–188, mar 2011.

[47] P. Ferrin, D. Simonetti, S. Kandoi, E. Kunkes, J. A. Dumesic, J. K. Nørskov, and M. Mavrikakis, "Modeling ethanol decomposition on transition metals: a combined application of scaling and Brønsted-Evans-Polanyi relations.," *Journal of the American Chemical Society*, vol. 131, pp. 5809–15, apr 2009.

[48] J. K. Nørskov, T. Bligaard, J. Rossmeisl, and C. H. Christensen, "Towards the computational design of solid catalysts.," *Nature chemistry*, vol. 1, pp. 37–46, apr 2009.

[49] I. a. Pašti and S. V. Mentus, "Modification of electronic properties of Pt(111) surface by means of alloyed and adsorbed metals: DFT study," *Russian Journal of Physical Chemistry A*, vol. 83, pp. 1531–1536, aug 2009.

[50] K. Reuter, D. Frenkel, and M. Scheffler, "The Steady State of Heterogeneous Catalysis, Studied by First-Principles Statistical Mechanics," *Physical Review Letters*, vol. 93, p. 116105, sep 2004.

[51] S. Kandoi, J. Greeley, M. a. Sanchez-Castillo, S. T. Evans, A. a. Gokhale, J. a. Dumesic, and M. Mavrikakis, "Prediction of Experimental Methanol Decomposition Rates on Platinum from First Principles," *Topics in Catalysis*, vol. 37, pp. 17–28, mar 2006.

[52] A. Hellman, E. J. Baerends, M. Biczysko, T. Bligaard, C. H. Christensen, D. C. Clary, S. Dahl, R. van Harrevelt, K. Honkala, H. Jonsson, G. J. Kroes, M. Luppi, U. Manthe, J. K. Nørskov, R. a. Olsen, J. Rossmeisl, E. Skúlason, C. S. Tautermann, a. J. C. Varandas, and J. K. Vincent, "Predicting catalysis: understanding ammonia synthesis from first-principles calculations.," *The journal of physical chemistry. B*, vol. 110, pp. 17719–17735, sep 2006.

[53] J. Greeley and M. Mavrikakis, "Alloy catalysts designed from first principles.," *Nature materials*, vol. 3, pp. 810–5, nov 2004.

[54] M. Andersson, T. Bligaard, a. Kustov, K. Larsen, J. Greeley, T. Johannessen, C. Christensen, and J. Norskov, "Toward computational screening in heterogeneous catalysis: Pareto-optimal methanation catalysts," *Journal of Catalysis*, vol. 239, pp. 501–506, apr 2006.

[55] E. Kunkes, D. Simonetti, J. Dumesic, W. Pyrz, L. Murillo, J. Chen, and D. Buttrey, "The role of rhenium in the conversion of glycerol to synthesis gas over carbon supported platinum–rhenium catalysts," *Journal of Catalysis*, vol. 260, pp. 164–177, nov 2008.

[56] B. Grgur, N. Markovic, and P. Ross, "Electrooxidation of H2, CO and H2/CO mixtures on a well-characterized Pt–Re bulk alloy electrode and comparison with other Pt binary alloys," *Electrochimica Acta*, vol. 43, no. 24, pp. 3631–3635, 1998.

[57] J. Tayal, B. Rawat, and S. Basu, "Effect of addition of rhenium to Pt-based anode catalysts in electro-oxidation of ethanol in direct ethanol PEM fuel cell," *International Journal of Hydrogen Energy*, vol. 37, no. 5, pp. 4597–4605, 2012.

[58] J. Goel and S. Basu, "Pt-Re-Sn as Metal Catalysts for Electro-Oxidation of Ethanol in Direct Ethanol Fuel Cell," *Energy Procedia*, vol. 28, pp. 66–77, jan 2012.

[59] Z.-F. Xu and Y. Wang, "Effects of Alloyed Metal on the Catalysis Activity of Pt for Ethanol Partial Oxidation: Adsorption and Dehydrogenation on Pt(3)M (M=Pt, Ru, Sn, Re, Rh, and Pd).," *The journal of physical chemistry. C, Nanomaterials and interfaces*, vol. 115, pp. 20565–20571, oct 2011.

[60] L. An, T. Zhao, and Y. Li, "Carbon-neutral sustainable energy technology: Direct ethanol fuel cells," *Renewable and Sustainable Energy Reviews*, vol. 50, pp. 1462–1468, 2015.

[61] H. R. Corti and E. R. Gonzalez, "Introduction to Direct Alcohol Fuel Cells," in *Direct Alcohol Fuel Cells* (H. R. Corti and E. R. Gonzalez, eds.), pp. 1–32, Dordrecht: Springer Netherlands, 2014.

[62] J. Ling, G. Longtin, and O. Savadogo, "Comparison of ethanol and methanol crossover through different MEA components and structures by cyclic voltammetry," *Asia-Pacific Journal of Chemical Engineering*, vol. 4, pp. 25–32, jan 2009.

[63] Y. H. Chu and Y. G. Shul, "Alcohol crossover behavior in direct alcohol fuel cells (DAFCs) system," *Fuel Cells*, vol. 12, no. 1, pp. 109–115, 2012.

[64] S. Song, W. Zhou, J. Tian, R. Cai, G. Sun, Q. Xin, S. Kontou, and P. Tsiakaras, "Ethanol crossover phenomena and its influence on the performance of DEFC," *Journal of Power Sources*, vol. 145, no. 2, pp. 266–271, 2005.

[65] N. Shroti, L. Barbora, and A. Verma, "Neodymium triflate modified nafion composite membrane for reduced alcohol permeability in direct alcohol fuel cell," *International Journal of Hydrogen Energy*, vol. 36, no. 22, pp. 14907–14913, 2011.

[66] H. Maab and S. P. Nunes, "Modified SPEEK membranes for direct ethanol fuel cell," *Journal of Power Sources*, vol. 195, no. 13, pp. 4036–4042, 2010.

[67] K. S. Roelofs, T. Hirth, and T. Schiestel, "Dihydrogenimidazole modified silica-sulfonated poly(ether ether ketone) hybrid materials as electrolyte membranes for direct ethanol fuel cells," *Materials Science and Engineering: B*, vol. 176, no. 9, pp. 727–735, 2011.

[68] B. Y. Wang, C. K. Tseng, C. M. Shih, Y. L. Pai, H. P. Kuo, and S. J. Lue, "Polytetrafluoroethylene (PTFE)/silane cross-linked sulfonated poly(styrene-ethylene/butylene-styrene) (sSEBS) composite membrane for direct alcohol and formic acid fuel cells," *Journal of Membrane Science*, vol. 464, pp. 43–54, 2014.

[69] H. S. Thiam, W. R. W. Daud, S. K. Kamarudin, A. B. Mohammad, A. A. H. Kadhum, K. S. Loh, and E. H. Majlan, "Overview on nanostructured membrane in fuel cell applications," *International Journal of Hydrogen Energy*, vol. 36, no. 4, pp. 3187–3205, 2011.

[70] A. Brouzgou, S. Q. Song, and P. Tsiakaras, "Low and non-platinum electrocatalysts for PEMFCs: Current status, challenges and prospects," *Applied Catalysis B: Environmental*, vol. 127, pp. 371–388, 2012.

[71] H. R. Corti, "Membranes for Direct Alcohol Fuel Cells," in *Direct Alcohol Fuel Cells*, pp. 121–230, Dordrecht: Springer Netherlands, 2014.

[72] T. Lopes, E. Antolini, F. Colmati, and E. R. Gonzalez, "Carbon supported Pt-Co (3:1) alloy as improved cathode electrocatalyst for direct ethanol fuel cells," *Journal of Power Sources*, vol. 164, no. 1, pp. 111–114, 2007.

[73] T. Lopes, E. Antolini, and E. Gonzalez, "Carbon supported Pt–Pd alloy as an ethanol tolerant oxygen reduction electrocatalyst for direct ethanol fuel cells," *International Journal of Hydrogen Energy*, vol. 33, pp. 5563–5570, oct 2008.

[74] a. Y. Tsivadze, M. R. Tarasevich, a. V. Kuzov, I. a. Romanova, and D. a. Pripadchev, "New nanosized cathode electrocatalysts tolerant to ethanol," *Doklady Physical Chemistry*, vol. 421, no. 1, pp. 166–169, 2008.

[75] S. Meenakshi, K. Nishanth, P. Sridhar, and S. Pitchumani, "Spillover effect induced Pt-TiO2/C as ethanol tolerant oxygen reduction reaction catalyst for direct ethanol fuel cells," *Electrochimica Acta*, vol. 135, pp. 52–59, 2014.

[76] E. Antolini, "Catalysts for direct ethanol fuel cells," *Journal of Power Sources*, vol. 170, pp. 1–12, 2007.

[77] E. A. Ticianelli and F. H. B. Lima, "Nanostrutured Electrocatalysts for Methanol and Ethanol-Tolerant Cathodes," in *Direct Alcohol Fuel Cells*, pp. 99–119, Dordrecht: Springer Netherlands, 2014.

[78] D. Morales Acosta, D. López de la Fuente, L. G. Arriaga, G. Vargas Gutiérrez, and F. J. Rodriguez Varela, "Electrochemical Investigation of Pt-Co / MWCNT as an Alcohol- Tolerant ORR Catalyst for Direct Oxidation Fuel Cells," *Int. J. Electrochem. Sci*, vol. 6, pp. 1835–1853, 2011.

[79] F. J. Rodríguez Varela and O. Savadogo, "Ethanol-tolerant Pt-alloy cathodes for direct ethanol fuel cell (DEFC) applications," *Asia-Pacific Journal of Chemical Engineering*, vol. 4, pp. 17–24, jan 2009.

[80] F. C. Simões and P. Olivi, "Oxygen Reduction Reaction on Pt–NiO x /C, Pt–CoO x /C, and Pt–SnO2/C Electrodes in the Presence of Ethanol," *Electrocatalysis*, vol. 1, no. 2-3, pp. 163–168, 2010.

[81] J. Perez, V. a. Paganin, and E. Antolini, "Particle size effect for ethanol electro-oxidation on Pt/C catalysts in half-cell and in a single direct ethanol fuel cell," *Journal of Electroanalytical Chemistry*, vol. 654, no. 1-2, pp. 108–115, 2011.

[82] S. Song, W. Zhou, Z. Liang, R. Cai, G. Sun, Q. Xin, V. Stergiopoulos, and P. Tsiakaras, "The effect of methanol and ethanol cross-over on the performance of PtRu/C-based anode DAFCs," *Applied Catalysis B: Environmental*, vol. 55, no. 1, pp. 65–72, 2005.

[83] P. E. Tsiakaras, "PtM/C (M = Sn, Ru, Pd, W) based anode direct ethanol-PEMFCs: Structural characteristics and cell performance," *Journal of Power Sources*, vol. 171, no. 1, pp. 107–112, 2007.

[84] J. Ribeiro, D. M. dos Anjos, K. B. Kokoh, C. Coutanceau, J. M. Léger, P. Olivi, a. R. de Andrade, and G. Tremiliosi-Filho, "Carbon-supported ternary PtSnIr catalysts for direct ethanol fuel cell," *Electrochimica Acta*, vol. 52, no. 24, pp. 6997–7006, 2007.

[85] W. J. Zhou, B. Zhou, W. Z. Li, Z. H. Zhou, S. Q. Song, G. Q. Sun, Q. Xin, S. Douvartzides, M. Goula, and P. Tsiakaras, "Performance comparison of low-temperature direct alcohol fuel cells with different anode catalysts," *Journal of Power Sources*, vol. 126, no. 1-2, pp. 16–22, 2004.

[86] A. O. Neto, L. a. Farias, R. R. Dias, M. Brandalise, M. Linardi, and E. V. Spinacé, "Enhanced electro-oxidation of ethanol using PtSn/CeO2–C electrocatalyst prepared by an alcohol-reduction process," *Electrochemistry Communications*, vol. 10, no. 9, pp. 1315–1317, 2008.

[87] L. Jiang, G. Sun, S. Sun, J. Liu, S. Tang, H. Li, B. Zhou, and Q. Xin, "Structure and chemical composition of supported Pt-Sn electrocatalysts for ethanol oxidation," *Electrochimica Acta*, vol. 50, no. 27, pp. 5384–5389, 2005.

[88] L. Jiang, L. Colmenares, Z. Jusys, G. Q. Sun, and R. J. Behm, "Ethanol electrooxidation on novel carbon supported Pt/SnOx/C catalysts with varied Pt:Sn ratio," *Electrochimica Acta*, vol. 53, no. 2, pp. 377–389, 2007.

[89] M. Zhu, G. Sun, and Q. Xin, "Effect of alloying degree in PtSn catalyst on the catalytic behavior for ethanol electro-oxidation," *Electrochimica Acta*, vol. 54, no. 5, pp. 1511–1518, 2009.

[90] X. Xue, J. Ge, T. Tian, C. Liu, W. Xing, and T. Lu, "Enhancement of the electrooxidation of ethanol on Pt-Sn-P/C catalysts prepared by chemical deposition process," *Journal of Power Sources*, vol. 172, no. 2, pp. 560–569, 2007.

[91] S. Rousseau, C. Coutanceau, C. Lamy, and J. M. Léger, "Direct ethanol fuel cell (DEFC): Electrical performances and reaction products distribution under operating conditions with different platinum-based anodes," *Journal of Power Sources*, vol. 158, no. 1, pp. 18–24, 2006.

[92] E. Antolini, F. Colmati, and E. R. Gonzalez, "Effect of Ru addition on the structural characteristics and the electrochemical activity for ethanol oxidation of carbon supported Pt-Sn alloy catalysts," *Electrochemistry Communications*, vol. 9, pp. 398–404, mar 2007.

[93] J. Ribeiro, D. M. Dos Anjos, J. M. Léger, F. Hahn, P. Olivi, a. R. De Andrade, G. Tremiliosi-Filho, and K. B. Kokoh, "Effect of W on PtSn/C catalysts for ethanol electrooxidation," *Journal of Applied Electrochemistry*, vol. 38, no. 5, pp. 653–662, 2008.

[94] E. Lee, A. Murthy, and A. Manthiram, "Effect of Mo addition on the electrocatalytic activity of Pt-Sn-Mo/C for direct ethanol fuel cells," *Electrochimica Acta*, vol. 56, pp. 1611–1618, jan 2011.

[95] J. Tayal, B. Rawat, and S. Basu, "Bi-metallic and tri-metallic Pt-Sn/C, Pt-Ir/C, Pt-Ir-Sn/C catalysts for electro-oxidation of ethanol in direct ethanol fuel cell," *International Journal of Hydrogen Energy*, vol. 36, pp. 14884–14897, nov 2011.

[96] S. Beyhan, C. Coutanceau, J. M. Léger, T. W. Napporn, and F. Kadirgan, "Promising anode candidates for direct ethanol fuel cell: Carbon supported PtSn-based trimetallic catalysts prepared by Bönnemann method," *International Journal of Hydrogen Energy*, vol. 38, pp. 6830–6841, 2013.

[97] M. Brandalise, R. W. R. Verjulio-Silva, M. M. Tusi, O. V. Correa, L. a. Farias, M. Linardi, E. V. Spinacé, and a. O. Neto, "Electro-oxidation of ethanol using PtRuBi/C electrocatalyst prepared by borohydride reduction," *Ionics*, vol. 15, no. 6, pp. 743–747, 2009.

[98] E. Ribadeneira and B. A. Hoyos, "Evaluation of Pt–Ru–Ni and Pt–Sn–Ni catalysts as anodes in direct ethanol fuel cells," *Journal of Power Sources*, vol. 180, pp. 238–242, 2008.

[99] F. Colmati, E. Antolini, and E. R. Gonalez, "Ethanol Oxidation on Carbon Supported Pt-Sn Electrocatalysts Prepared by Reduction with Formic Acid," *Journal of The Electrochemical Society*, vol. 154, no. 1, p. B39, 2007.

[100] H. Li, G. Sun, L. Cao, L. Jiang, and Q. Xin, "Comparison of different promotion effect of PtRu/C and PtSn/C electrocatalysts for ethanol electro-oxidation," *Electrochimica Acta*, vol. 52, pp. 6622–6629, aug 2007.

[101] F. Vigier, C. Coutanceau, A. Perrard, E. Belgsir, and C. Lamy, "Development of anode catalysts for a direct ethanol fuel cell," *Journal of Applied Electrochemistry*, vol. 34, pp. 439–446, apr 2004.

[102] F. Colmati, E. Antolini, and E. R. Gonzalez, "Effect of temperature on the mechanism of ethanol oxidation on carbon supported Pt, PtRu and Pt3Sn electrocatalysts," *Journal of Power Sources*, vol. 157, pp. 98–103, jun 2006.

[103] F. Lima, D. Profeti, W. Lizcano-Valbuena, E. Ticianelli, and E. Gonzalez, "Carbon-dispersed Pt-Rh nanoparticles for ethanol electro-oxidation. Effect of the crystallite size and of temperature," *Journal of Electroanalytical Chemistry*, vol. 617, pp. 121–129, jun 2008.

[104] F. Kadirgan, S. Beyhan, and T. Atilan, "Preparation and characterization of nano-sized Pt-Pd/C catalysts and comparison of their electro-activity toward methanol and ethanol oxidation," *International Journal of Hydrogen Energy*, vol. 34, pp. 4312–4320, may 2009.

[105] E. Antolini and E. Gonzalez, "Effect of synthesis method and structural characteristics of Pt-Sn fuel cell catalysts on the electro-oxidation of CH3OH and CH3CH2OH in acid medium," *Catalysis Today*, vol. 160, pp. 28–38, feb 2011.

[106] F. Colmati, E. Antolini, and E. R. Gonzalez, "Ethanol oxidation on a carbon-supported Pt75Sn25 electrocatalyst prepared by reduction with formic acid: Effect of thermal treatment," *Applied Catalysis B: Environmental*, vol. 73, pp. 106–115, apr 2007.

[107] E. V. Spinace, R. R. Dias, A. O. Neto, and M. Linardi, *Scientific Bases for the Preparation of Heterogeneous Catalysts*, vol. 162 of *Studies in Surface Science and Catalysis*. Elsevier, 2006.

[108] D. Godoi, J. Perez, and H. Villullas, "Alloys and oxides on carbon-supported Pt-Sn electrocatalysts for ethanol oxidation," *Journal of Power Sources*, vol. 195, pp. 3394–3401, jun 2010.

[109] S. C. Zignani, V. Baglio, J. J. Linares, G. Monforte, E. R. Gonzalez, and A. S. Aricò, "Performance and selectivity of Pt xSn/C electro-catalysts for ethanol oxidation prepared by reduction with different formic acid concentrations," *Electrochimica Acta*, vol. 70, pp. 255–265, 2012.

[110] K. Artyushkova, B. Halevi, M. Padilla, P. Atanassov, and E. a. Baranova, "Mechanistic Study of Electrooxidation of Ethanol on PtSn Nanoparticles in Alkaline and Acid Media," *Journal of the Electrochemical Society*, vol. 162, no. 6, pp. H345–H351, 2015.

[111] Y. Wang, S. Song, G. Andreadis, H. Liu, and P. Tsiakaras, "Understanding the electrocatalytic activity of PtxSny in direct ethanol fuel cells," *Journal of Power Sources*, vol. 196, no. 11, pp. 4980–4986, 2011.

[112] G. Wu, R. Swaidan, and G. Cui, "Electrooxidations of ethanol, acetaldehyde and acetic acid using PtRuSn/C catalysts prepared by modified alcohol-reduction process," *Journal of Power Sources*, vol. 172, no. 1, pp. 180–188, 2007.

[113] A. O. Neto, R. R. Dias, M. M. Tusi, M. Linardi, and E. V. Spinacé, "Electro-oxidation of methanol and ethanol using PtRu/C, PtSn/C and PtSnRu/C electrocatalysts prepared by an alcohol-reduction process," *Journal of Power Sources*, vol. 166, pp. 87–91, mar 2007.

[114] E. Cunha, J. Ribeiro, K. Kokoh, and A. de Andrade, "Preparation, characterization and application of Pt-Ru-Sn/C trimetallic electrocatalysts for ethanol oxidation in direct fuel cell," *International Journal of Hydrogen Energy*, vol. 36, pp. 11034–11042, aug 2011.

[115] W. Zhou, W. Li, S. Song, Z. Zhou, L. Jiang, G. Sun, Q. Xin, K. Poulianitis, S. Kontou, and P. Tsiakaras, "Bi- and tri-metallic Pt-based anode catalysts for direct ethanol fuel cells," *Journal of Power Sources*, vol. 131, no. 1-2, pp. 217–223, 2004.

[116] A. Bonesi, M. Moreno, W. Triaca, and a. C. Luna, "Modified catalytic materials for ethanol oxidation," *International Journal of Hydrogen Energy*, vol. 35, pp. 5999–6004, jun 2010.

[117] T. S. Almeida, K. B. Kokoh, and a. R. De Andrade, "Effect of Ni on Pt/C and PtSn/C prepared by the Pechini method," *International Journal of Hydrogen Energy*, vol. 36, no. 6, pp. 3803–3810, 2011.

[118] P. D. S. Correa, E. L. da Silva, R. F. da Silva, C. Radtke, B. Moreno, E. Chinarro, and C. D. F. Malfatti, "Effect of decreasing platinum amount in Pt-Sn-Ni alloys supported on carbon as electrocatalysts for ethanol electrooxidation," *International Journal of Hydrogen Energy*, vol. 37, pp. 9314–9323, jun 2012.

[119] L. S. Parreira, J. C. M. da Silva, M. D'Villa -Silva, F. C. Simões, S. Garcia, I. Gaubeur, M. A. L. Cordeiro, E. R. Leite, and M. C. dos Santos, "PtSnNi/C nanoparticle electrocatalysts for the ethanol oxidation reaction: Ni stability study," *Electrochimica Acta*, vol. 96, pp. 243–252, 2013.

[120] S. Beyhan, J. M. Léger, and F. Kadirgan, "Pronounced synergetic effect of the nano-sized PtSnNi/C catalyst for ethanol oxidation in direct ethanol fuel cell," *Applied Catalysis B: Environmental*, vol. 130-131, pp. 305–313, 2013.

[121] Z.-B. Wang, G.-P. Yin, J. Zhang, Y.-C. Sun, and P.-F. Shi, "Investigation of ethanol electrooxidation on a Pt–Ru–Ni/C catalyst for a direct ethanol fuel cell," *Journal of Power Sources*, vol. 160, no. 1, pp. 37–43, 2006.

[122] R. E. Ribadeneira and B. A. Hoyos, "CO-CATALYTIC EFFECT OF NICKEL IN Pt-Ru/C AND Pt-Sn/C ELEC- TROCATALYSTS FOR ETHANOL ELECTROOXIDATION," *Latin American Applied Research*, vol. 118, pp. 113–118, 2010.

[123] E. Antolini, F. Colmati, and E. Gonzalez, "Ethanol oxidation on carbon supported (PtSn)alloy/SnO2 and (PtSnPd)alloy/SnO2 catalysts with a fixed Pt/SnO2 atomic ratio: Effect of the alloy phase characteristics," *Journal of Power Sources*, vol. 193, no. 2, pp. 555–561, 2009.

[124] T. Almeida, A. Van Wassen, R. VanDover, A. de Andrade, and H. Abruña, "Combinatorial PtSnM (Fe, Ni, Ru and Pd) nanoparticle catalyst library toward ethanol electrooxidation," *Journal of Power Sources*, vol. 284, pp. 623–630, 2015.

[125] G. García, N. Tsiouvaras, E. Pastor, M. a. Peña, J. L. G. Fierro, and M. V. Martínez-Huerta, "Ethanol oxidation on PtRuMo/C catalysts: In situ FTIR spectroscopy and DEMS studies," *International Journal of Hydrogen Energy*, vol. 37, pp. 7131–7140, apr 2012.

[126] Z.-B. Wang, G.-P. Yin, and Y.-G. Lin, "Synthesis and characterization of PtRuMo/C nanoparticle electrocatalyst for direct ethanol fuel cell," *Journal of Power Sources*, vol. 170, no. 2, pp. 242–250, 2007.

[127] R. De Souza, L. Parreira, J. Silva, F. Simões, M. Calegaro, M. Giz, G. Camara, A. Neto, and M. Santos, "PtSnCe/C electrocatalysts for ethanol oxidation: DEFC and FTIR "in-situ" studies," *International Journal of Hydrogen Energy*, vol. 36, no. 18, pp. 11519–11527, 2011.

[128] R. De Souza, J. Silva, M. Assumpção, A. Neto, and M. Santos, "Ethanol Oxidation Reaction Using PtSn/C+Ce/C Electrocatalysts: Aspects of Ceria Contribution," *Electrochimica Acta*, vol. 117, pp. 292–298, 2014.

[129] J. M. Jacob, P. G. Corradini, E. Antolini, N. A. Santos, and J. Perez, "Electro-oxidation of ethanol on ternary Pt–Sn–Ce/C catalysts," *Applied Catalysis B: Environmental*, vol. 165, pp. 176–184, 2015.

[130] D. Chu, Z. Li, X. Yuan, J. Li, X. Wei, and Y. Wan, "Electrocatalytic properties of carbon nanotubes supported ternary PtSnIn catalysts for ethanol electro-oxidation," *Electrochimica Acta*, vol. 78, pp. 644–648, 2012.

[131] J. Thepkaew, S. Therdthianwong, A. Kucernak, and A. Therdthianwong, "Electrocatalytic activity of mesoporous binary/ternary PtSn-based catalysts for ethanol oxidation," *Journal of Electroanalytical Chemistry*, vol. 685, pp. 41–46, 2012.

[132] P. G. Corradini, E. Antolini, and J. Perez, "Electro-oxidation of ethanol on ternary non-alloyed Pt–Sn–Pr/C catalysts," *Journal of Power Sources*, vol. 275, pp. 377–383, 2015.

[133] N. Nakagawa, Y. Kaneda, M. Wagatsuma, and T. Tsujiguchi, "Product distribution and the reaction kinetics at the anode of direct ethanol fuel cell with Pt/C, PtRu/C and PtRuRh/C," *Journal of Power Sources*, vol. 199, pp. 103–109, 2012.

[134] S. Beyhan, J. M. Léger, and F. Kadirgan, "Adsorption and oxidation of acetaldehyde on carbon supported Pt, PtSn and PtSn-based trimetallic catalysts by in situ Fourier transform infrared spectroscopy," *Journal of Power Sources*, vol. 242, pp. 503–509, 2013.

[135] a. Kowal, M. Li, M. Shao, K. Sasaki, M. B. Vukmirovic, J. Zhang, N. S. Marinkovic, P. Liu, a. I. Frenkel, and R. R. Adzic, "Ternary Pt/Rh/SnO2 electrocatalysts for oxidizing ethanol to CO2.," *Nature materials*, vol. 8, pp. 325–30, apr 2009.

[136] S. Beyhan, J.-M. Léger, and F. Kadırgan, "Understanding the influence of Ni, Co, Rh and Pd addition to PtSn/C catalyst for the oxidation of ethanol by in situ Fourier transform infrared spectroscopy," *Applied Catalysis B: Environmental*, vol. 144, pp. 66–74, 2014.

[137] M. Li, D. A. Cullen, K. Sasaki, N. S. Marinkovic, K. More, and R. R. Adzic, "Ternary electrocatalysts for oxidizing ethanol to carbon dioxide: making ir capable of splitting C-C bond.," *Journal of the American Chemical Society*, vol. 135, pp. 132–41, jan 2013.

[138] S. Beyhan, J.-M. Léger, and F. Kadırgan, "In situ FTIR investigation of acetic acid electrooxidation on carbon supported Pt–Sn based trimetallic catalysts: Influence of the nature of the third metal," *Applied Surface Science*, vol. 321, pp. 426–431, 2014.

[139] A. Bach Delpeuch, F. Maillard, M. Chatenet, P. Soudant, and C. Cremers, "Ethanol oxidation reaction (EOR) investigation on Pt/C, Rh/C, and Pt-based bi- and tri-metallic electrocatalysts: A DEMS and in situ FTIR study," *Applied Catalysis B: Environmental*, vol. 181, pp. 672–680, 2016.

[140] M. Li, W.-P. Zhou, N. Marinkovic, K. Sasaki, and R. Adzic, "The role of rhodium and tin oxide in the platinum-based electrocatalysts for ethanol oxidation to CO2," *Electrochimica Acta*, vol. 104, pp. 454–461, aug 2013.

[141] L. C. Silva-Junior, G. Maia, R. R. Passos, E. a. de Souza, G. a. Camara, and M. J. Giz, "Analysis of the selectivity of PtRh/C and PtRhSn/C to the formation of CO2 during ethanol electrooxidation," *Electrochimica Acta*, vol. 112, pp. 612–619, 2013.

[142] S. García-Rodríguez, S. Rojas, M. Peña, J. Fierro, S. Baranton, and J. Léger, "An FTIR study of Rh-PtSn/C catalysts for ethanol electrooxidation: Effect of surface composition," *Applied Catalysis B: Environmental*, vol. 106, no. 3-4, pp. 520–528, 2011.

[143] E. a. de Souza, M. Giz, G. a. Camara, E. Antolini, and R. R. Passos, "Ethanol electro-oxidation on partially alloyed Pt-Sn-Rh/C catalysts," *Electrochimica Acta*, vol. 147, pp. 483–489, nov 2014.

[144] E. Higuchi, T. Takase, M. Chiku, and H. Inoue, "Preparation of ternary Pt/Rh/SnO2 anode catalysts for use in direct ethanol fuel cells and their electrocatalytic activity for ethanol oxidation reaction," *Journal of Power Sources*, vol. 263, pp. 280–287, oct 2014.

[145] L. Zhao, S. Mitsushima, A. Ishihara, K. Matsuzawa, and K.-i. Ota, "Pt-Ir-SnO2/C Electrocatalysts for Ethanol Oxidation in Acidic Media," *Chinese Journal of Catalysis*, vol. 32, pp. 1856–1863, nov 2011.

[146] W. Du, Q. Wang, D. Saxner, N. A. Deskins, D. Su, J. E. Krzanowski, A. I. Frenkel, and X. Teng, "Highly Active Iridium/Iridium-Tin/Tin Oxide Heterogeneous Nanoparticles as Alternative Electrocatalysts for the Ethanol Oxidation Reaction," *Journal of the American Chemical Society*, vol. 133, pp. 15172–15183, 2011.

[147] R. Burch, "The Oxidation State of Rhenium and Its Role in Platinum-Rhenium Reforming Catalysts," *Platinum Metals Rev*, vol. 22, no. 2, pp. 57–60, 1978.

[148] Z. Wei, A. M. Karim, Y. Li, D. L. King, and Y. Wang, "Elucidation of the roles of Re in steam reforming of glycerol over Pt-Re/C catalysts," *Journal of Catalysis*, vol. 322, pp. 49–59, 2015.

[149] M. Salciccioli, M. Stamatakis, S. Caratzoulas, and D. Vlachos, "A review of multiscale modeling of metal-catalyzed reactions: Mechanism development for complexity and emergent behavior," *Chemical Engineering Science*, vol. 66, no. 19, pp. 4319–4355, 2011.

[150] T. Liang, Y. K. Shin, Y.-T. Cheng, D. E. Yilmaz, K. G. Vishnu, O. Verners, C. Zou, S. R. Phillpot, S. B. Sinnott, and A. C. T. van Duin, "Reactive Potentials for Advanced Atomistic Simulations," *Annual Review of Materials Research*, vol. 43, no. 1, pp. 109–129, 2013.

[151] M. Boronat, A. Corma, F. Illas, J. Radilla, T. Ródenas, and M. J. Sabater, "Mechanism of selective alcohol oxidation to aldehydes on gold catalysts: Influence of surface roughness on reactivity," *Journal of Catalysis*, vol. 278, no. 1, pp. 50–58, 2011.

[152] Q. S. Meng, Y. L. Shen, J. Xu, and J. L. Gong, "Mechanistic Insights into Selective Oxidation of Ethanol on Au(111): A DFT Study," *Chinese Journal of Catalysis*, vol. 33, no. 3, pp. 407–415, 2012.

[153] A. O. Pereira and C. R. Miranda, "Atomic scale insights into ethanol oxidation on Pt, Pd and Au metallic nanofilms: A DFT with van der Waals interactions," *Applied Surface Science*, vol. 288, pp. 564–571, 2014.

[154] M. Li, W. Guo, R. Jiang, L. Zhao, and H. Shan, "Decomposition of ethanol on Pd(111): a density functional theory study.," *Langmuir : the ACS journal of surfaces and colloids*, vol. 26, no. 3, pp. 1879–88, 2010.

[155] G. Cui, S. Song, P. K. Shen, A. Kowal, and C. Bianchini, "First-Principles Considerations on Catalytic Activity of Pd toward Ethanol Oxidation," *The Journal of Physical Chemistry C*, vol. 113, pp. 15639–15642, sep 2009.

[156] Y. Choi and P. Liu, "Understanding of ethanol decomposition on Rh(111) from density functional theory and kinetic Monte Carlo simulations," *Catalysis Today*, vol. 165, no. 1, pp. 64–70, 2011.

[157] J. Courtois, W. Du, E. Wong, X. Teng, and N. A. Deskins, "Screening iridium-based bimetallic alloys as catalysts for direct ethanol fuel cells," *Applied Catalysis A: General*, vol. 483, pp. 85–96, aug 2014.

[158] R. Alcalá, M. Mavrikakis, and J. a. Dumesic, "DFT studies for cleavage of C-C and C-O bonds in surface species derived from ethanol on Pt(111)," *Journal of Catalysis*, vol. 218, pp. 178–190, 2003.

[159] R. R. Davda, R. Alcala, J. Shabaker, G. Huber, R. D. Cortright, M. Mavrikakis, and J. a. Dumesic, "DFT and experimental studies of C-C and C-O bond cleavage in ethanol and ethylene glycol on Pt catalysis," *Science and Technology in Catalysis 2002*, vol. 145, pp. 79–84, 2003.

[160] M. Koehle and A. Mhadeshwar, "Microkinetic modeling and analysis of ethanol partial oxidation and reforming reaction pathways on platinum at short contact times," *Chemical Engineering Science*, vol. 78, pp. 209–225, 2012.

[161] Y. Shibuta, K. Shimamura, R. Arifin, and F. Shimojo, "Ab initio molecular dynamics simulation of ethanol decomposition on platinum cluster at initial stage of carbon nanotube growth," *Chemical Physics Letters*, vol. 636, pp. 110–116, 2015.

[162] R. Alcala, J. W. Shabaker, G. W. Huber, M. a. Sanchez-Castillo, and J. a. Dumesic, "Experimental and DFT studies of the conversion of ethanol and acetic acid on PtSn-based catalysts.," *The journal of physical chemistry. B*, vol. 109, pp. 2074–85, feb 2005.

[163] Y. Wang, Y. Mi, N. Redmon, and J. Holiday, "Understanding Electrocatalytic Activity Enhancement of Bimetallic Particles to Ethanol Electro-oxidation: (1) Water Adsorption and Decomposition on Pt(n)M (n=2,3 and 9; M=Pt, Ru, Sn).," *The journal of physical chemistry. C, Nanomaterials and interfaces*, vol. 114, pp. 317–326, jan 2010.

[164] K. Kholmurodov, E. Dushanov, K. Yasuoka, H. Khalil, A. Galal, S. Ahmed, N. Sweilam, and H. Moharram, "Molecular dynamics study of ethanol solvated by water on the Pt (111) surface," *Chemical Physics*, vol. 402, pp. 41–47, 2012.

[165] J. E. Mueller, A. C. T. Van Duin, and W. A. Goddard, "Development and validation of reaxff reactive force field for hydrocarbon chemistry catalyzed by nickel," *Journal of Physical Chemistry C*, vol. 114, no. 11, pp. 4939–4949, 2010.

[166] J. E. Mueller, A. C. T. Van Duin, and W. A. Goddard, "Application of the ReaxFF reactive force field to reactive dynamics of hydrocarbon chemisorption and decomposition," *Journal of Physical Chemistry C*, vol. 114, no. 12, pp. 5675–5685, 2010.

[167] W. Somers, A. Bogaerts, A. C. T. Van Duin, and E. C. Neyts, "Plasma species interacting with nickel surfaces: Toward an atomic scale understanding of plasma-catalysis," *Journal of Physical Chemistry C*, vol. 116, no. 39, pp. 20958–20965, 2012.

[168] C. W. Bauschlicher, T. Qi, E. J. Reed, A. Lenfant, J. W. Lawson, and T. G. Desai, "Comparison of ReaxFF, DFTB, and DFT for phenolic pyrolysis. 2. Elementary reaction paths," *Journal of Physical Chemistry A*, vol. 117, no. 44, pp. 11126–11135, 2013.

[169] C. Zou, A. C. T. Van Duin, and D. C. Sorescu, "Theoretical investigation of hydrogen adsorption and dissociation on iron and iron carbide surfaces using the ReaxFF reactive force field method," *Topics in Catalysis*, vol. 55, no. 5-6, pp. 391–401, 2012.

[170] D. Rapaport, *The Art of Molecular Dynamics Simulation*. Cambridge University Press, second ed., 2006.

[171] D. Marx and J. Hutter, *Ab Initio Molecular Dynamics: Basic Theory and Advanced Methods*. Cambridge University Press, 2009.

[172] H. M. Aktulga, S. A. Pandit, A. C. T. van Duin, and A. Y. Grama, "Reactive Molecular Dynamics: Numerical Methods and Algorithmic Techniques," *SIAM Journal on Scientific Computing*, vol. 34, pp. C1–C23, jan 2012.

[173] M. E. Tuckerman and G. J. Martyna, "Understanding Modern Molecular Dynamics: Techniques and Applications," *The Journal of Physical Chemistry B*, vol. 104, no. 2, pp. 159–178, 2000.

[174] A. C. T. van Duin, C. Zou, K. Joshi, V. Bryantsev, and W. a. Goddard, "A Reaxff Reactive Forcefield for Proton Transfer Reactions in Bulk Water and its Applications to Heterogeneous Catalysis," *Computational Catalysis*, no. 14, pp. 223–243, 2013.

[175] J. K. Norskov, F. Studt, F. Abild-Pedersen, and T. Bligaard, *Fundamental Concepts in Heterogeneous Catalysis*. John Wiley & Sons, Inc., 2014.

[176] A. Asthagiri and M. J. Janik, eds., *Computational Catalysis*. RSC Catalysis Series, Cambridge: Royal Society of Chemistry, 2013.

[177] H. Knozinger and O. Deutschmann, "Heterogeneous Catalysis and Solid Catalysts.," in *Ullmann's Encyclopedia of Industrial Chemistry*, Weinheim, Germany: Wiley-VCH Verlag GmbH & Co. KGaA, jun 2009.

[178] A. Gross, *Theoretical Surface Science*. Berlin, Heidelberg: Springer Berlin Heidelberg, 2009.

[179] M. G. Evans and M. Polanyi, "Inertia and driving force of chemical reactions," *Transactions of the Faraday Society*, vol. 34, p. 11, 1938.

[180] S. Wang, V. Vorotnikov, J. E. Sutton, and D. G. Vlachos, "Brønsted–Evans–Polanyi and Transition State Scaling Relations of Furan Derivatives on Pd(111) and Their Relation to Those of Small Molecules," *ACS Catalysis*, vol. 4, no. 2, pp. 604–612, 2014.

[181] S. Wang, B. Temel, J. Shen, G. Jones, L. C. Grabow, F. Studt, T. Bligaard, F. Abild-Pedersen, C. H. Christensen, and J. K. Nørskov, "Universal Brønsted-Evans-Polanyi Relations for C–C, C–O, C–N, N–O, N–N, and O–O Dissociation Reactions," *Catalysis Letters*, vol. 141, no. 3, pp. 370–373, 2011.

[182] A. Michaelides, Z. P. Liu, C. J. Zhang, A. Alavi, D. a. King, and P. Hu, "Identification of general linear relationships between activation energies and enthalpy changes for dissociation reactions at surfaces," *Journal of the American Chemical Society*, vol. 125, no. 13, pp. 3704–3705, 2003.

[183] J. K. Nørskov, "Universality in Heterogeneous Catalysis," *Journal of Catalysis*, vol. 209, pp. 275–278, jul 2002.

[184] A. Balandin, "Modern State of the Multiplet Theor of Heterogeneous Catalysis," *Advances in Catalysis*, vol. 19, pp. 1–210, 1969.

[185] J. K. Nørskov, T. Bligaard, B. Hvolbaek, F. Abild-Pedersen, I. Chorkendorff, and C. H. Christensen, "The nature of the active site in heterogeneous metal catalysis.," *Chemical Society reviews*, vol. 37, pp. 2163–71, oct 2008.

[186] B. Hammer and J. Nørskov, "Theoretical surface science and catalysis: calculations and concepts," *Advances in catalysis*, vol. 45, 2000.

[187] H. S. Taylor, "A Theory of the Catalytic Surface," *Proceedings of the Royal Society A: Mathematical, Physical and Engineering Sciences*, vol. 108, pp. 105–111, may 1925.

[188] C. H. Christensen and J. K. Nørskov, "A molecular view of heterogeneous catalysis.," *The Journal of chemical physics*, vol. 128, p. 182503, may 2008.

[189] W. Kolos, "Adiabatic Approximation and Its Accuracy," *Advances in Quantum Chemistry*, vol. 5, no. C, pp. 99–133, 1970.

[190] M. Born and R. Oppenheimer, "Zur quantentheorie der molekeln," *Annalen der Physik*, vol. 20, no. 84, pp. 457–484, 1927.

[191] W. Kohn, "Nobel Lecture: Electronic structure of matter—wave functions and density functionals," *Reviews of Modern Physics*, vol. 71, pp. 1253–1266, oct 1999.

[192] J. G. Lee, *Computational Materials Science: An Introduction*. CRC Press, 2012.

[193] D. Sholl and J. Steckel, *Density Functional Theory: A Practical Introduction*, vol. 7. Hoboken, New Jersey: John Wiley & Sons, Inc., aug 2009.

[194] W. Koch and M. C. Holthausen, *A Chemist's Guide to Density Functional Theory*. WILEY-VCH Verlag GmbH, second ed., 2001.

[195] P. Hohenberg and W. Kohn, "Inhomogeneous Electron Gas," *Physical Review*, vol. 136, pp. B864–B871, nov 1964.

[196] W. Kohn and L. J. Sham, "Self-Consistent Equations Including Exchange and Correlation Effects," *Physical Review*, vol. 140, pp. A1133–A1138, nov 1965.

[197] J. P. Perdew and A. Zunger, "Self-interaction correction to density-functional approximations for many-electron systems," *Physical Review B*, vol. 23, pp. 5048–5079, may 1981.

[198] J. P. Perdew and Y. Wang, "Accurate and simple analytic representatio of the electron-gas correlation energy," *Physical Review B*, vol. 45, no. 23, pp. 244–249, 1992.

[199] J. P. Perdew, "Unified Theory of Exchange and Correlation Beyond the Local Density Approximation," in *Electronic Structure of Solids '91* (P. Ziesche and H. Eschrig, eds.), pp. 11–20, Akademie Verlag, Berlin, 1991.

[200] J. P. Perdew, K. Burke, and M. Ernzerhof, "Generalized Gradient Approximation Made Simple," *Physical Review Letters*, vol. 77, pp. 3865–3868, oct 1996.

[201] A. D. Becke, "Density-functional exchange-energy approximation with correct asymptotic behavior," *Physical Review A*, vol. 38, pp. 3098–3100, sep 1988.

[202] C. Lee, W. Yang, and R. Parr, "Development of the Colle-Salvetti correlation-energy formula into a functional of electron dnsity," *Physical Review B*, vol. 37, no. 2, 1988.

[203] W. E. Pickett, "Pseudopotential methods in condensed matter applications," *Computer Physics Reports*, vol. 9, pp. 115–197, apr 1989.

[204] D. Vanderbilt, "Soft self-consistent pseudopotentials in a generalized eigenvalue formalism," *Physical Review B*, vol. 41, pp. 7892–7895, apr 1990.

[205] N. Troullier and J. L. Martins, "Efficient pseudopotentials for plane-wave calculations," *Physical Review B*, vol. 43, pp. 1993–2006, jan 1991.

[206] M. Murakami and Y. Ito, "Cleavage of Carbon—Carbon Single Bonds by Transition Metals," in *Activation of Unreactive Bonds and Organic Synthesis*, vol. 3, Springer Berlin Heidelberg, 1999.

[207] B. Predel, "Pt-Re (Platinum-Rhenium)," in *Phase Equilibria, Crystallographic and Thermodynamic Data of Binary Alloys: Ni-Np – Pt-Zr* (O. Madelung, ed.), vol. 3, p. 1990, Springer Berlin Heidelberg, 1998.

[208] F. Murnaghan, "The compressibility of media under extreme pressures," *Proc Natl Acad Sci U S A*, vol. 30, no. 9, pp. 244–247, 1944.

[209] A. Michaelides and M. Scheffler, "An introduction to the theory of crystalline elemental solids and their surfaces," in *Surface and Interface Science: Concepts and Methods Science* (K. Wandelt, ed.), pp. 13–172, Weinheim: Wiley-VCH, 2012.

[210] P. Giannozzi and S. Baroni, "QUANTUM ESPRESSO: a modular and open-source software project for quantum simulations of materials," *Journal of Physics: ...*, p. 36, jun 2009.

[211] B. Hammer, L. Hansen, and J. Nørskov, "Improved adsorption energetics within density-functional theory using revised Perdew-Burke-Ernzerhof functionals," *Physical Review B*, vol. 59, no. 11, pp. 7413–7421, 1999.

[212] A. E. Mattsson, R. Armiento, P. a. Schultz, and T. R. Mattsson, "Nonequivalence of the generalized gradient approximations PBE and PW91," *Physical Review B*, vol. 73, no. 19, p. 195123, 2006.

[213] D. C. Patton, D. V. Porezag, and M. R. Pederson, "Simplified generalized-gradient approximation and anharmonicity: Benchmark calculations on molecules," *Physical Review B*, vol. 55, no. 12, pp. 7454–7459, 1997.

[214] Y. J. Wang and J. W. Davenport, "Relativistic effects on the s -¿ d promotion energy and spin-polarization energy of the transition metals," *Physical Review A*, vol. 41, pp. 4690–4695, may 1990.

[215] M. A. Van Hove, "The Adsorption Sites of CO and NO Molecules on Metal Surfaces," *Israel Journal of Chemistry*, vol. 38, no. 4, pp. 349–352, 1998.

[216] Y. Ishikawa, M.-S. Liao, and C. R. Cabrera, "Energetics of H2O dissociation and COads+OHads reaction on a series of Pt–M mixed metal clusters: a relativistic density-functional study," *Surface Science*, vol. 513, pp. 98–110, jul 2002.

[217] J. Greeley and M. Mavrikakis, "Near-surface alloys for hydrogen fuel cell applications," *Catalysis Today*, vol. 111, no. 1-2, pp. 52–58, 2006.

[218] A. Ramstad, F. Strisland, S. Raaen, A. Borg, and C. Berg, "CO and O2 adsorption on the Re/Pt(111) surface studied by photoemission and thermal desorption.," *Surface Science*, vol. 440, pp. 290–300, oct 1999.

[219] A. Ramstad, F. Strisland, S. Raaen, T. Worren, A. Borg, and C. Berg, "Growth and alloy formation studied by photoelectron spectroscopy and STM," *Surface Science*, vol. 425, pp. 57–67, apr 1999.

[220] D. Ogletree, M. Van Hove, and G. Somorjai, "LEED intensity analysis of the structures of clean Pt(111) and of CO adsorbed on Pt(111) in the c(4 x 2) arrangement," *Surface Science*, vol. 173, no. 2-3, pp. 351–365, 1986.

[221] R. McCabe and L. Schmidt, "binding states of CO and H2 on clean and oxidized (111)Pt," *Surface Science*, vol. 65, no. 1, pp. 189–209, 1977.

[222] T. H. Lin and G. a. Somorjai, "Modulated molecular beam scattering of CO and NO from Pt(111) and the stepped Pt(557) crystal surfaces," *Surface Science Letters*, vol. 107, p. A233, 1981.

[223] B. Poelsema, R. L. Palmer, and G. Comsa, "A thermal He scattering study of CO adsorption on Pt(111)," *Surface Science*, vol. 136, no. 1, pp. 1–14, 1984.

[224] A. Cudok, H. Froitzheim, and M. Schulze, "Low-temperature adsorption kinetics of CO on Pt(111) derived from nonequilibrium time-resolved electron-energy-loss spectroscopy measurements," *Physical Review B*, vol. 47, pp. 13682–13686, may 1993.

[225] Y. Y. Yeo, L. Vattuone, and D. A. King, "Calorimetric heats for CO and oxygen adsorption and for the catalytic CO oxidation reaction on Pt{111}," *The Journal of Chemical Physics*, vol. 106, no. 1, p. 392, 1997.

[226] M. Kinne, T. Fuhrmann, C. M. Whelan, J. F. Zhu, J. Pantförder, M. Probst, G. Held, R. Denecke, and H. P. Steinrück, "Kinetic parameters of CO adsorbed on Pt(111) studied by in situ high resolution x-ray photoelectron spectroscopy," *Journal of Chemical Physics*, vol. 117, no. 23, pp. 10852–10859, 2002.

[227] F. Abild-Pedersen and M. Andersson, "CO adsorption energies on metals with correction for high coordination adsorption sites – A density functional study," *Surface Science*, vol. 601, no. 7, pp. 1747–1753, 2007.

[228] H. Steininger, S. Lehwald, and H. Ibachi, "On the adsorption of CO on Pt(111)," *Surface Science Letters*, vol. 123, no. 2-3, p. A453, 1982.

[229] E. Schweizer, B. Persson, M. Tüshaus, D. Hoge, and a.M. Bradshaw, "The potential energy surface, vibrational phase relaxation and the order-disorder transition in the adsorption system Pt{111}-CO," *Surface Science Letters*, vol. 213, p. A212, 1989.

[230] B. N. J. Persson, M. Tushaus, and a. M. Bradshaw, "On the nature of dense CO adlayers," *Journal of Chemical Physics*, vol. 92, no. 8, pp. 5034–5046, 1990.

[231] A. Hightower, M. D. Perez, and B. E. Koel, "An IRAS study of CO bonding on Sn/Pt(111) surface alloys at maximal pressures of 10Torr," *Surface Science*, vol. 603, no. 3, pp. 455–461, 2009.

[232] P. J. Feibelman, B. Hammer, F. Wagner, M. Scheffler, R. Stumpf, R. Watwe, and J. Dumesic, "The CO/Pt(111) Puzzle," *The Journal of Physical Chemistry B*, no. 111, pp. 4018–4025, 2001.

[233] G. Kresse, a. Gil, and P. Sautet, "Significance of single-electron energies for the description of CO on Pt(111)," *Physical Review B*, vol. 68, no. 7, pp. 3–6, 2003.

[234] R. A. Olsen, P. H. T. Philipsen, and E. J. Baerends, "CO on Pt(111): A puzzle revisited," *Journal of Chemical Physics*, vol. 119, no. 8, pp. 4522–4528, 2003.

[235] H. Orita, N. Itoh, and Y. Inada, "All electron scalar relativistic calculations on adsorption of CO on Pt(1 1 1) with full-geometry optimization: A correct estimation for CO site-preference," *Chemical Physics Letters*, vol. 384, no. 4-6, pp. 271–276, 2004.

[236] L. Schimka, J. Harl, a. Stroppa, a. Grüneis, M. Marsman, F. Mittendorfer, and G. Kresse, "Accurate surface and adsorption energies from many-body perturbation theory," *Nature Materials*, vol. 9, no. 9, pp. 741–744, 2010.

[237] I. Grinberg, Y. Yourdshahyan, and A. M. Rappe, "CO on Pt(111) puzzle: A possible solution," *The Journal of Chemical Physics*, vol. 117, no. 5, p. 2264, 2002.

[238] S. E. Mason, I. Grinberg, and A. M. Rappe, "First-principles extrapolation method for accurate CO adsorption energies on metal surfaces," *Physical Review B - Condensed Matter and Materials Physics*, vol. 69, no. 16, pp. 1–4, 2004.

[239] D. J. Godbey, "The Adsorption and Desorption of Hydrogen and Carbon Monoxide on Bimetallic Re-Pt(111) Surfaces," *Surface Science*, vol. 204, pp. 301–318, 1988.

[240] C. Pauls, D. Przyrembel, and K. Christmann, "Dissociation of carbon monoxide on the rhenium(10-10) Surface," *Journal of Physical Chemistry B*, vol. 108, no. 38, pp. 14749–14758, 2004.

[241] M. Gajdo, A. Eichler, and J. Hafner, "CO adsorption on close-packed transition and noble metal surfaces: trends from ¡i¿ab initio¡/i¿ calculations," *Journal of Physics: Condensed Matter*, vol. 16, no. 8, pp. 1141–1164, 2004.

[242] C. J. Zhang, R. J. Baxter, P. Hu, A. Alavi, and M.-H. Lee, "A density functional theory study of carbon monoxide oxidation on the CuPt(111) alloy surface: Comparison with the reactions on Pt(111) and Cu(111)," *The Journal of Chemical Physics*, vol. 115, no. 11, p. 5272, 2001.

[243] M. Lynch and P. Hu, "A density functional theory study of CO and atomic oxygen chemisorption on Pt(111)," *Surface Science*, vol. 458, no. 1-3, pp. 1–14, 2000.

[244] W. Liu, Y. F. Zhu, J. S. Lian, and Q. Jiang, "Adsorption of CO on surfaces of 4d and 5d elements in group VIII," *Journal of Physical Chemistry C*, vol. 111, no. 2, pp. 1005–1009, 2007.

[245] E. D. German and M. Sheintuch, "Comparative Theoretical Study of CO Adsorption and Desorption Kinetics on (111) Surfaces of Transition Metals," *J. Phys. Chem. C*, vol. 112, no. 111, pp. 14377–14384, 2008.

[246] K. Hahn and M. Mavrikakis, "Atomic and Molecular Adsorption on Re(0001)," *Topics in Catalysis*, vol. 57, pp. 54–68, feb 2014.

[247] R. Ducros, B. Tardy, and J. Bertolini, "Carbon monoxide adsorption on Re(0001) between 120 and 600 K studied by vibrational electron energy loss spectroscopy," *Surface Science*, vol. 128, pp. L219–L223, jan 1983.

[248] F. Solymosi and T. Bansagi, "CO-Induced Changes in Structure of Supported Rhenium l a," *Journal of Physical Chemistry*, vol. 96, no. C, pp. 1349–1355, 1992.

[249] J. Anderson, F. Chong, and C. Rochester, "IR study of CO adsorption on Pt, Re and Pt–Re/Al 2 O 3 catalysts before and after coking," *Journal of Molecular Catalysis A: Chemical*, vol. 140, pp. 65–80, 1999.

[250] C. Lucas, N. Marković, and P. Ross, "The adsorption and oxidation of carbon monoxide at the Pt(111)/electrolyte interface: atomic structure and surface relaxation," *Surface Science*, vol. 425, pp. L381–L386, 1999.

[251] C. A. Lucas and N. M. Markovic, "In-situ Surface X-ray Scattering and Infrared Reflection Adsorption Spectroscopy of CO Chemisorption at the Electrochemical Interface," in *In-situ Spectroscopic Studies of Adsorption at the Electrode and Electrocatalysis*, pp. 339–381, Elsevier, 2007.

[252] M. Zhang, K. Yang, X. Zhang, and Y. Yu, "Effect of Ni(111) surface alloying by Pt on partial oxidation of methane to syngas: A DFT study," *Surface Science*, vol. 630, pp. 236–243, 2014.

[253] Y. Chen and D. G. Vlachos, "Hydrogenation of Ethylene and Dehydrogenation and Hydrogenolysis of Ethane on Pt (111) and Pt (211): A Density Functional Theory Study," *Journal of Physical Chemistry C*, vol. 114, no. 11, pp. 4973–4982, 2010.

[254] R. Zhang, L. Song, and Y. Wang, "Applied Surface Science Insight into the adsorption and dissociation of CH 4 on Pt (h k l) surfaces : A theoretical study," *Applied Surface Science*, vol. 258, no. 18, pp. 7154–7160, 2012.

[255] J. A. Herron, S. Tonelli, and M. Mavrikakis, "Atomic and molecular adsorption on Ru(0001)," *Surface Science*, vol. 614, pp. 64–74, aug 2013.

[256] T. Fromherz, C. Mendoza, and F. Ruette, "Chemisorption of atomic H, C, N and O on a cluster-model graphite surface," *Monthly Notices of the Royal Astronomical Society*, vol. 263, no. 4, p. 851, 1993.

[257] J.-F. Paul and P. Sautet, "Chemisorption and Transformation of CH x Fragments (x = 0-3) on a Pd(111) Surface: A Periodic Density Functional Study," *The Journal of Physical Chemistry B*, vol. 102, pp. 1578–1585, feb 1998.

[258] J. Kua, F. Faglioni, and W. a. Goddard, "Thermochemistry for Hydrocarbon Intermediates Chemisorbed on Metal Surfaces: CH n-m(CH3)m with n = 1, 2, 3 on Pt, Ir, Os, Pd, Rh, and Ru," *Journal of the American Chemical Society*, vol. 122, no. 5, pp. 2309–2321, 2000.

[259] W. Yang and R. G. Parr, "Hardness, softness, and the fukui function in the electronic theory of metals and catalysis.," *Proceedings of the National Academy of Sciences of the United States of America*, vol. 82, pp. 6723–6726, 1985.

[260] S. Linic, N. Schweitzer, H. Xin, E. Nikolla, and J. T. Miller, "Establishing Relationships Between the Geometric Structure and Chemical Reactivity of Alloy Catalysts Based on Their Measured Electronic Structure," *Topics in Catalysis*, vol. 53, pp. 348–356, feb 2010.

[261] P.-O. Löwdin, "On the Non-Orthogonality Problem Connected with the Use of Atomic Wave Functions in the Theory of Molecules and Crystals," *The Journal of Chemical Physics*, vol. 18, no. 3, pp. 365–375, 1950.